9-26-2008

Cardioprotective Signal Transduction to Mitochondria

Casey Lee Quinlan
Portland State University

CARDIOPROTECTIVE SIGNAL TRANSDUCTION TO

MITOCHONDRIA

by

CASEY LEE QUINLAN

A dissertation submitted in partial fulfillment of the
requirements for the degree of

DOCTOR OF PHILOSOPHY
in
BIOLOGY

Portland State University
2008

DISSERTATION APPROVAL

The abstract and dissertation of Casey Lee Quinlan for the Doctor of Philosophy in Biology were presented September 26, 2008, and accepted by the dissertation committee and the doctoral program.

COMMITTEE APPROVALS:

Keith D. Garlid, Chair

Stan S. Hillman

Michael S. Bartlett

Jason E. Podrabsky

David H. Peyton

Representative of the Office of Graduate Studies

DOCTORAL PROGRAM APPROVAL:

Suzanne Estes, Director
Biology Ph.D. Program

ABSTRACT

An abstract of the dissertation of Casey Lee Quinlan for the Doctor of Philosophy in Biology, presented September 26, 2008.

Title: Cardioprotective Signal Transduction to Mitochondria

Intracellular responses to external stimuli require reception of the message at the plasma membrane followed by encoding and transmission of the message to its effectors downstream. In this process, diverse cellular responses are mediated by many redundant molecular players. The apparent generality and redundancy of many kinases, such as the mitogen-activated protein kinases (MAPKs), suggests that signal transduction must gain specificity through tight regulation. Diffusion and random collisions of relevant signaling components seem insufficient to explain the multilayered complexity observed in cell signaling cascades. Emerging hypotheses suggest that signaling machinery may achieve enhanced specificity and control by exploiting the compartmentalization capabilities of plasma membrane microdomains. This study examines the hypothesis that treatment of the heart with the cardioprotective agents, ouabain or bradykinin, instigates formation of a signaling platform (or signalosome) that encompasses all the enzymes of the receptor-mediated pathway. The signalosome serves to compartmentalize and deliver the signaling

components to mitochondria where it facilitates opening of the mitochondrial

ATP-sensitive K^+ channel and instigation of an intramitochondrial signaling

pathway that mediates cardioprotection.

DEDICATION

The work presented here is dedicated to John R. Quinlan.

ACKNOWLEDGMENTS

TABLE OF CONTENTS

LIST OF FIGURES

LIST OF ABBREVIATIONS

5-HD - 5-hydroxydecanoate

AAR - Area at risk

ANT - adenine nucleotide translocase

BCECF - pH sensitive fluorescent probe

Bk - Bradykinin

CCCP - Carbonyl cyanide m- chlorophenylhydrazone

Dzx - Diazoxide

eNOS - Endothelial nitric oxide synthase

GC - guanylyl cyclase

GPCR - G-protein coupled receptor

H_2O_2 - Hydrogen peroxide

IMS - Intermembrane space

IPC - ischemic preconditioning

KCO - K^+ channel openers

KT - KT5823

LL - light layer fraction

LVEDP - Left ventricular end diastolic pressure

MAPK - mitogen-activated protein kinase

miCK - Mitochondrial creatine kinase

$mitoK_{ATP}$ - Mitochondrial ATP-sensitive K^+ channel

MOM - mitochondrial outer membrane

MPG - 2-mercaptopropionyl glycine

MPT - Mitochondrial Permeability Transition

NO - Nitric oxide

NOS - Nitric oxide synthase

ODQ - 1H-[1,2,4]Oxadiazole[4,3-a]quinoxalin-1-one

PBFI - K^+ sensitive fluorescent probe

PC - Preconditioning

Pi - Inorganic phosphate

PI3-k - Phophatidylinostitol 3-kinase

PKC - Protein kinase C

PKG - cGMP-dependent protein kinase G

PLL - Purified light layer fraction

PMA - Phorbal 12-myristate 13-acetate

PP2 - 4-Amino-5-(4-chlorophenyl)-7-(t-butyl)pyrazolo[3,4-d] pyrimidine

PP2A - Protein phosphatase 2A

RACK - receptor for activated C kinase

ROS - Reactive oxygen species

RPP - Rate-pressure product

SUR - Sulfonylurea receptors

TEA^+ - Tetraethylammonium cation

TPP^+ - Tetraphenylphosphonium cation

TTC - Thiphenyltetrazolium chloride

Val - Valinomycin

VDAC - Voltage-dependent anion channel

1. Introduction

1.1 Cardioprotection and Mitochondria

Heart attacks and their associated ischemic events are together a major cause of death in the United States and world wide. According to the American Heart Association, there are 1.2 million new and recurrent coronary attacks per year, and of these about 38 percent result in death (191). Investigations into the damage-causing mechanisms of a heart attack have revealed that both apoptotic and necrotic cell death pathways are triggered downstream of the coronary thrombosis, and this cell death is at the root of the observed injury (52, 223). Necrotic and apoptotic cell death pathways are distinct in many respects, but both have been shown to involve mitochondria (37, 77, 90, 126). In this regard, many agents that affect mitochondria have been shown to reduce ischemic damage; treatments that reduce such injury are referred to as cardioprotective.

The 1986 discovery of the phenomenon known as ischemic preconditioning (IPC), whereby cardioprotection is achieved through brief cycles of ischemia and reperfusion prior to a significant ischemic event, has spurred significant interest in the mechanisms of protection from cardiac injury (148). Since the discovery of IPC, many drugs have been shown to mimic its

effects, including a number of G-coupled receptor agonists, agents that target specific kinases, and (of particular interest to this study) activation of the mitochondrial ATP-sensitive K^+ channel (mitoK$_{ATP}$)(50, 71). These disparate treatments all hold in common their ability to affect mitochondria and limit necrotic and apoptotic cell death pathways.

Mitochondria are well characterized as the ubiquitous organelles of aerobic metabolism. Beyond this definition, their role can be expanded to include critical importance in the processes of reactive oxygen species (ROS) production, intracellular signaling pathways and, as mentioned above, apoptotic/necrotic death pathways (5, 6, 50, 108, 146). All known cardioprotective pathways inhibit cellular necrosis, which itself is a direct manifestation of the mitochondrial permeability transition (MPT). MPT is a large-conductance pore that allows the passage of solutes of up to 1500 Da. The occurrence of this pathology results in the loss of mitochondrial membrane integrity and membrane potential, which in turn compromises ATP production (40). The exact molecular identity of MPT is unknown; it is hypothesized to be a multiprotein pore composed of such prevalent membrane proteins as the adenine nucleotide translocase (ANT) and voltage-dependent anion channel (VDAC), but the only proven pore component is cyclophilin D (10). Cyclosporin A, the best known pharmacologic inhibitor of MPT, binds to cyclophilin D (39). Activation of the mitoK$_{ATP}$ channel has been shown to

inhibit pathological manifestations of MPT (32).

The mitoK$_{ATP}$ channel was simultaneously discovered by two labs in 1991. Patch clamp studies and reconstitution assays both found evidence for the presence of a potassium uniport pathway in the mitochondrial inner membrane (84, 91). In the years that have followed, work in our laboratory has focused on the role that mitoK$_{ATP}$ plays in cellular physiology and pathology. We, and others, have found that mitoK$_{ATP}$ is a receptor for cardioprotective potassium-channel openers (64, 71, 72, 82). We have shown that opening mitoK$_{ATP}$ is cardioprotective through a mechanism involving mitochondrial ROS production and inhibition of cellular necrosis (4, 32). In Chapter 2, an analysis of the direct physiological effects of mitoK$_{ATP}$-opening is discussed.

As stated above, all methods of cardioprotection protect the mitochondria from the pathological occurrence of MPT. In this respect, MPT could be considered the "end-effector" of cardioprotection; triggers of this end-effect are numerous. IPC, the gold standard of cardioprotection, generates several cardioprotective G-protein coupled receptor (GPCR) agonists such as adenosine, opioids, and bradykinin. When bound to their receptors these compounds instigate activation of a number of downstream targets, such as Akt, protein kinase C (PKC), nitric oxide synthase (NOS), protein kinase G (PKG), and activation of mitoK$_{ATP}$ (12, 26, 79, 146, 224, 232, 239).

MitoK$_{ATP}$ activation is known to be a crucial component of

cardioprotection. Its inhibition blocks all known forms of cardioprotection (82, 88). Opening of mitoK_{ATP}, either directly by pharmacological means or by activation of upstream signaling pathways, leads to the instigation of the intramitochondrial signaling pathway which involves multiple steps and will be detailed in the following section.

1.2 Intramitochondrial signaling

The diagram in Fig. 1.1 summarizes several years of studies on intramitochondrial signaling (4, 31, 32, 34, 35, 62, 93, 186). The primary function of this pathway is to inhibit MPT opening, which is widely considered to be the cause of cell death after ischemia-reperfusion (7, 38, 45).

Step one - opening mitoK_{ATP}

Direct mitoK_{ATP} opening by K_{ATP} channel openers (KCO)

The ability of KCOs to open mitoK_{ATP} in their therapeutic dose range was described in 1996 (72). KCOs act on the regulatory sulfonylurea receptors (SUR) of K_{ATP} channels. Pinacidil, cromakalim, and nicorandil are effective openers of cardiac K_{ATP} through their action on SUR2A, but ineffective on the pancreatic beta cell K_{ATP}, which uses SUR1. Conversely, diazoxide is an effective opener of beta cell K_{ATP}, but ineffective on the cardiac channel (145). All KCOs we have examined, including those listed above, open mitoK_{ATP} and protect the heart from ischemia-reperfusion injury (35, 71, 72, 81, 94, 115, 162, 185).

Figure 1.1 **The intramitochondrial signaling pathways.** The pathways leading to mitoK$_{ATP}$ opening, ROS production, and MPT inhibition are shown. Positive and negative regulation of pathway components is indicated by plus (+) and minus (-) symbols, respectively. MitoK$_{ATP}$ is opened by activation of PKG, and stimulation of PKCε1. MPT is inhibited by the mitoK$_{ATP}$-induced ROS activation of PKCε2, or exogenous addition of activators such PMA. Please see the text for a complete description. This figure has been modified from Costa and Garlid (34).

Figure 1.1
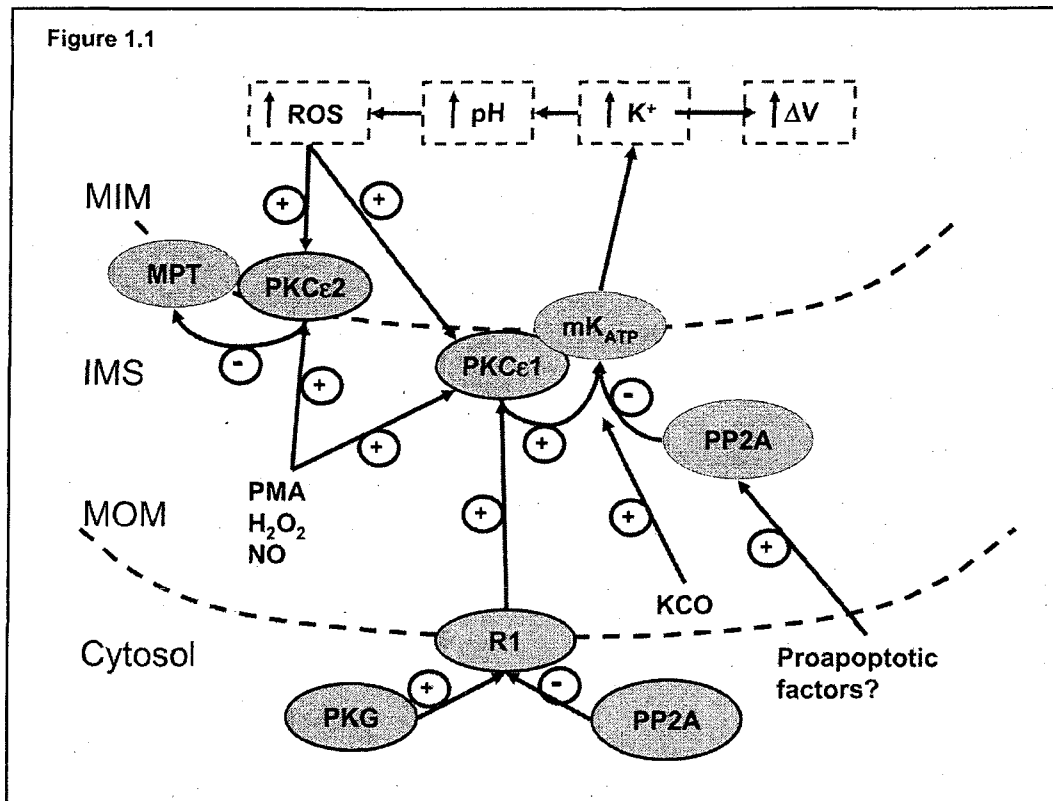
Indirect mitoK$_{ATP}$ opening, by signaling to PKCε1

Ischemic preconditioning, ischemic postconditioning, and pharmacological preconditioning via plasma membrane receptor agonists cause mitoK$_{ATP}$ opening by activating a signaling pathway that signals to a constitutive mitochondrial Protein kinase C epsilon, PKCε. Our studies suggest that this PKCε lies directly upstream of mitoK$_{ATP}$ (32, 34, 93). The PKCε-specific peptide agonist ΨεRACK and the general PKCε agonists H$_2$O$_2$, NO, and phorbol 12-myristate 13-acetate (PMA) each open mitoK$_{ATP}$ (34).(190). That these agents were acting via PKCε ("PKCε1" in Fig. 1.1) was verified by showing that the PKCε-specific binding antagonist εV$_{1-2}$ blocked all four modes of PKCε activation of mitoK$_{ATP}$, but did not block pharmacological mitoK$_{ATP}$ opening by diazoxide (34, 93). Moreover, the PKC inhibitor Gö6983, which inhibits the PKC isoforms PKCα, PKCβ, PKCγ, and PKCζ, did not block PKCε-dependent mitoK$_{ATP}$ opening, excluding a role for these isoforms (31).

PKCε requires anionic phospholipids for activity and is activated physiologically by diacylglycerol (or phorbol ester) or by a sulfydryl oxidizing agent, such as H$_2$O$_2$ (212) or NO (34). PMA or H$_2$O$_2$ opens up one of the two zinc fingers in PKCε (104, 113). In mitochondria, the phospholipid requirement is met by cardiolipin, which is abundant. ΨεRACK, PMA, H$_2$O$_2$, or NO cause conformational changes that expose the substrate domain on

PKCε, allowing for the active conformation of the enzyme (190). ΨεRACK is a PKCε-specific peptide agonist that acts by regulating intramolecular PKCε binding, and εV$_{1-2}$ is a PKCε-specific peptide antagonist that acts by preventing protein-protein interactions between PKCε and its binding protein (97, 190, 210). PKCε has been shown to be crucial for cardioprotection in a number of models (11, 58, 198).The specific activators and inhibitors of PKCε have been shown to modulate cardioprotection in both isolated cardiomyocytes as well as perfused heart studies (147).

Jaburek, et al. (93) showed in reconstituted liposomes that the PKCε agonist ΨεRACK opens, and the antagonist εV$_{1-2}$ closes, the partially in reconstituted liposomes. This, together with the finding that PKCε remains associated with mitochondria in mitoplasts (32), raises the possibility that PKCε and mitoK$_{ATP}$ are part of a functional complex. In studies performed in mitoplasts, mitochondria lacking their outer membrane, the protein phosphatase PP2A prevents mitoK$_{ATP}$-dependent swelling induced by PKCε agonists (34), and we conclude that PKCε-dependent mitoK$_{ATP}$ opening requires inner membrane phosphorylation, perhaps of mitoK$_{ATP}$ itself.

Step two - mitochondrial K^{+} uptake and its consequences

Once mitoK$_{ATP}$ is opened, the increase in K$^+$ uptake leads to several changes in the matrix. Electrophoretic K$^+$ influx is balanced by electrogenic H$^+$ efflux driven by the respiratory chain. Uncompensated, this would cause an increase of matrix pH by about 2 pH units (4). Partial compensation is provided by electroneutral uptake of substrate anions, such as phosphate. The compensation is partial because the concentration of phosphate in the cytosol is much lower than that of K$^+$, and this imbalance leads to matrix alkalinization (4, 35, 70).

Matrix alkalinization now releases the K$^+$/H$^+$ antiporter from inhibition by matrix protons (17), causing K$^+$ efflux to increase in response to increased K$^+$ uptake until a new K$^+$ steady state is achieved. The uncoupling caused by increased futile cycling of K$^+$ is about 3% of the maximum activity of the electron transport chain. This low level of uncoupling reflects the low activity of mitoK$_{ATP}$, a property that is essential for mitochondrial survival. Thus, if we add sufficient amounts of the K$^+$ ionophore valinomycin to double the electrophoretic K$^+$ influx, the MOM will rupture with loss of cytochrome c and respiratory inhibition (35). This is an important point, mitoK$_{ATP}$ catalyzes sufficiently low K$^+$ conductance that membrane integrity is not compromised by its activity.

Uptake of K$^+$ salts and osmotically obligated water leads to increased matrix volume ("ΔV" in Fig. 1.1), which is the basis of the light scattering (LS)

assay for mitoK$_{ATP}$ activity (35). LS is the only practical method to study this

process in isolated mitochondria, because mitoK$_{ATP}$-dependent K$^+$ flux is

rapid (t$_{1/2}$ ~ 30 s) and, as stated above, minimal. This technique has been

successfully employed by several laboratories to measure K$^+$ flux in

mitochondria (54, 174, 189, 192, 233).

MitoK$_{ATP}$-dependent matrix alkalinization plays an essential role in

intramitochondrial signaling. It causes a slight reduction in the rate of electron

transport and concomitant increase in ROS production at Complex I (4). As

seen below, the ROS produced by this mechanism play two important roles in

cardioprotection, through their ability to activate PKCε.

We note that each of the consequences of mitoK$_{ATP}$ opening are due

specifically to the increased K$^+$ influx. Thus, when mitoK$_{ATP}$ is inhibited, the K$^+$

ionophore valinomycin (approximately 1 pmol/mg mitochondria) duplicates the

effects of the channel in terms of K$^+$ uptake, respiration, matrix alkalinization,

volume increase, and ROS production (4, 35).

Step three - activation of PKCε by endogenous ROS

ROS activation of PKCε2 and inhibition of MPT.

The increased ROS activates a second mitochondrial PKCε, "PKCε2"

in Fig. 1.1, which inhibits the mitochondrial permeability transition ("MPT") in a

phosphorylation-dependent reaction (32). The evidence for two distinct

mitochondrial $PKC\varepsilon$, one acting on $mitoK_{ATP}$ and the other on MPT, is as follows: (1) PMA or H_2O_2 opens $mitoK_{ATP}$ and inhibits MPT. εV_{1-2} blocks both of these effects of PMA or H_2O_2, indicating that the effects are due to $PKC\varepsilon$ activation. However, glibenclamide or 5-HD blocks only $mitoK_{ATP}$ opening and has no effect on MPT inhibition. This indicates that $PKC\varepsilon 2$ can inhibit MPT directly, without the intervention of $mitoK_{ATP}$ (32). H_2O_2 and NO, but not superoxide, also activate $PKC\varepsilon 2$ and inhibit MPT (32, 34). The dichotomy between protective and damaging ROS was strikingly demonstrated in a series of experiments to assay MPT. MPT is induced in vitro and in vivo under conditions of high ROS (damaging, 100 μM H_2O_2). Interestingly, conditioning the mitochondria with a low amount of ROS (2 μM H_2O_2) 1 min prior to administering the damaging ROS will inhibit the onset of MPT (32). This same effect has been observed in the isolated perfused heart as well. Hearts have been shown to be protected from a lethal ischemic event by preconditioning with 2 μM H_2O_2 (237). Thus, the redundant modes of cardioprotective $mitoK_{ATP}$ opening described above lead to inhibition of MPT, and, therefore, to reduction of cell death after ischemia-reperfusion injury (7, 38, 45).

ROS activation of $PKC\varepsilon 1$ and feedback $mitoK_{ATP}$ opening.

The $mitoK_{ATP}$-dependent increase in ROS plays an additional role in cardioprotection. Note in Fig. 1.1 that $PKC\varepsilon 1$ is bypassed when KCOs are

10

administered to the heart; however, we have found that PKCε1 is soon

activated by mitoK$_{ATP}$-dependent ROS, leading to a persistent

phosphorylation-dependent open state of mitoK$_{ATP}$ (34). These data define a

new, positive feedback loop for mitoK$_{ATP}$ opening, whose existence, which has

been suggested by a number of authors (101, 106, 124), means that mitoK$_{ATP}$

may be either upstream or downstream of PKCε, depending on the triggering

stimulus. We suggest that feedback phosphorylation of mitoK$_{ATP}$ is the

mechanism of memory, which is seen with all PC triggers (49, 165). Thus,

cardioprotective stimuli can be washed away from the system and the

perfused heart remains protected from a major ischemic assault, thanks to

phosphorylation of mitoK$_{ATP}$. We infer, but have not demonstrated, that

mitoK$_{ATP}$ opening is eventually reversed by an endogenous phosphatase

("PP2A" in Fig. 1.1) within the intermembrane space. For example, PP2A has

been found in mitochondria where it is activated by proapoptotic factors (111).

Support for the intramitochondrial signaling model

The model in Fig. 1.1 helps to support and extend results of previous

studies. Jiang *et al* (96) observed PKC and 5-HD regulation of the human

cardiac mitoK$_{ATP}$ in lipid bilayers. Garg and Hu (61) showed that PKCε

modulates mitoK$_{ATP}$ activity in cardiomyocytes and COS-7 cells. Penna *et al*

(177) demonstrated that protection by postconditioning protection involves a redox mechanism and persistent activation of $mitoK_{ATP}$ and PKC. Facundo et $al.$ (54) showed that H_2O_2 induces $mitoK_{ATP}$ activity in isolated mitochondria, but did not identify participation of PKCε. Zhang et $al.$ (244) found that superoxide anion activated $mitoK_{ATP}$ in planar bilayers, and we showed that this effect is mediated, not by superoxide, but by H_2O_2 acting indirectly via PKCε1 (34). Sasaki, et al. (197) suggested that NO may open $mitoK_{ATP}$ directly; however $mitoK_{ATP}$ opening by NO is blocked by $εV_{1-2}$ (34), showing that NO opens $mitoK_{ATP}$ indirectly through PKCε1. Several authors have shown that exogenous and endogenous NO are cardioprotective and have attributed this effect to MPT inhibition (24, 99, 109, 227). Brookes, et al. (24) showed that NO inhibited MPT and cytochrome c release in isolated liver mitochondria. We showed that this effect is independent of $mitoK_{ATP}$ activity and occurs via activation of PKCε2 (34). Korge, et al. (112) found that diazoxide prevented MPT opening and cytochrome c loss, and that both effects were mimicked by the PKC activator PMA and blocked by 5-HD. Kim, et al. (110) found that a cytosolic extract, together with cGMP and ATP, blocked MPT in isolated mitochondria, an effect that was blocked by PKG inhibition. Forbes, et al (56) and Pain, et al (165) found that N-acetylcysteine or MPG reversed the protective effect of diazoxide in perfused hearts. Our data suggests that blockade of protection occurred because $mitoK_{ATP}$-

dependent ROS was scavenged and unavailable to activate PKCε2 and inhibit MPT. Lebuffe, et al (124) found that PMA-induced protection was blocked by 5-HD and that this block was reversed by coadministration of H_2O_2 and NO. This is also consistent with the model of Fig. 1.1 in that H_2O_2 and NO can bypass the blocked mitoK$_{ATP}$ and act directly on PKCε2, thereby inhibiting MPT and protecting the heart.

1.3 Study compounds: Bradykinin and Ouabain

This study examines the cardioprotective profiles of two compounds, ouabain and bradykinin. The rational behind the selection of these two agents is that they activate distinct cardioprotective pathways that converge on mitoK$_{ATP}$-opening. The pharmacological differences between these compounds as well as their cardioprotective profile will be discussed.

Figure 1.2

Bradykinin

Ouabain

Arg - Pro - Pro - Gly - Phe - Ser - Pro - Phe - Arg
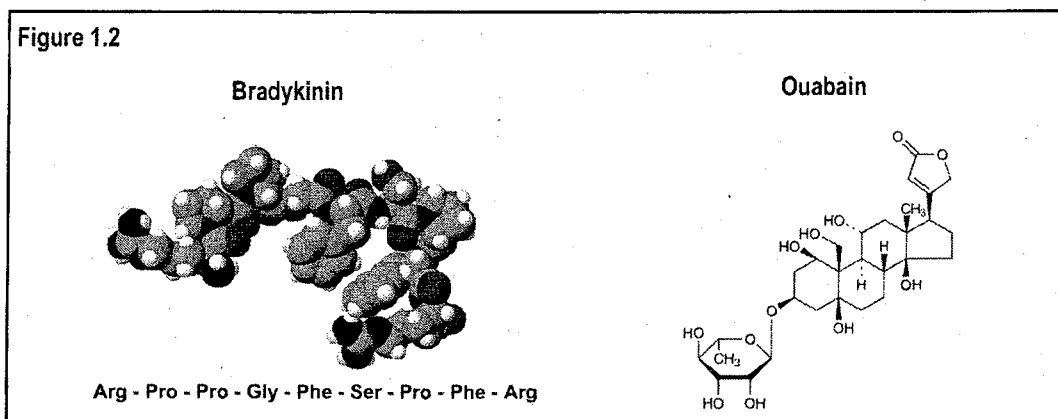
Figure 1.2 **Study compounds: Bradykinin and Ouabain.** A pictorial representation of the two drugs used in this study. Bradykinin, a 9-amino acid peptide, and ouabain a steroidal compound.

Bradykinin

Bradykinin is one of a number of short biologically active peptides called kinins. Since its discovery in 1949, many physiological and pathological manifestations of bradykinin have been investigated (100, 176) In the

cardiovascular system, bradykinin is a classic vasodilator mediated by the release of nitric oxide and prostacylin (176). Interestingly, several actions of bradykinin in the heart are independent of its action as vasodilatory peptide.

The precursor to bradykinin is circulating kininogen released from the liver. Bradykinin is produced from the proteolytic cleavage of kininogen by kallikrein, a serine protease (25, 176). In plasma, activation of kallikrein is a feature of the intrinsic clotting cascade, the first step of which is the activation of factor XII (Hageman factor). This is by far the more complex pathway and not presumed to be the pathway in most tissues. Vascular endothelial cells are the primary source of bradykinin in the heart. In this case, enzymatic cleavage of pre-kallikrein generates kallikrein at the endothelial cell surface, which then cleaves kinongens to produce bradykinin (176).

Bradykinin binds to two cell surface GPCRs in cardiomyocytes, the constitutively expressed B2 and the stress induced B1 (76). The B2 receptor is of the greatest interest here as it is known to mediate the effects of cardioprotection (79, 114, 161, 238, 239). Bradykinin, administered at a dose below that which induces coronary vasodilation, instigates a cellular signaling pathway that has been well described in the literature (160). Interaction of bradykinin with its receptor causes activation of phosphatidylinositol 3-kinase (PI3K), which phosphorylates membrane phospholipids to yield phosphatidylinositol trisphosphate, which then activates phospholipid

dependent kinases (PDK), which in turn causes phosphorylation and activation of Akt. Akt phosphorylates endothelial nitric oxide synthase (eNOS), causing it to increase generation of NO. NO activates soluble guanylyl cyclase (GC), causing it to synthesize cGMP which then activates protein kinase G (PKG). PKG acts on the mitochondrial outer membrane (MOM), causing opening of inner membrane mitoK$_{ATP}$ channels (31) and inhibition of MPT (32). As in all signaling pathways, there are multiple enzymes interacting in complex ways to mediate the end effect. In chapter 4 of this text, I investigate the hypothesis that this signaling complexity and specificity is attained by means of compartmentalization of bradykinin pathway components.

Ouabain

Cardiac glycosides, such as digitalis and ouabain, have been used in the treatment of congestive heart failure for at least 200 years (125). Ouabain, a water-soluble cardiotonic steroid derived from the *Ouabaio* tree, acts as a specific inhibitor of the N$^+$,K$^+$-ATPase in the plasma membrane. Its binding to and inhibition of the N$^+$,K$^+$-ATPase generates a condition of increased contractility in the heart referred to as positive inotropy. It is suggested that the positive inotropic response is due to the increased intracellular Na$^+$ concentrations that occur when the N$^+$,K$^+$-ATPase is inhibited. The Na$^+$ increase activates the Na$^+$/Ca^{2+} exchanger leading to increased intracellular Ca^{2+} (204), and Ca^{2+} is integral to the contractile response of muscle tissue.

Since its discovery in 1957, the N^+,K^+-ATPase has been well described as the "sodium pump" responsible for the formation and maintenance of the plasma membrane ionic gradient and membrane potential (213). Also in the ensuing decades it has become clear that the N^+,K^+-ATPase performs functions that are distinct from its role as an ion pump. For example, it has been known for some time that the N^+,K^+-ATPase is capable of modulating its own gene expression and the expression of genes involved in cell growth (150, 158), suggesting a signaling capacity of the enzyme. Interestingly, the same nontoxic concentrations of ouabain that induce a positive inotropic response have also been linked to nonproliferative cell growth (hypertrophy) in the heart (234). This suggests an inducible change in gene expression and an interesting model for examining heart failure. The work of Xie, Askari, and colleagues has contributed much to this field. They have found that the instigation of hypertrophy is through signal transduction pathways that originate at the N^+,K^+-ATPase and induce a number of early response proto-oncogenes, activate transcription factors activator protein-1 (AP-1) and NF-κB, and induce or repress the transcription of several cardiac marker genes known to be involved in the hypertrophic response (144, 235). Ouabain, when used to precondition the heart, has been shown to initiate the formation of a signaling module between N^+,K^+-ATPase, Src, and PKCε that mediates the cardioprotective effect. It is within the capacity as a signal transducing

receptor that the N^+,K^+-ATPase and its ligand ouabain will be discussed here.

In Chapter 3 of this text, ouabain's cardioprotective profile is examined in the isolated heart and skinned cardiac fiber models. Preconditioning with ouabain was found to reduce infarction, protect heart function, and preserve adenine nucleotide compartmentation in mitochondria. We compared ouabain cardioprotection with bradykinin and found, through the use of inhibitors, that both pathways depend on src kinase, mitoK$_{ATP}$, and ROS. We also show that the ouabain pathway does not utilize PKG, which is surprising because most known forms of cardioprotection seem to be mediated by PKG.

In Chapter 5, the ouabain mechanism of cardioprotection is further explored. This study examines the hypothesis that ouabain binding to the N^+,K^+-ATPase instigates the formation of a signaling platform that recruits the enzymes of the cascade into a signalosome that mediates opening of the mitoK$_{ATP}$ channel. It is shown that the terminal kinases upstream of mitochondria are Src and PKCϵ, and that these phosphorylate and activate p38 MAPK located in mitochondria.

1.4 Compartmentalization of Signaling Components

The vast majority of signaling accomplished by hormones and neurotransmitters in the cardiovascular system is exerted through G-protein coupled receptors (GPCRs), which are receptors with the characteristic 7-transmembrane domain morphology. Agonist stimulation causes

conformational change of the receptor and association with heterotrimeric G-proteins within the plasma membrane. This interaction causes binding of GTP to the Gα subunit, followed by disassociation of the G$\beta\gamma$ subunit, and ultimately regulation of various effectors such as enzymes or ion channels (179). Despite the redundancy of many of the enzymes in these pathways, impressive specificity is observed in GPCR signaling.

Much of the research on signaling pathways has focused on identifying the linear progression of pathway components. This approach has yielded crucial information regarding the G-proteins involved in pathways and their cognate downstream effectors. In this light, the current dogma suggests that this linear "bucket brigade" means of signal transduction gains specificity by diffusion and high-affinity protein-protein interactions. However, many GPCRs appear to elicit diverse cellular effects through coupling to the same the G-protein or by activating seemingly redundant pathways (163). The inability of this simple explanation to account for the observed complexity in signaling has prompted many investigators to propose enhanced spacial and temporal levels of control, such as membrane scaffolding and new roles for endocytosis (107, 135, 175, 203).

The hypothesis that membrane microdomains may act as signaling scaffolds is not a new one per se; the concentration of G-protein coupled GPCRs in so-called lipid rafts, subdomains enriched in cholesterol and

glycosphingolipids, is well supported in the literature, i.e. the andrenergic, angiotensin, and bradykinin receptors have all been found enriched in lipid rafts or caveolae (19, 122). Interestingly, the Na^+,K^+-ATPase is known to associate with caveolar microdomains as well (131). The membrane microdomains, caveolae, are often discussed interchangeably with lipid rafts because of their similar biochemical properties (28, 57, 170). Caveolae, however, are morphologically distinct 50-100 nm "flask-like" membrane invaginations which contain the integral membrane protein caveolin. Caveolin exists in three isoforms: Caveolin-1 and -2 are expressed in a variety of cell types including endothelial, epithelial, and fibroblasts; whereas caveolin-3 appears to be muscle-tissue specific (51, 116, 167, 200). Lipid rafts/caveolae are often described biochemically by their well defined buoyancy in density gradients and resistance to nonionic detergents like Triton-X 100 (3, 206). Caveolae have been shown to be involved in endocytic events on a broad scale. They have been implicated in the internalization of macromolecules such as albumin, and have been suggested to modulate receptor desensitization in a complimentary pathway to clathrin-coated pits (41, 171, 194).

The interesting biochemical properties of caveolae as well as their ability to sequester and regulate signaling molecules has brought them to the forefront of many signaling hypotheses. Caveolins have been shown to

intimately regulate signaling pathway components, in particular those molecules with lipid-modified groups such as heterotrimeric G-proteins, PI3-kinase, and eNOS (55, 128, 209). The work described in the following chapters will explore the hypothesis that caveolar "signalosomes" provide a means of scaffolding and delivery of the message of ouabain- or bradykinin-induced cardioprotection to mitochondria.

1.5 Research focus and synopsis

In this study I present a hypothesis for signal transduction in a cardiac model. Specifically, it is proposed that hearts treated with the cardioprotective agents ouabain or bradykinin are protected from the damage of a heart attack because of the formation of a signalosome that serves to scaffold the signaling enzymes into a platform that modulates the opening $mitoK_{ATP}$. Figure 1.3 is a model based on the hypotheses discussed in the following pages.

This work begins with a description and analysis of the physiological properties of the $mitoK_{ATP}$ channel in heart. A description and comparison of the cardioprotective profiles of the two study compounds, ouabain and bradykinin, follows. The remaining chapters explore the signalosome hypothesis in detail.

Figure 1.3 Signalosome hypothesis. Upon binding to their receptors, bradykinin and ouabain elicit the assembly of signalosomes that phosphorylate thier receptors, R1 and R2, on the mitochondrial outer membrane (MOM). Each signalosome contains its respective receptor and a full complement of enzymes for their respective signaling pathway. The terminal kinase of the bradykinin signalosome is PKG, which phosphorylates R1 at a Ser/Thr residue. The terminal kinases of the ouabain signalosome are Src and PKCε, which act in parallel to phosphorylate R2 at a Tyr and Ser/Thr residue, respectively. Following phosphorylation of the outer membrane, the mitochondrial PKCε (PKCε1) is activated by an unknown mechanism. Activation of PKCε1 phosphorylates mitoK$_{ATP}$ and causes it to open, with consequent increase in production of protective H_2O_2 (4). The H_2O_2 then activates PKCε2, which leads to reduction in necrosis through inhibition of the mitochondrial permeability transition (MPT) (32).

Bradykinin signalosome   **Ouabain signalosome**

BK2 receptor   Na,K-ATPase
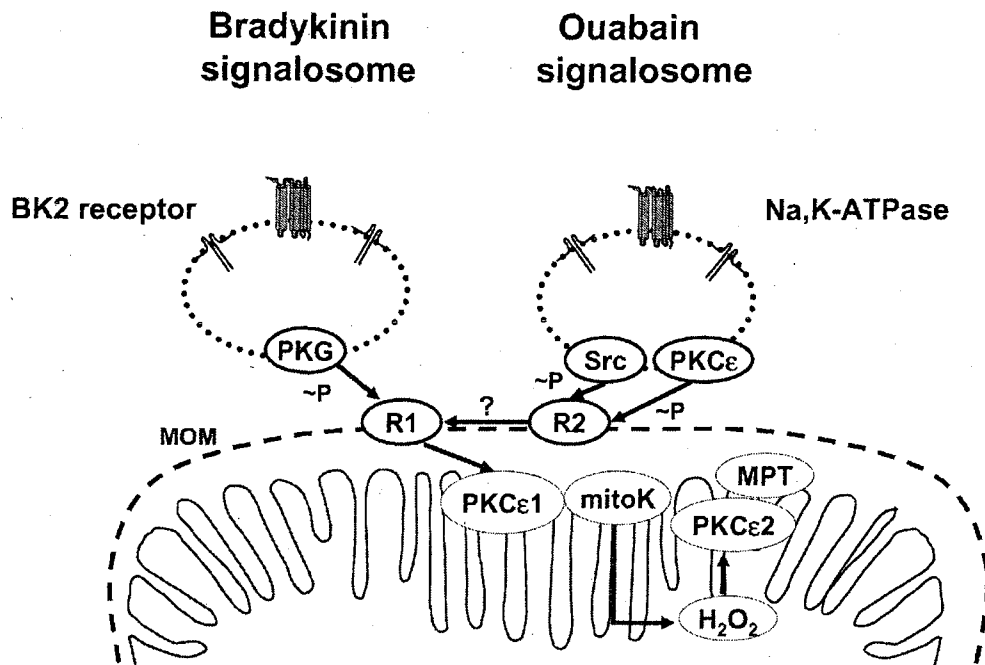
2. The Direct Physiological Effects of MitoK$_{ATP}$ Opening on Heart Mitochondria[1]

2.1 Summary

As much of the work presented in the following chapters will address the physiological roles of the mitochondrial ATP-sensitive K$^+$ channel (mitoK$_{ATP}$), this chapter will provide a description of the direct physiological effects of channel opening in mitochondria. MitoK$_{ATP}$ has been assigned multiple roles in cell physiology and in cardioprotection. Each of these roles must arise from basic consequences of mitoK$_{ATP}$ opening that should be observable at the level of the mitochondrion. MitoK$_{ATP}$ opening has been proposed to have three direct effects on mitochondrial physiology — an increase in steady-state matrix volume, respiratory stimulation (uncoupling), and matrix alkalinization. Here, we examine the evidence for these hypotheses through experiments on

---

isolated rat heart mitochondria. Using perturbation techniques, we show that matrix volume is the consequence of a steady-state balance between K^+ influx, caused either by mitoK$_{ATP}$ opening or valinomycin, and K^+ efflux caused by the mitochondrial K^+/H^+ antiporter. We show that increasing K^+ influx with valinomycin uncouples respiration like a classical uncoupler with the important difference that uncoupling via K^+ cycling soon causes rupture of the outer mitochondrial membrane and release of cytochrome *c*. By loading the fluorescence probe PBFI into the matrix, we show directly that K^+ influx is increased by diazoxide and inhibited by ATP and 5HD. By loading the fluorescence probe BCECF into the matrix, we show directly that increasing K^+ influx with either valinomycin or diazoxide causes matrix alkalinization. Finally, by comparing the effects of mitoK$_{ATP}$ openers and blockers with those of valinomycin, we show that four independent assays of mitoK$_{ATP}$ activity yield quantitatively identical results for mitoK$_{ATP}$-mediated K^+ transport. These results provide decisive support for the hypothesis that mitochondria contain an ATP-sensitive K^+ channel and establish the physiological consequences of mitoK$_{ATP}$ opening for mitochondria.

2.2 Introduction

The mitochondrial ATP-sensitive K^+ channel (mitoK$_{ATP}$) is a receptor for K$_{ATP}$ channel openers (72) and blockers (94). Their identification and subsequent use in the perfused heart model (71) provided strong evidence for the hypothesis that mitoK$_{ATP}$ opening protects the perfused heart against ischemia-reperfusion injury. Thus, the mitoK$_{ATP}$-selective openers, diazoxide and BMS191095, were found to be cardioprotective (71, 81), and the mitoK$_{ATP}$-selective blocker, 5-hydroxydecanoate (5HD), was found to block protection by both ischemic preconditioning (8, 80) and K$_{ATP}$ channel openers (71). MitoK$_{ATP}$ has been proposed to play multiple roles in cardioprotection (69, 159), and the mechanisms underlying these roles must arise from one of the direct effects of mitoK$_{ATP}$ opening on mitochondrial physiology. We have proposed three effects of increasing K^+ influx in normoxic mitochondria — matrix swelling, mild uncoupling, and matrix alkalinization (70). Important aspects of cardioprotection have been attributed to each of these effects.

Matrix swelling is a simple osmotic consequence of net uptake of K^+ and phosphate into the matrix. The K^+/H^+ antiporter is designed to balance K^+ uptake and thereby provide volume homeostasis (70). We have proposed that the K^+/H^+ antiporter can only be activated by increased volume itself, so it follows that increasing K^+ influx should cause volume to move to a higher steady-state value with greater underlying K^+ cycling, which, in turn, will lead to

increased energy dissipation (uncoupling). The concept that uncoupling through K^+ cycling is necessarily associated with matrix swelling has not previously been explored.

It has been known for some time that scavengers of reactive oxygen species (ROS) block cardioprotection (9, 30, 165, 221), leading Downey and coworkers to propose that mitoK_{ATP} opening is a trigger of cardioprotection (165) via mitoK_{ATP}-dependent ROS signaling. Our finding that mitoK_{ATP} opening leads to a moderate increase in mitochondrial production of reactive oxygen species (ROS) in cardiomyocytes (64, 217) has been confirmed in vascular smooth muscle cells (117) and perfused hearts (56, 155). Thus, mitoK_{ATP} opening causes an increase in mitochondrial ROS, which serve as second messengers to activate kinases within the cardioprotective signaling pathway (43). We have hypothesized that the increased ROS production is caused by matrix alkalinization secondary to increased K^+ influx (70); however matrix alkalinization secondary to mitoK_{ATP} opening has not yet been demonstrated.

We have investigated the physiological consequences of increasing the K^+ conductance of the inner membrane in isolated rat heart mitochondria, with the following results: [a] Steady-state perturbation experiments show that changes in K^+ conductance cause mitochondrial volume to move between true steady states in which total K^+ influx equals total K^+ efflux via the K^+/H^+

antiporter. [b] The increased K^+ cycling caused by mitoK$_{ATP}$ opening leads to very limited uncoupling that is associated with matrix swelling. We have found a very narrow margin of safety between K^+ uptake due to mitoK$_{ATP}$ opening and K^+ uptake that causes cytochrome c loss due to matrix swelling and outer membrane rupture. [c] K^+ influx caused by mitoK$_{ATP}$ opening is demonstrated directly, as measured with the matrix-loaded fluorescence probe, PBFI. [d] MitoK$_{ATP}$ opening leads to matrix alkalinization, as measured with the matrix-loaded fluorescence probe, BCECF. [e] The effects of ATP, diazoxide, and 5HD on K^+ flux in heart mitochondria are shown to be qualitatively and quantitatively the same when measured by four independent techniques — light scattering, respiration, K^+ flux, and H^+ flux. These results lay the groundwork for studies of how the direct physiological consequences of mitoK$_{ATP}$ opening are translated into cardioprotection.

2.3 Methods

Mitochondrial isolation

Two male Sprague-Dawley rats (220 - 240 g) were anesthetized with CO_2 and immediately decapitated. The hearts were removed and washed in ice-cold Buffer A (250 mM sucrose, 10 mM HEPES pH 7.2, and 5 mM K-EGTA). The tissue was finely minced in the presence of 1 mg/ml protease (type XXIV Sigma), and the suspension was diluted 3-fold with Buffer A supplemented with 0.5% fatty acid-free BSA. We observed that $mitoK_{ATP}$ activity depends critically on the time between decapitation and completion of homogenization. This period was kept as brief as possible and was completed within 2 min. The suspension was homogenized with a motorized teflon pestle and centrifuged for 3 min at 1500 g. The supernatant was centrifuged for 5 min at 9000 g, and the resulting pellets were resuspended in Buffer A lacking BSA and centrifuged for 3 min at 2300 g. This supernatant was centrifuged for 5 min at 9000 g. For respiration measurements and at least one of each light scattering experiment, mitochondria were further purified in a self-generating 28% Percoll gradient. The compact, hemoglobin-free mitochondrial pellet was resuspended at 35 - 40 mg protein/ml and kept on ice. Mitochondrial protein concentration was estimated using the Biuret reaction (75). This procedure is in accordance with the Guiding Principles in the Care and Use of Animals and was approved by the IACUC at Portland

State University.

Measurements of mitochondrial matrix volume and oxygen consumption

Changes in mitochondrial matrix volume, which accompany net salt transport into mitochondria, were followed using a quantitative light scattering technique. This technique is based on the observation that the inverse absorbance of the mitochondrial suspension (1/A), when corrected for the extrapolated value at infinite protein concentration ($1/A_\infty$), is linearly related to matrix volume within well-defined regions (16, 67). Light scattering changes of 0.1 mg/ml mitochondrial suspensions were followed at 520 nm and 25 °C and are reported as β, which is inverse absorbance normalized for protein concentration, P_s:

$$\beta = P_s \, (1/A - 1/A_\infty)$$

Mitochondria were suspended in a buffered salt medium containing K^+, tetraethylammonium (TEA^+), Na^+, or Li^+ salts of Cl^- (120 mM), HEPES (10 mM), EGTA (0.1 mM) , succinate (10 mM) and phosphate (P_i) (5 mM), pH 7.2. The osmolality of these media ranged between 275 to 280 mOsm. For assays of nonelectrolyte transport, mitochondria were suspended in the same medium, except that 264 mM erythritol or malonamide was substituted for the Cl^- salt. All media also contained 0.5 mM $MgCl_2$, 5 μM rotenone (to inhibit

reverse electron transfer from Complex II to Complex I) and 0.67 μM

oligomycin (to inhibit ATP synthesis by the F_oF_1-ATP synthase and the

consequent drecrease in membrane potential).

In these experiments, diazoxide (in DMSO) was always added to the

suspension 2 s after mitochondria to ensure even distribution of this

hydrophobic compound. It should also be noted that diazoxide is ineffective

unless ATP is already present, because the opener cannot open an already

open channel. Similarly, 5HD is ineffective unless ATP and an opener

diazoxide are also present, because 5HD does not itself block the channel, but

rather prevents the opening effect of diazoxide (94). The same observations

hold for cromakalim and glibenclamide. Light scattering traces were initiated

by addition of the mitochondrial suspension; the first 5-7 seconds of each

trace, containing the transient from the mitochondrial addition, were omitted for

clarity.

Oxygen consumption was measured with a Clark type electrode (Yellow

Springs Instruments) in a temperature-controlled chamber, using the same

buffered KCl medium described above and in the presence of ATP (200 μM).

Oxygen concentration dissolved in our media was taken to be 480 ng atom O/

ml at 25 °C.

Measurement of K^+ influx into PBFI-loaded mitochondria.

The final mitochondrial pellet was resuspended to 20 mg/ml in Buffer A supplemented with 10 mM pyruvate and 10 mM malate. This suspension was incubated with 20 μM Potassium Binding Fluorescent Indicator acetoxymethyl ester (PBFI-AM), under stirring for 10 minutes at 25 °C. PBFI-AM was dissolved in DMSO and mixed in a 2:1 ratio (v/v) with the non-ionic surfactant pluronic F-127 in prior to addition to the mitochondrial suspension. The mitochondrial suspension was then diluted to 5 - 7 mg/ml with TEA$^+$ medium containing 175 mM sucrose, 50 mM TEA-Cl, 10 mM HEPES, 5 mM pyruvate, 5 mM malate, 5 mM succinate, 5 mM P_i, 0.1 mM EGTA, and 0.5 mM $MgCl_2$, and incubated for 2 minutes under stirring at 25°C. This incubation was designed to substitute matrix K$^+$ with TEA$^+$ in order to bring matrix [K$^+$] into the sensitivity range of PBFI — under our experimental conditions, PBFI exhibited an apparent K_d for K$^+$ of about 8 mM, determined as in ref. (95). The brief period of TEA$^+$-loading had no effect on respiration or respiratory control. The 2 ml suspension was then diluted with ice cold Buffer A to 35 ml and centrifuged twice at 10,000 x g for 3 minutes. The resulting pellet was resuspended in Buffer A at 30 mg/ml and kept on ice. For the assays, aliquots of this suspension (0.25 mg/ml) were transferred to 2 ml of the same potassium medium used for the light scattering assay, at 25°C. PBFI fluorescence, which increases with increasing K$^+$ concentration (95) was measured with an SLM/Aminco 8000C fluorescence spectrophotometer using

an excitation ratio technique (λex = 340/380, λem = 500) in which the signal at 340 nm correspond to the maximal sensitivity of the probe to K^+ and the signal at 380 nm corresponds to isosbestic point of the probe. Ratiometric measurements reduce variations in the measured fluorescence intensity that may arise from competing factors, indicator concentration, excitation path length, excitation intensity and detection efficiency (23). A calibration was carried out on each preparation. The fluorescence ratios, R, were found to be hyperbolically dependent on potassium concentrations, and were converted to potassium concentration using the equation $[K^+] = K_d *(R - R_0) / (R_{max} - R)$, where K_d is the dissociation constant (~ 8 Mm) experimentally determined, as previously described (95). R_0 is the fluorescence signal after lysis, and R_{max} is the maximum signal obtained after probe saturation with KCl .

Measurement of pH changes in BCECF-loaded mitochondria.

Matrix pH was measured in isolated rat heart mitochondria as described by Jung *et al* (102). Briefly, isolated rat heart mitochondria were incubated with 8 μM 2',7' -bis-(2-carboxyethyl)-5-(and-6)-carboxyfluorescein, acetoxymethyl ester (BCECF, AM) in Buffer A for 10 minutes at room temperature with stirring and oxygen access. The suspension was then diluted 10-fold with Buffer A and centrifuged at 9000 *x g* for 5 min to remove excess probe. Mitochondria were then resuspended in Buffer A and stored on ice.

Assays were carried with 0.25 mg/ml mitochondrial protein at 30 °C. BCECF

fluorescence, which increases with increasing pH, was measured with an

SLM/Aminco 8000C fluorescence spectrophotometer (λex = 509, λem = 535).

Statistical analysis

Data are presented as mean ± standard deviation (SD) of the mean.

Data were analyzed using unpaired Student's t-test of the means using

Microcal Origin software (Northampton, MA, USA). A value of $p < 0.05$ was

considered statistically significant.

Chemicals

PBFI-AM and BCECF-AM were obtained from Molecular Probes, Inc

(Eugene, OR, USA). Pluronic F-127 was obtained from Calbiochem (San

Diego, CA, USA). All other chemicals used were from Sigma Chemical Co.

(St. Louis, MO, USA).

2.4 Results

The effects of ATP, diazoxide, and 5HD on matrix swelling are potassium-specific.

The diagram in Fig. 2.1 describes the underlying processes by which respiring mitochondria take up K^+, phosphate, and osmotically obligated water when suspended in potassium medium . K^+ influx is driven by the proton pumps of the electron transport chain and occurs via the parallel pathways of diffusion and mitoK$_{ATP}$. K^+ efflux is driven by the pH gradient and mediated by the K^+/H^+ antiporter, which is regulated in such a way that its activity increases with matrix volume. Therefore, K^+ influx proceeds with matrix swelling until it is matched by increased K^+ efflux and a new steady-state volume is achieved (70).

Figure 2.1. The K⁺ cycle in heart mitochondria. In mitochondria respiring *in vivo* or *in vitro,* electrophoretic K^+ or TEA^+ influx is always balanced by electrogenic H^+ ejection by the electron transport chain ("ETS"). During steady-state K^+ cycling, K^+ influx via diffusion ("leak") and $mitoK_{ATP}$ ("K_{ATP}") is also balanced by K^+ efflux on the K^+/H^+ antiporter ("K/H"). The phosphate transporter ("P_i") is highly active, such that P_i is in near-equilibrium with the pH gradient (ΔpH). Thus, there is no net P_i movement associated with steady-state K^+ cycling, because there is no change in ΔpH. Increasing K^+ influx, either by opening $mitoK_{ATP}$ or by adding valinomycin, results in an imbalance between K^+ influx and efflux, causing matrix pH to increase. This leads to net uptake of phosphoric acid via the phosphate transporter. Net salt uptake is associated with osmotically obligated water, resulting in matrix swelling. Matrix alkalinization releases the K^+/H^+ antiporter from allosteric inhibition by protons (17), and its activity increases to match the new level of K^+ influx. The system then reaches a new steady state at a higher matrix volume.

Fig. 2.1

35
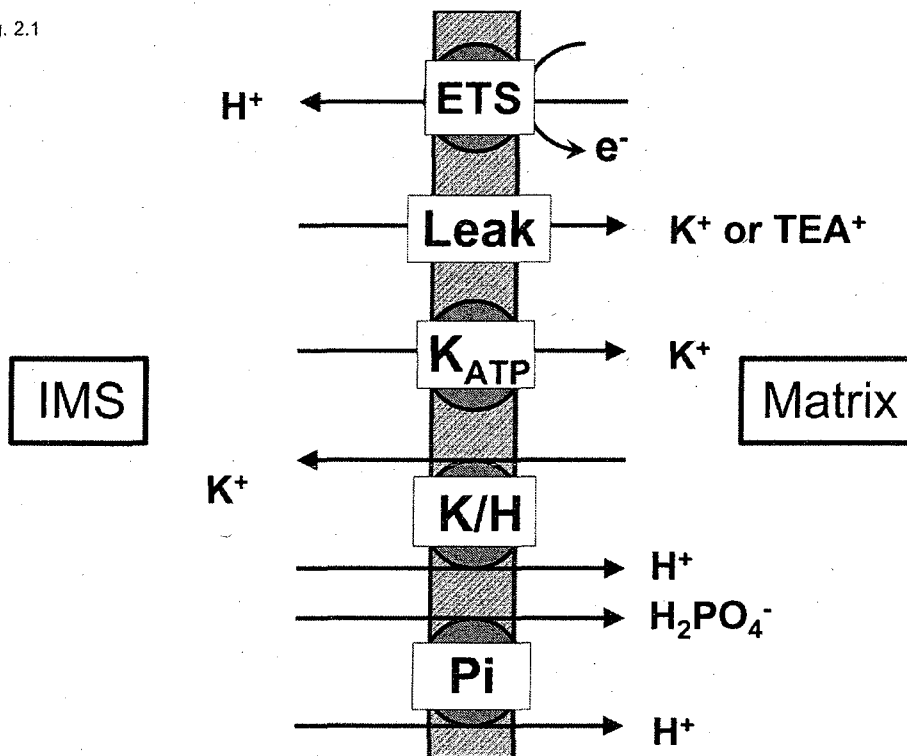
Matrix swelling is proportional to net salt influx and leads to increased

light scattering (16, 67). Fig. 2.2A contains typical light scattering traces from

heart mitochondria respiring in K^+ medium. In the absence of ATP ("none"),

the matrix swelled to a higher steady-state volume. Addition of 200 μM ATP

resulted in a lower swelling rate and consequently a lower steady-state volume

("ATP"). ATP inhibition was reversed by 30 μM diazoxide ("ATP + DZX"), and

the diazoxide-opening was blocked by 300 μM 5HD ("ATP + DZX + 5HD").

The results obtained with the combination diazoxide + 5HD (Fig. 2A) were

reproduced by the combinations diazoxide + glibenclamide (10 μM),

cromakalim (50 μM) + 5HD or cromakalim + glibenclamide (5 independent

experiments for each combination, data not shown).

Fig. 2.2 B contains typical light scattering traces from heart

mitochondria respiring in potassium-free TEA^+ medium. Electrophoretic influx

of TEA^+ occurs solely by diffusion. Because there is no efflux pathway for this

cation, mitochondria take up TEA^+, phosphate, and water until K^+ efflux via the

K^+/H^+ antiporter equals TEA^+ influx, at which point a steady-state volume is

achieved (at 60 - 90 s, Fig. 2.2 B). This steady state is short-lived, because

mitochondria soon lose all their K^+ via K^+/H^+ exchange, a phenomenon first

described in 1979 (66). After matrix potassium is exhausted (at about 120s,

Fig. 2.2 B), uptake of TEA^+ can no longer be balanced by K^+ extrusion, and

matrix swelling proceeds at a rate proportional to the uncompensated TEA^+

36

influx. Note that light scattering in TEA$^+$ medium is unaffected by ATP, diazoxide, or 5HD (Fig. 2.2 B) and is also unaffected by cromakalim or glibenclamide (not shown). We have also found in experiments not shown that light scattering in Li$^+$ or Na$^+$ media is similarly unaffected by these agents.

Fig. 2.2 C contains light scattering traces from mitochondria suspended in the same K$^+$ medium as was used in Fig. 2.2 A. These data show that inhibition of K$^+$ influx by ATP or tetraphenylphosphonium cation (TPP$^+$) is reversed by the presence of 0.9 pmol valinomycin per mg of protein, and that the matrix swelling induced by this concentration of valinomycin is qualitatively and quantitatively similar to that induced by diazoxide in Fig. 2.2 A. Moreover, 5HD and glibenclamide (not shown) did not inhibit swelling caused by valinomycin, confirming the mitoK$_{ATP}$-specific effects of 5HD. Glibenclamide was also not able to inhibit swelling caused by valinomycin (not shown).

To further investigate whether ATP has artifactual effects on the light scattering signal, we examined the effects of ATP on nonelectrolyte transport in respiring mitochondria, with typical results contained in Fig. 2.3. Heart mitochondria rapidly take up erythritol and malonamide with osmotically obligated water, and malonamide is transported about 5 times faster than erythritol, as previously shown in liver mitochondria (67). Note that

Figure 2.2. K⁺-selective effects of ATP, diazoxide, and 5HD on matrix swelling. Light scattering traces (β) of rat heart mitochondria respiring on succinate. (*A*) Mitochodria were respiring in K⁺ medium. The traces labeled "none" and "ATP + DZX" are nearly superimposable, as are the traces labeled "ATP" and "ATP + DZX + 5HD". (*B*) Mitochodria were respiring in TEA⁺ medium. All four traces are superimposable. (*C*) Mitochodria were respiring in K⁺ medium and ATP was present in all traces. The traces "Val", "Val + TPP⁺" and "Val + 5HD" are nearly superimposable, and the traces "none", "TPP⁺" and "DZX + 5HD" are superimposable. Mitochondria were suspended at 0.1 mg/ml and assayed as described in "Methods". ATP (200 μM), TPP⁺ (0.5 μM) and 5HD (300 μM) were present at the beginning of each corresponding trace. Diazoxide (30 μM) and valinomycin (0.9 pmol per mg of protein) were added 2 seconds after the addition of mitochondria. These traces are representative of at least 8 independent experiments.
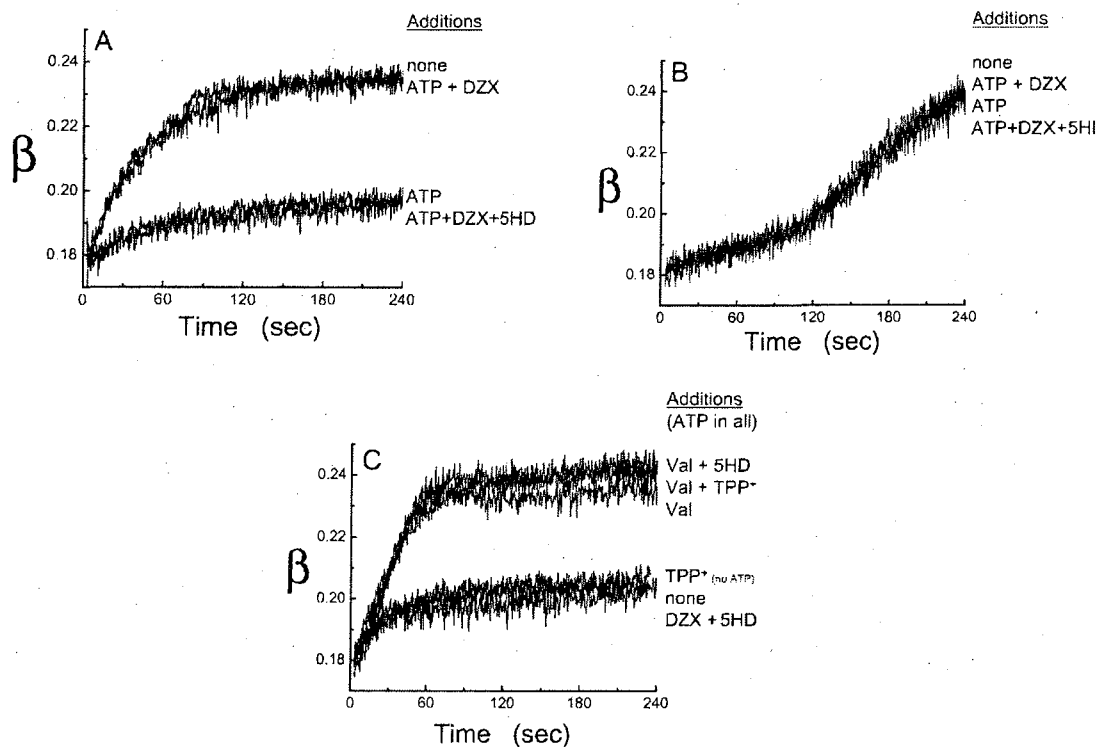
Figure 2.3. ATP has no effect on nonelectrolyte transport in heart mitochondria. Light scattering traces (β) of rat heart mitochondria respiring on succinate in malonamide or erythritol medium in the presence or absence of 200 μM ATP. Mitochondria were suspended at 0.1 mg/ml and assayed as described in "Methods". In these experiments, mitochondria swell due to uptake of permeant nonelectrolyte and osmotically obligated water. The paired traces ("+/- ATP") for each nonelectrolyte are nearly superimposable. These traces are representative of 4 independent experiments.

Fig. 2.3.

malonamide
+/- ATP

erythritol
+/- ATP
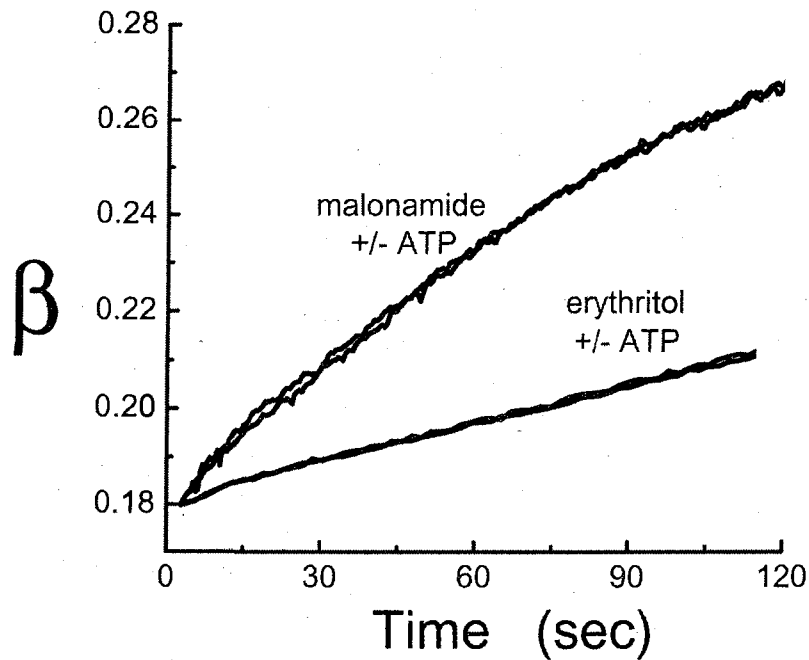
the presence of 200 μM ATP had no effect on the rate of swelling, confirming

that ATP does not introduce an artifact into the light scattering assay when

added before the mitochondria. We also observed no effect of diazoxide or 5-

HD on matrix swelling in erythritol and malonamide (data not shown).

Perturbation of steady-state volume by modifying K$^+$ flux

It was stated above that matrix volume approaches a steady state that

reflects underlying K$^+$ cycling and that the K$^+$/H$^+$ antiporter is volume-

dependent. We tested these assertions through steady-state perturbation

experiments. First, the putative steady state was perturbed with quinine, which

inhibits the K$^+$/H$^+$ antiporter (68, 153). (Quinine may have other effects on

mitochondria; however it behaves in the predicted manner as a K$^+$/H$^+$

antiporter inhibitor under all experimental conditions tested). It can be seen in

Fig. 2.4 A that addition of quinine is followed by a rapid swelling due to

uncompensated K$^+$ uptake, confirming that the observed constant volume is

the result of steady-state potassium cycling. Subtle changes in steady-state

volume can also be elicited by increasing K$^+$ influx or efflux with low

concentrations of valinomycin or nigericin, respectively (46). Typical results

from such experiments (Fig. 2.4 B) show, as expected, that valinomycin

induces matrix expansion while nigericin induces matrix contraction. When

quinine was added at the steady state, the resulting net flux must correspond to

40

net K^+ influx, which in turn must equal that part of the K^+/H^+ exchange removed by quinine inhibition. The results in Figs. 2.4 A and B therefore demonstrate that K^+/H^+ antiporter activity increases as matrix volume is increased.

The consequences of uncoupling via increasing activity of the K^+ cycle

The K^+ cycle (Fig. 2.1) catalyzes net proton influx, as do the classical protonophoretic uncouplers, but the two processes are not identical in all their effects. Fig. 2.5 contains data from mitochondria in which respiration was titrated with the potassium ionophore valinomycin (Fig. 2.5 A) or the protonophoretic uncoupler CCCP (Fig. 2.5 B) in the presence and absence of 10 μM cytochrome c. A typical feature of uncoupling, seen in both panels, is that respiration increases up to the V_{max} of electron transport, after which respiration is constant (at high concentrations, CCCP inhibits electron transport, as seen in the slight decline in rates at 500 nM CCCP). Note that valinomycin is expressed in units per mg of protein, whereas CCCP is expressed in molar units. The practical reason for this is that the valinomycin partition coefficient between membrane and aqueous medium is very high, so that most of the ionophore is in the mitochondria. CCCP is much less hydrophobic and most of this ionophore is in the aqueous medium.

Figure 2.4. Steady-state perturbations of mitochondrial matrix volume by valinomycin, nigericin, and quinine. Light scattering traces (β) of rat heart mitochondria respiring on succinate in K^+ medium. (*A*) The two superimposed upper traces were obtained with no additions and with diazoxide + ATP. The two superimposed lower traces were obtained with ATP and with diazoxide + ATP + 5HD. To inhibit the K^+/H^+ antiporter, quinine (500 μM) was added where indicated ("quinine"). (*B*) After a steady-state volume was achieved,1 pmol per mg of protein of nigericin (Nig) or valinomycin (Val) were added ("ionophores"). After the new steady state was achieved, quinine was added ("quinine"). Two superimposable traces for each experiment are presented. Mitochondria were suspended at 0.1 mg/ml and assayed as described in "Methods". Other conditions and concentrations of tested compounds were exactly as described for Fig. 2.2. These traces are representative of at least 4 independent experiments.
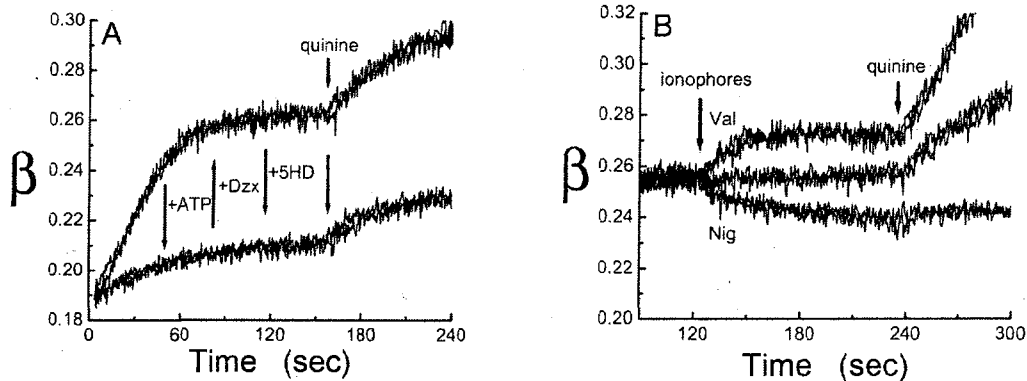
Figure 2.5. Uncoupling of respiration by K⁺ cycling causes rupture of the outer mitochondrial membrane. Oxygen consumption rates (V_{resp}) of rat heart mitochondria respiring on succinate in K⁺ medium. (*A*) Valinomycin titrations in the presence (○) or absence (☆) of cytochrome *c*. The dashed line represents the rate of diazoxide-induced oxygen consumption (in the presence (☆) or absence (★) of cytochrome *c*), being equal to the rate induced by about 1 pmol of valinomycin per mg of protein. (*B*) CCCP titration in the presence (●) or absence (◆) of cytochrome *c*. Exogenous cytochrome *c* had little effect on oxygen consumption rates induced by CCCP; thus the data points are nearly superimposable. Mitochondria were suspended at 0.25 mg/ml and assayed as described in "Methods". The data are shown as the average ± S.D of 5 independent experiments.
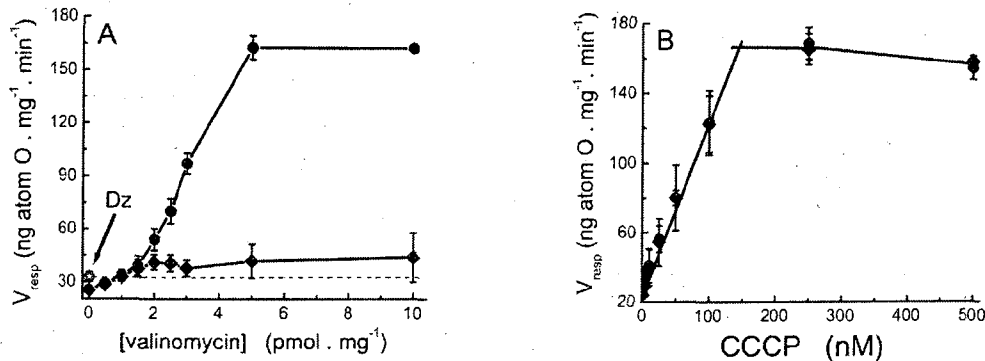
Several features of the data in Fig. 2.5 A are noteworthy. [a] The respiratory rate induced by our standard concentration of diazoxide (dashed line in Fig. 5A) is about the same as that induced by 1 pmol valinomycin per mg of protein, a result similar to that obtained with light scattering (Fig. 2.2) (115). Similar rates of oxygen consumption were observed when 50 μM cromakalim was used instead of diazoxide (n=3, data not shown). [b] The respiratory stimulation induced by diazoxide is a very small

fraction (less than 5%) of respiratory capacity, which is similar in magnitude to diffusive leak of K^+. [c] In the absence of added exogenous cytochrome c, no further acceleration of respiration occurs at valinomycin concentrations greater than 1.5 pmol/mg. Our interpretation is that the swelling consequent on increased K^+ cycling permeabilizes or ruptures the outer mitochondrial membrane with the release of endogenous cytochrome c. The inner membrane clearly remains intact. [d] The fact that exogenous cytochrome c restores the acceleration of respiration confirms that the outer membrane (OM) has become permeable to cytochrome c.

In contrast to the results with valinomycin, CCCP does not exhibit dependence on added cytochrome c (Fig. 2.5 B). CCCP does not rupture the OM at any concentration, because uncoupling by means of increased proton

cycling has no direct effect on matrix volume, and the OM maintains its integrity.

Net K⁺ uptake causes matrix alkalinization.

Net K^+ influx is balanced exactly by net electrogenic proton ejection by the electron transport chain, leading to matrix alkalinization. This will be partially compensated by electroneutral Pi uptake, which delivers protons to the matrix. However, the cytosolic concentration of potassium is much greater than those of P_i and other substrate anions that undergo electroneutral exchange across the inner mitochondrial membrane. Consequently, these anion movements cannot fully compensate the alkalinizing effect of net K^+ influx. We have hypothesized

that this normal imbalance must inevitably lead to matrix alkalinization as a consequence of net K^+ uptake via mitoK$_{ATP}$ (70).

To test this hypothesis, we measured changes in both matrix $[K^+]$ and matrix pH by loading the matrix with the K^+-selective fluorescent probe, PBFI (95), and the pH-selective fluorescent probe, BCECF (22). PBFI is insensitive to changes in matrix K^+ at normal levels of matrix $[K^+]$ (about 150 mM), because the probe (Kd ~ 8 mM) is saturated at these levels, so we first depleted K^+ by a brief incubation in TEA$^+$ salts with substrate (66), resulting in a matrix $[K^+]$ of 10 - 20 mM. This substitution had no effect on respiration rate or respiratory

control (data not shown). One of the earliest reported features of the K^+/H^+ antiporter is that it responds to changes in pH and volume, but not K^+ (63, 66). Thus, when part of matrix K^+ is replaced by TEA^+, the K^+/H^+ antiporter responds exactly as if the matrix contained all K^+. This leads to the prediction that the TEA^+ will replace K^+ and mitochondria will reach a new steady-state at a lower K^+ concentration. This is exactly what is observed, as shown in the K^+ influx data in Fig. 2.6 A. The results of experiments measuring matrix pH are reported in Fig. 2.6 B. The results obtained with diazoxide and 5HD (Fig. 2.6) were duplicated by 50 μM cromakalim and 10 μM glibenclamide, respectively (n=3, data not shown). These results show directly that K^+ channel openers increase net K^+ influx and that net uptake of K^+ by respiring mitochondria causes matrix alkalinization (70).

Four independent assays of mitoK$_{ATP}$ activity in isolated mitochondria.

Our studies show that the effects of ATP, diazoxide, cromakalim, glibenclamide, 5HD, and valinomycin on light scattering (Fig. 2.2 A and 2.2C) are qualitatively identical to their effects on K^+ influx (Fig. 2.6 A) and H^+ efflux (Fig. 2.6 B). These results also demonstrate that the effect of valinomycin on these parameters affords a means of quantitating mitoK$_{ATP}$-dependent K^+ flux.

Fig. 2.7 summarizes the results of experiments comparing diazoxide with valinomycin in the light scattering assay (Fig. 2.7 A) and the respiration assay (Fig. 2.7 B). In both assays, mitoK$_{ATP}$ activity corresponded, by

Fig. 2.6. K⁺ influx and matrix alkalinization induced by mitoK$_{ATP}$ activity.

(A) Representative traces of PBFI-detected matrix K⁺ concentration. (B) Representative traces of BCECF-detected matrix pH changes. Mitochondria were loaded with either PBFI or BCECF and assayed at 0.25 mg/ml in K⁺ medium as described in "Methods". Where indicated, ATP (200 μM) and 5HD (300 μM) were present at the beginning of each trace. Diazoxide (30 μM) and valinomycin (0.9 pmol per mg of protein) were added 2 seconds after the addition of mitochondria. Traces are representative of at least 4 independent experiments.
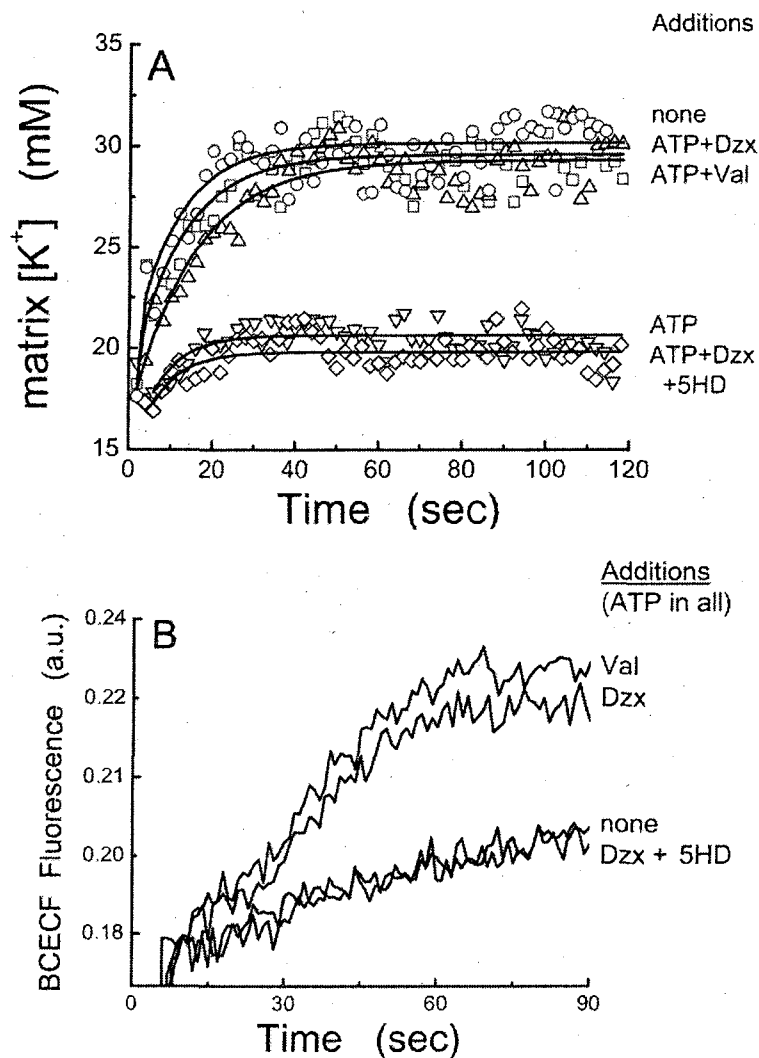
Fig. 2.7. Quantitative comparison of the light scattering and respiration assays of mitoK$_{ATP}$ activity. (A) Relative rates of matrix volume changes (LS rate) in rat heart mitochondria respiring on succinate in K$^+$ medium. Mitochondria were suspended at 0.1 mg/ml and assayed as described in "Methods". The rates in the absence and presence of ATP were set as 100 and 0%, respectively. (B) Oxygen consumption rates (V$_{resp}$) in rat heart mitochondria respiring on succinate in K$^+$ medium. Mitochondria were suspended at 0.25 mg/ml and assayed in K$^+$ medium as described in "Methods". For both experiments, ATP (200 µM), diazoxide (30 µM), valinomycin (0.5, 1 or 1.5 pmol per mg of protein) and 5HD (300 µM) were present as indicated. Error bars represent standard deviations from the average of at least three independent experiments. *p<0.05 vs control, **p<0.05 vs ATP, ***p<0.05 vs Dzx.

48
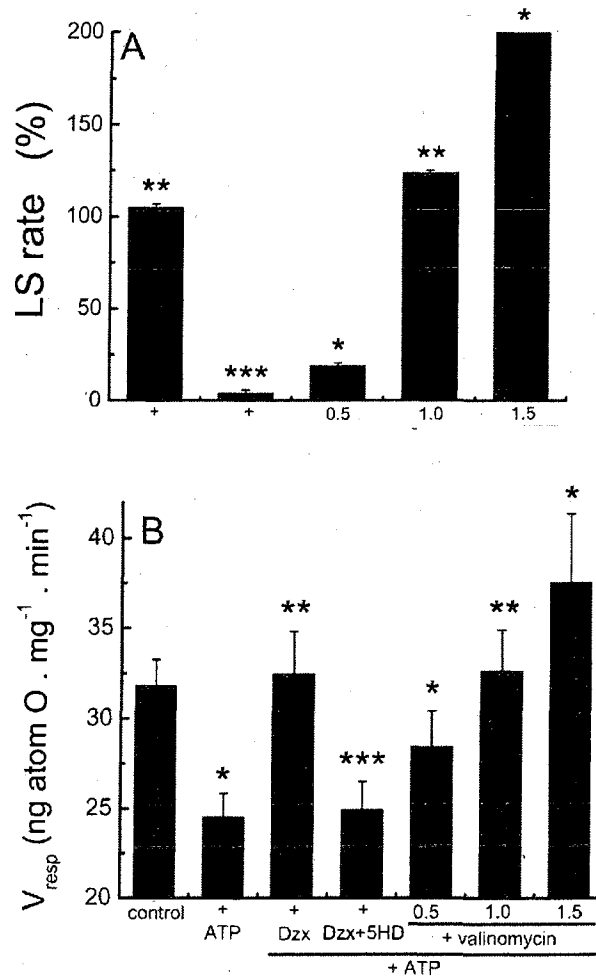
interpolation, to 1.0 ± 0.2 pmol valinomycin per mg of protein (5 independent experiments). Fig. 2.8 summarizes the results from the PBFI (Fig. 2.8 A) and BCECF (Fig. 2.8 B) experiments, together with a comparison with the effects of 1 pmol valinomycin per mg of protein. In both assays, mitoK$_{ATP}$ activity corresponded again to 1.0 ± 0.2 pmol valinomycin per mg of protein (3 independent experiments). Thus, the data contained in Figs. 2.7 and 2.8 show that four independent assays yield quantitatively identical results, establishing not only the capacity of the endogenous ATP-inhibitable and diazoxide-openable K$^+$ channel, but also the validity of each of these assays in monitoring that capacity. These experiments were also duplicated by substituting cromakalim and glibenclamide for diazoxide and 5HD (as described for Fig. 2.2 A, data not shown).

Fig. 2.8. Quantitative comparison of PBFI and BCECF assays of mitoK$_{ATP}$ activity. (A) Relative rates of PBFI-detected K$^+$ influx of rat heart mitochondria respiring on succinate in K$^+$ medium. (B) Relative rates of BCECF-detected matrix pH changes of rat heart mitochondria respiring on succinate in K$^+$ medium. Mitochondria were loaded with either PBFI or BCECF and assayed at 0.25 mg/ml in K$^+$ medium as described in "Methods". The rates in the presence of ATP were set as 100%. For both set of experiments, ATP (200 μM), diazoxide (30 μM), valinomycin (1 pmol per mg of protein) and 5HD (300 μM) were present as indicated. Error bars represent standard deviations from the average of the at least three individuals. experiment *p<0.05 vs ATP, **p<0.05 vs Dzx.

50
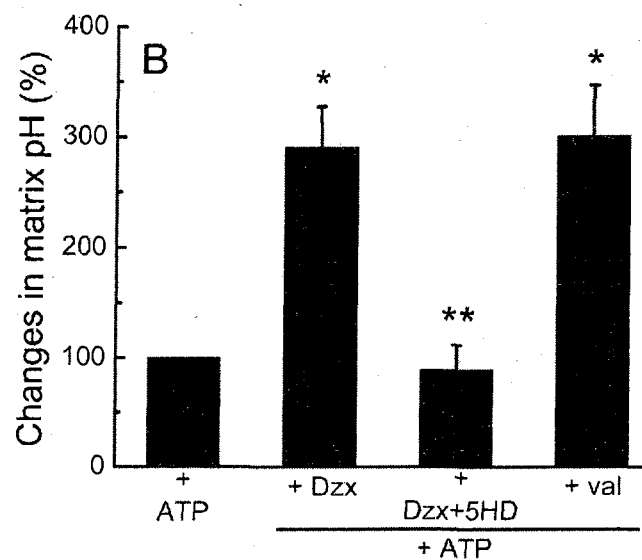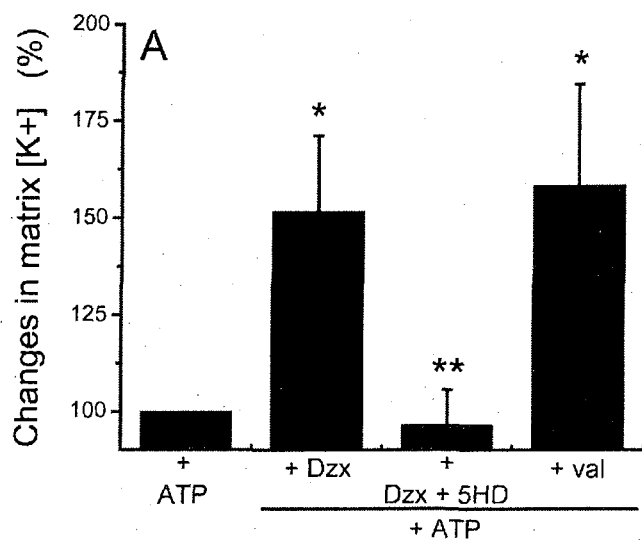
2.5 Discussion

MitoK$_{ATP}$ has been assigned multiple roles in cell physiology in general, and in cardioprotection in particular (69). These include providing efficient energy transfer between mitochondria and cellular ATPases (47), preservation of ADP from deamination during ischemia (47), prevention of Ca^{2+} overload (47, 89, 133), inhibition of the mitochondrial permeability transition (MPT) (112), prevention of apoptosis (1), and cell signaling (159, 165). Each of these roles must arise from direct effects at the level of the mitochondrion, and the motivation for these studies was to examine in detail the direct physiological effects of mitoK$_{ATP}$ opening on isolated heart mitochondria. Three such effects have been proposed — to increase matrix volume, to cause mild uncoupling, and to cause matrix alkalinization (70). Any other effect must be downstream of one or another of these three.

MitoK$_{ATP}$ maintains matrix volume during ischemia. During ischemia, the matrix will contract due to the decreased membrane potential. Matrix contraction will cause reciprocal expansion of the intermembrane space (IMS), resulting in increased outer membrane permeability to ADP and ATP, which promotes rapid hydrolysis of cellular ATP by mitochondria. MitoK$_{ATP}$ opening increases potassium conductance to compensate for the lower electrical driving force, thereby maintaining matrix volume, IMS volume, and low outer membrane permeability to ATP and ADP. It was shown that

mitoK$_{ATP}$ opening causes a large _overall_ reduction in ATP hydrolysis during simulated ischemia, an effect that preserves adenine nucleotides by delaying their degradation, thereby preserving ADP for an appropriate response to reperfusion (47, 112). We also showed that segregation of ATP and ADP by this mechanism increases the _localized_ ATP hydrolysis within the mitochondrial compartment, thereby lowering the membrane potential. Membrane depolarization, in turn, will reduce Ca^{2+} uptake and prevent Ca^{2+} overload, as suggested by Liu, et al. (133) and Korge, et al. (112). The only point of disagreement on this issue is the mechanism of the membrane depolarization. Liu, et al. (133) and Korge, et al. (112) attribute it to uncoupling. Although a significant uncoupling during ischemia cannot be excluded, we have shown that the mitoK$_{ATP}$-dependent depolarization observed in simulated ischemia is associated with _reduced_ ATP hydrolysis. This depolarization cannot be due to uncoupling, which would _increase_ ATP hydrolysis (47).

MitoK$_{ATP}$ increases matrix volume during normoxia. As described in Fig. 2.1, mitoK$_{ATP}$ opening adds a parallel inner membrane K$^+$ conductance leading to increased K$^+$ influx. K$^+$ is accompanied by P$_i$ and water, leading to matrix swelling, as shown by the light scattering traces in Fig. 2.2 A and in ref. (115). The increase in matrix volume is inhibited by ATP; ATP inhibition is reversed by K$_{ATP}$ channel openers such as diazoxide; and channel opening is

prevented by K_{ATP} channel blockers, such as 5HD. Attribution of these responses to mitoK$_{ATP}$ activity is supported by the finding that they do not occur in K$^+$-free medium (Fig. 2.2 B). Nor do they occur in K$^+$ medium when K$^+$ influx is increased with valinomycin (Fig. 2.2 C). As shown in Fig. 2.2 C, mitochondria treated with valinomycin exhibit the same response as mitochondria treated with diazoxide, except that the effects of valinomycin do not require ATP and are not inhibited by 5HD.

Based on the known behavior of the K$^+$/H$^+$ antiporter, we have asserted that the increase in matrix K$^+$ due to mitoK$_{ATP}$ opening simply shifts matrix volume to a higher steady-state value (70). The K$^+$/H$^+$ antiporter is not very susceptible to regulation by changes in its substrate concentrations, because [K$^+$] and [H$^+$] do not change very much, even with rather large amounts of net K$^+$ uptake (63). Instead, the antiporter is regulated allosterically by matrix [Mg^{2+}] (63) and [H$^+$] (17), which sense *changes* in matrix volume (70). This means that the K$^+$/H$^+$ antiporter will mitigate, but not prevent, volume changes due to increased K$^+$ uptake. Fig. 2.4 contains strong support for this hypothesis. Matrix volume was perturbed by opening and closing mitoK$_{ATP}$ (Fig. 2.4 A) or by adding ionophores (Fig. 2.4 B). The effects of quinine, which inhibits the K$^+$/H$^+$ antiporter (153), confirm that the preceding volume was a true steady state and also demonstrate that K$^+$/H$^+$ antiporter activity increases with increasing matrix volume.

MitoK$_{ATP}$ opening causes mild uncoupling. The steady-state K$^+$ cycle described in Fig. 2.1 is a futile cycle and dissipates energy. We have found that, provided K$^+$ influx and efflux are balanced with the aid of ionophores, the result of the futile K$^+$ cycle is exactly the same as that of a futile protonophoretic cycle caused by adding an uncoupler such as CCCP (data not shown). However, when K$^+$ influx and efflux must rely on endogenous pathways, the results are not identical, as shown in Fig. 2.5. As valinomycin-mediated uncoupling increases, the volume must also increase, as described in the preceding section. This will eventually cause the outer membrane to rupture with loss of cytochrome *c* and inhibition of respiration (Fig. 2.5 A). This is not observed during CCCP-mediated uncoupling (Fig. 2.5 B), which is not associated with matrix swelling. Valinomycin-induced uncoupling causes loss of outer membrane integrity at about 1.5 pmol valinomycin per mg of protein, and mitoK$_{ATP}$ opening causes uncoupling at an equivalent valinomycin dose of about 1 pmol per mg of protein (dashed line in Fig. 2.5 A). Thus, mitochondria have a very narrow margin of safety with respect to K$^+$ cycling, and a low mitoK$_{ATP}$ activity is essential for preserving the integrity of the outer membrane. Indeed, the K$^+$ flux catalyzed by mitoK$_{ATP}$ is so small that it is estimated to cause a decrease in mitochondrial membrane potential of only 1 - 2 mV in normoxic hearts (115). For this reason, we believe that a decrease in membrane potential is not one of the significant effects of mitoK$_{ATP}$ opening in

the normoxic heart. Other laboratories have also shown that mitoK$_{ATP}$ opening

does not cause detectable uncoupling of respiration *in vivo* or in isolated

myocytes (83, 123, 164).

MitoK$_{ATP}$ opening causes matrix alkalinization. The theoretical

basis for the hypothesis that net K$^+$ uptake results in matrix alkalinization is

best understood in the context of Fig. 2.1. Since overall transport must be

electroneutral, electrophoretic K$^+$ influx will be balanced exactly by the

electrogenic H$^+$ efflux driven by electron transport. If this were all that

happened, the K$^+$ for H$^+$ exchange would increase matrix pH by an amount

determined by the buffering power of the matrix (70). For example, if 20 mM

K$^+$ were added to the matrix by this process, matrix pH would increase by

about 1 pH unit. But in fact, this loss of matrix protons is partially compensated

by electroneutral uptake of phosphoric acid via the Pi transporter. The

compensation is limited, however, by the fact that Pi is in equilibrium with the

pH gradient and, because the cytosolic concentration of Pi is much lower than

that of K$^+$, Pi uptake is limited by its equilibrium distribution. For these

reasons, the P$_i$ equivalents taken up will always be less than those of K$^+$ during

net K$^+$ uptake, and it is this imbalance that leads to matrix alkalinization. The

data in Figs. 2.6 A and 2.6 B show directly that the increase in matrix K$^+$,

mediated either by mitoK$_{ATP}$ or by valinomycin, is accompanied by matrix

alkalinization. This effect is germane to the role of mitoK$_{ATP}$ in

cardioprotection, because matrix alkalinization appears to be the cause of mitoK$_{ATP}$-dependent increases in production of reactive oxygen species (A. Andrukhiv and K. D. Garlid, unpublished observations).

MitoK$_{ATP}$ - its existence and its assay. The theoretical, experimental, and quantitative basis of the light scattering assay for ion transport in mitochondria were developed 20 years ago (16, 67), and application of this assay to the study of mitoK$_{ATP}$ was described 12 years ago (18). Despite a robust body of evidence in support of this application (13, 18, 72, 94, 115), its validity was recently questioned by Halestrap and coworkers (44). They carried out light scattering experiments with heart mitochondria in which they observed ATP inhibition of matrix swelling in K$^+$ medium but failed to observe any effects of diazoxide or 5HD. The latter finding caused these authors to raise the question of whether mitochondria possess a K$_{ATP}$ channel. To explain the effect of ATP, they attributed the apparent inhibition by ATP to a light scattering artifact rather than to inhibition of K$^+$ flux.

The results in this chapter address these concerns as follows: [a] ATP, diazoxide, cromakalim, glibenclamide and 5HD affect matrix swelling only in K$^+$ medium and not in TEA$^+$, Li$^+$, Na$^+$ or nonelectrolyte media (Figs. 2.2A, 2.2B, 2.3, and data not shown). [b] ATP, diazoxide, and 5HD have no effect in K$^+$ medium when K$^+$ conductance is increased by valinomycin. [c] Direct measurement of K$^+$ influx (Fig. 2.6 A) and the accompanying matrix

alkalinization (Fig. 2.6 B) confirm the effects of ATP, diazoxide, cromakalim, glibenclamide, and 5HD on K^+ influx in mitochondria. [d] When valinomycin-mediated K^+ influx was used for calibration, mitoK$_{ATP}$-mediated K^+ influx was found to be quantitatively identical to that induced either by diazoxide or cromakalim in four independent assays — light scattering, respiration, K^+ influx, and H^+ efflux (Figs. 2.7 and 2.8). In our judgement, these findings provide decisive support for the existence of mitoK$_{ATP}$ and for the validity of the light scattering technique for its assay. This is very important, because light scattering is the only practical means of studying K^+ transport in isolated mitochondria, and such studies are essential for future progress toward understanding the role of mitoK$_{ATP}$ in cardioprotection.

It seems likely that all of the effects of mitoK$_{ATP}$ opening arise from increasing the K^+ conductance of the inner mitochondrial membrane, although unrecognized consequences of protein-protein interactions cannot be excluded. We believe that the only known direct effect of mitoK$_{ATP}$ opening *during ischemia* is to maintain matrix and intermembrane space volumes (47). We have now established three direct effects of mitoK$_{ATP}$ opening that occur *during normoxia* — matrix swelling, mild uncoupling, and matrix alkalinization. The unknown mechanisms by which mitoK$_{ATP}$ opening confers cardioprotection must ultimately derive from one of these effects, and it is hoped that these findings will help in the search for these mechanisms.

3. Ouabain protects rat hearts against ischemia-reperfusion injury *via* a pathway involving src kinase, mitoK$_{ATP}$, and ROS[2]

3.1 Summary

This chapter introduces the cardioprotective profile of ouabain and contrasts it to that of bradykinin. As these drugs are discussed in this context throughout this text, this overview is important. Here, we investigated whether exposure to ouabain was cardioprotective, and began to map the signaling pathways linking ouabain to the opening of mitoK$_{ATP}$.

In Langendorff-perfused rat hearts, 10-80 μM ouabain given before the onset of ischemia resulted in cardioprotection against ischemia-reperfusion injury, as documented by an improved recovery of contractile function and a reduction of infarct size. In skinned cardiac fibers, a ouabain-induced protection of mitochondrial outer membrane integrity, adenine nucleotide compartmentation and energy transfer efficiency was evidenced by a

---

decreased release of cytochrome c and preserved $K_{1/2}$ (ADP) and ANT-miCK

coupling, respectively. Ouabain-induced positive inotropy was dose-

dependent over the range studied, whereas ouabain-induced cardioprotection

was maximal at the lowest dose tested. When compared to bradykinin (BK)-

induced preconditioning, ouabain was equally efficient. However, the two

ligands clearly diverge in the intracellular steps leading to mitoK$_{ATP}$ opening

from their respective receptors. Thus, BK-induced cardioprotection was

blocked by inhibitors of PKG or guanylyl cyclase (GC), whereas ouabain-

induced protection was not blocked by either agent. Interestingly, however,

ouabain-induced inotropy appears to require PKG and GC. Thus, 5-HD (a

selective mitoK$_{ATP}$ inhibitor), MPG (a reactive oxygen species scavenger),

ODQ (a GC inhibitor), PP2 (a src kinase inhibitor), and KT 5823 (a Protein

kinase G inhibitor) abolished preconditioning by bradykinin and blocked the

inotropic response to ouabain. However, only PP2, 5-HD, and MPG blocked

ouabain-induced cardioprotection.

3.2 Introduction

Preconditioning the heart prior to prolonged ischemia results in protection

against ischemia-reperfusion injury. Preconditioning begins with activation of

cell surface receptors, which leads in turn to initiation of intracellular signal

transduction pathways. These have been extensively studied and reviewed by

Downey and coworkers (29, 49, 152) and by Gross and Gross (79). The signaling cascades lead to mitochondria, where they cause opening of mitoK$_{ATP}$ and subsequent release of ROS from mitochondria (4). Further downstream effects occur, including inhibition of the mitochondrial permeability transition (MPT) and prevention of cellular necrosis (32).

Ouabain, a member of the oldest class of drugs used in the treatment of heart failure, has generally not been viewed as a potential cardioprotective agent. Indeed, Ishida, et al. (92) employed high concentrations of ouabain to induce Ca^{2+} overload in heart and to show that the toxic effects of Ca^{2+} overload were blunted by the mitoK$_{ATP}$ opener diazoxide. Nevertheless, several lines of evidence raised the possibility that ouabain may be cardioprotective in the therapeutic dose range. First, it has been known for several years that ouabain interaction with the Na,K-ATPase activates a cellular signaling cascade (reviewed in (236)) that resembles the signaling cascade of cardioprotection (69). Second, we showed that low concentrations of ouabain stimulated mitochondrial production of reactive oxygen species (ROS) in rat cardiac myocytes and that this ROS production was blocked by 5-hydroxydecanoate (5-HD) (217). Third, we reported that mitoK$_{ATP}$ is required for increased contractility by various positive inotropic agents including ouabain, further suggesting that wired mechanisms link the activation of Na,K-ATPase signaling complex to mitoK$_{ATP}$ opening (73). Because mitoK$_{ATP}$

opening and increased mitochondrial ROS production are critical for cardioprotection, we decided to investigate whether ouabain is capable of preconditioning the isolated rat heart.

At first glance, the physiology of inotropy and the pathophysiology of cardioprotection appear to have little in common, but a closer analysis of mitochondrial bioenergetics revealed that mitoK$_{ATP}$ opening should be critically important in both mechanisms. During both inotropic stimulation and ischemia, the mitochondrial membrane potential ($\Delta\Psi$) decreases. As a consequence, K$^+$ diffusion into the matrix decreases and the mitochondrial matrix contracts, resulting in an expansion of the mitochondrial intermembrane space (IMS). IMS expansion disrupts the coupling between the outer membrane voltage-dependent anion channel (VDAC), the inner membrane adenine nucleotide translocase (ANT), and the mitochondrial creatine kinase (miCK) leading to an increased outer membrane permeability to ADP and ATP and decreased efficiency of energy transfer (47, 48, 69). Thus, energy transfer from mitochondria to cytosolic ATPases is impaired when it is most needed, whether during inotropic stimulation or reperfusion following ischemia. This effect is prevented by mitoK$_{ATP}$ opening, which prevents IMS expansion by adding a parallel K$^+$ conductance to compensate for the decrease in K$^+$ driving force (47, 48, 69).

The present study focuses on ouabain-induced cardioprotection and

begins an investigation of the signaling pathway involved. We show that preconditioning with ouabain protects against infarction, protects heart function, and preserves adenine nucleotide compartmentation in mitochondria. We compared ouabain cardioprotection with the well-characterized cardioprotection by bradykinin and found, through the use of inhibitors, that both pathways depend on src kinase, $mitoK_{ATP}$, and ROS. We also observed important differences in the signaling pathways for ouabain cardioprotection. First, ouabain protection was not affected by inhibitors of cGMP-dependent protein kinase (PKG) or guanylyl cyclase, whereas bradykinin protection was abolished by these agents. Second, cardioprotection was more sensitive to ouabain than was the inotropic response; that is, protection was observed at ouabain concentrations that induced little or no inotropic response. Third, whereas inhibitors of PKG or guanylyl cyclase had no effect on ouabain-induced cardioprotection, they abolished the inotropic response to ouabain. These divergences suggest that the intracellular signaling steps leading to $mitoK_{ATP}$ opening differ between ouabain and bradykinin and, moreover, that ouabain-induced increases in contractility require an additional signaling pathway in parallel with that which opens $mitoK_{ATP}$.

3.3 Materials and Methods

Chemicals and reagents

1H-[1,2,4]Oxadiazole[4,3-a]quinoxalin-1-one (**ODQ**), KT5823 (**KT**), and 4-Amino-5-(4-chlorophenyl)-7-(*t*-butyl)pyrazolo[3,4-d] pyrimidine (**PP2**) were purchased from Calbiochem (San Diego, CA). Bradykinin (**Bk**), ouabain (**Ouab**), 5-hydroxydecanoate (**5-HD**), N-2-mercaptopropionyl glycine (**MPG**), and all other reagents were all purchased from Sigma-Aldrich Corp. (St. Louis, MO). 8-(4-chlorophenylthio)-guanosine 3',5'-cyclic monophosphate (**CPT-cGMP**) was purchased from BIOLOG, Inc. (Hayward, CA).

Langendorff Perfusion

Different perfusion protocols were conducted in Bordeaux and Portland, respectively (Fig 3.1). They differ slightly based on established practices in each laboratory and required adaptations for preparation and analysis of skinned fibers. The experimental protocols used in these studies were performed in compliance with the American Physiological Society *Guiding Principles in the Use and Care of Animals* and were approved by Institutional Animal Care and Use Committee at Portland State University.

Assessment of ouabain-induced cardioprotection and effects on mitochondrial function.

Male Sprague-Dawley rats weighing 250 to 375g were anesthetized with 40 mg of sodium pentobarbital injected intraperitoneally. The thorax was opened, hearts were rapidly excised, immediately cooled in iced Krebs buffer and perfused by an aortic canula delivering warm (37 °C), buffer at a constant pressure of 100 mmHg. Hearts were perfused with a modified Krebs-Henseleit solution containing in mM: NaCl 118, KCl 5.9, $CaCl_2$ 1.75, $MgSO_4$ 1.2, EDTA 0.5, $NaHCO_3$ 25, Glucose 16.7. The perfusate was gassed with $95\%O_2$ - $5\%CO_2$ which resulted in a pO_2 above 600 mmHg at the level of the aortic canula and a buffer pH of 7.4. The pulmonary artery was transacted to facilitate coronary venous drainage and a left ventricular polyethylene apical drain was inserted through a left atrial incision to allow Thebesien venous drainage. Left ventricular pressure was monitored from a water-filled latex balloon placed through the left atrial appendage, and connected to a Statham P23Db pressure transducer. The volume of the balloon was adjusted to obtain a left ventricular diastolic pressure around 7 mmHg and kept constant throughout the entire experiment. Hearts were not paced and mechanical performance was evaluated as the product of heart rate and developed pressure (RPP).

Mitochondrial and heart function were assessed in five groups (n = 6 in

each group) as described in Fig. 3.1, Protocol A. The control group was perfused under aerobic conditions during 90 minutes. The ischemia-reperfusion group (IR) was allowed to stabilize under aerobic conditions during 40 min prior to a 30-min zero-flow global ischemia period followed by 20 min of reperfusion. The global zero-flow ischemia model was chosen in this case because is it more adapted to the assessment of left ventricular functional alterations and preparation of skinned fibers. Ouabain- treated groups (Ouab) were allowed to stabilize under aerobic condition during 20 min, before 20 min perfusion with a buffer containing ouabain. This was followed by 30 min zero-flow ischemia and 20 min reperfusion without ouabain. Mitochondrial function was assessed on permeabilized fibers of left ventricle obtained immediately at the end of the 20 min of reperfusion. Protocols for their preparation and assay have been extensively described and discussed in earlier studies (47, 73, 222). Following incubation with saponin to permeabilize the muscle, fibers were washed in buffer to remove adenine nucleotides, phosphocreatine, and saponin. The oxygen consumption of skinned fibers (0.5-0.75 mg dry weight) was measured polarographically at 25°C using a Clark-type oxygen electrode (Oroboros oxygraph, Paar, Graz Austria). Data were recorded at sampling intervals of 1 s (Datlab Acquisition Software, Oroboros, Innsbruck, Austria).

To determine control of respiration by ADP and creatine, oxygen consumption of skinned fibers was measured in medium containing (in mM):

CaK$_2$EGTA 2.77 ; K$_2$EGTA 7.23 (pCa =7) ; MgCl$_2$ 1.38 ; DTT 0.5 ; MES 100 ; imidazole 20 ; taurine 20 ; KH$_2$PO$_4$ 3; pyruvate 10 ; and malate 5 mM. pH was adjusted to 7.1 with KOH 10 M at 25°C and 2 mg/ml of bovine serum albumin was added. To determine the half saturation constant of respiration for ADP ($K_{1/2}^{ADP}$), the dependence of respiration on ADP concentration in the presence and absence of 20 mM exogenous creatine was calculated by nonlinear regression (Kaleidagraph software).

To examine permeability of the outer mitochondrial membrane to cytochrome *c* following ischemia-reperfusion, respiration was measured in 2 ml of KCl buffer containing (in mM) : KCl 125 ; HEPES 20 ; pyruvate 10 ; malate 5 ; Mg acetate 3 ; KH$_2$PO$_4$ 5 ; EGTA 0.4 ; DTT 0.3. pH was adjusted to 7.1 with KOH 10 M at 25 °C and 2 mg/ml of bovine serum albumin was added. Respiration was stimulated by the addition of ADP at a final concentration of 1 mM, which induced a maximal activation. Cytochrome c was then added at a final concentration of 8 mM to test the intactness of the outer mitochondrial membrane.

Infarct size (IS) was determined in five groups of 4 to 6 hearts as described in Fig. 3.1, protocol B. The ischemia-reperfusion group (IR) was allowed to stabilize under aerobic conditions during 40 min prior to a 40-min regional zero-flow ischemia period followed by 120 min of reperfusion. Ouabain-treated groups (Ouab) were allowed to stabilize under aerobic

condition during 20 min, before 15 min perfusion with a buffer containing ouabain. This was followed by 40 min zero-flow ischemia and 120 min reperfusion without ouabain. Regional ischemia was achieved by occlusion of the left anterior descending coronary artery. The model of regional zero-flow ischemia was chosen here to mimic the coronary artery occlusion encountered in the clinical setting at the acute phase of myocardial infarction. The coronary artery was reoccluded at the end of reperfusion, and the area at risk (AAR) was determined by negative

Figure 3.1   Rat heart perfusion protocols.

Timing of interventions is shown in relation to the zero-flow ischemia. Protocol A was used to characterize the protective effect of ouabain on heart function (see figure 3.2), in relation with mitochondrial respiratory function in skinned fibers prepared after 20 min reperfusion (see figures 3.4 and 3.5).   Ouabain (Ouab) concentrations were 10 μM, 20 μM, or 80 μM. Protocol B was used to address the question of the role of mitoK$_{ATP}$ in ouabain effect and compare the mechanism of ouabain preconditioning to bradykinin preconditioning. After ischemia, all hearts were reperfused with standard Krebs-Henseleit solution for 120 min (see figure 3.3 and 3.6-8) . Ouabain concentrations were 1 nM,10 μM, 20 μM, 50 μM,80 μM, or 1 mM.

Protocol A : Assessment of ouabain-induced cardioprotection and effects on mitochondrial function
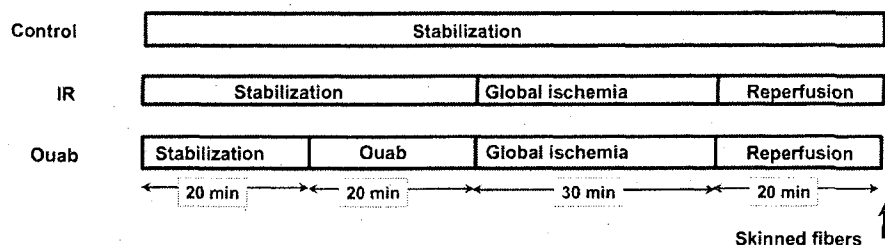
Protocol B: Comparison of ouabain- and bradykinin-induced cardioprotection
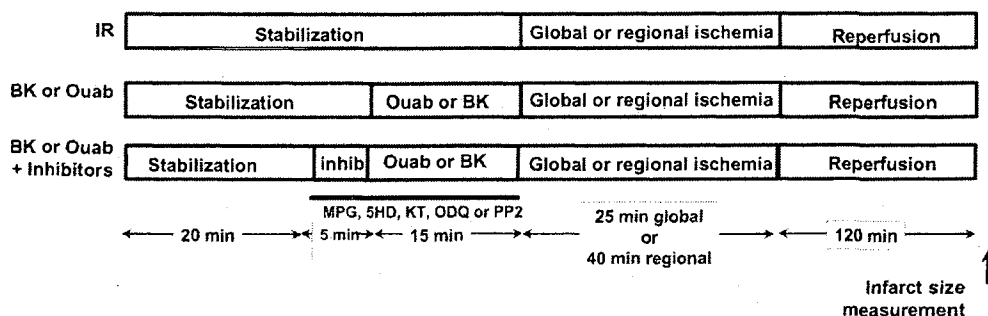
staining after perfusion of phtalocyanin blue (SP chaux, matière & couleurs, Bordeaux, France). This allowed for the delineation of the normal, aerobically perfused area, stained blue, versus the AAR, not stained. The heart was then removed from the perfusion apparatus, rinsed of excess blue dye, trimmed of right ventricle and atrial tissue, and cut into six cross-sectional pieces. Slices of the left ventricle were incubated without agitation in 1% (w/v) Thiphenyltetrazolium chloride (TTC) solution for 12 min at 37°C and pH 7.4. TTC stains the viable tissue in a brick-red color, which allows the discrimination between viable (red) and nonviable (pale yellow) tissue. The samples were then fixed in 3.5% (w/v) formalin solution for 24 hours at 4°C and weighed. Both sides of each slice were photographed. The area of each region, delineated with SigmaScan Pro software were averaged from the photographs of each side for each slice and multiplied by the weight of the slice. Infarct size was finally expressed both as percentage of total left ventricular mass and as a percentage of AAR.

Comparison of ouabain- and bradykinin-induced cardioprotection

Perfusion conditions were identical with those in Bordeaux with slight modification in the perfusion buffer containing in mM: NaCl 118.5, KCl 4.7, $MgSO_4$ 1.2, KH_2PO_4 1.2, $NaHCO_3$ 25, $CaCl_2$ 1.7, glucose 10, and pyruvate 1.2, gassed with 95% O_2–5% CO_2. Ten groups of hearts were studied (n = 3-6 in each group) as described in figure 3.1B. Following stabilization and

pretreatment, all groups were exposed to 25-min zero-flow global ischemia followed by 120 min of reperfusion with standard Krebs solution. The ischemia-reperfusion group (IR) was allowed to stabilize under aerobic conditions for 40 min. Prior to ischemia, the ouabain- (Ouab) and bradykinin- (BK) treated groups were allowed to stabilize under aerobic conditions for 25 min, followed by 15 min perfusion with a buffer containing 50 mM of ouabain or 100 nM bradykinin, respectively. Where used, ODQ (2 μM), 5-HD (300 μM), KT5823 (1 μM), MPG (1 mM), or PP2 (1 μM) were added to the perfusate 5 min before ouabain or bradykinin, and included in the perfusate during the subsequent 15 min perfusion with ouabain or bradykinin. In the experiments with the PKG activator, CMP-cGMP was added simultaneously with ODQ 5 min before the additon of ouabain.

The hearts in each group were reperfused for 120 min after which infarct size was estimated by the method of Ytrehus, et al. (241). 15 ml of 1% wt/vol TTC in phosphate–buffered saline pH 7.4 at 37 °C was infused into the coronary circulation at a rate of 0.5 ml/gm/min. The eluted stain from the cardiac veins was collected and recirculated. After approximately 15 min of perfusion the epicardial surface was deep red. Hearts were then removed from the cannula and fixed overnight in 10 % Formalin. Hearts were removed from formalin, sectioned along the atrioventricular plane into ~1mm sections. Sections were placed between two microscope slides and computerized area

analysis was performed using Scion image and the infarct size of each heart was expressed as a fraction of the total area at risk. Infarct size for each heart was determined by averaging the infarct area of the 5-6 sections. The RPP data shown if Fig. 3.8 were calculated using the average RPP measured· during the 15-min drug treatment for each experimental condition (Figure 3.1 protocol B).

3.4 Results

Effects of ouabain concentration on cardiac function

Hemodynamic data shown in Fig. 3.2 were obtained in experimental conditions described in Fig. 3.1, protocol A. As shown in Fig. 3.2A, the control group was hemodynamically stable, with less than 12% decline in RPP over the 90-min perfusion period. The average control RPP was 33800 ± 1200 mm Hg.min. Ischemia resulted in immediate cardiac arrest. Upon reperfusion, a limited recovery of systolic function was observed with maximal RPP values at the end of the reperfusion period corresponding to 17% of control values. As shown in Fig. 3.2B, diastolic pressure remained constant in the control group. In the IR group, ischemic contracture was observed after 15 min of ischemia with a maximum of 24 ± 4 mm Hg (Figure 3.2B, $p < 0.01$ *vs.* control). Overall, these data show the early occurrence of contracture during ischemia and a poor early recovery of systolic function after reperfusion.

Perfusion of ouabain induced a concentration-dependent increase in RPP (Fig. 3.2A), with the maximum increase (57%) being achieved with 80 µM ouabain. The inotropic effect was due exclusively to an increase in developed pressure with no significant associated change in heart rate or left ventricular diastolic pressure (not shown). All three doses of ouabain prevented ischemic

Figure 3.2. *Effects of ouabain on left ventricular function.*
A: Rate pressure product (RPP), and **B**: left ventricular end diastolic
pressure (LVEDP) obtained from control , Ischemia-reperfusion (IR) ,
Ouab 10, Ouab 20, and Ouab 80 groups of Langendorff perfused rat
hearts. See "Materials and Methods" and "protocol A" of Fig. 3.1 for
details on perfusion protocols. Values are means of 6 separate
experiments. §= $p < 0.05$ *vs* IR.
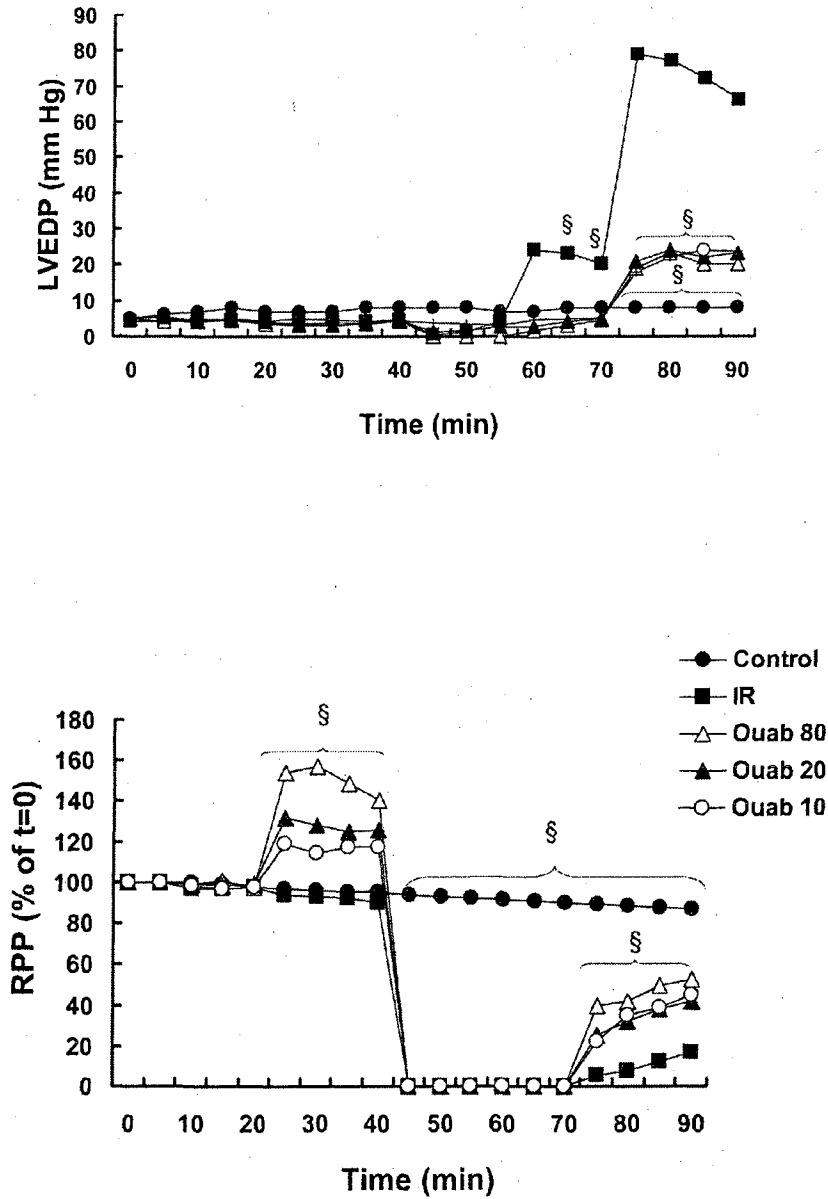
Figure 3.3. Effect of ouabain dose on infarct size.
Infarct size expressed as a percentage of the area at risk in Langendorff-perfused rat hearts subjected to 40 minutes regional ischemia followed by 120 minutes reperfusion as described in "Materials and Methods" and "protocol B" of Fig. 3.1. * = p < 0.05 vs. IR.
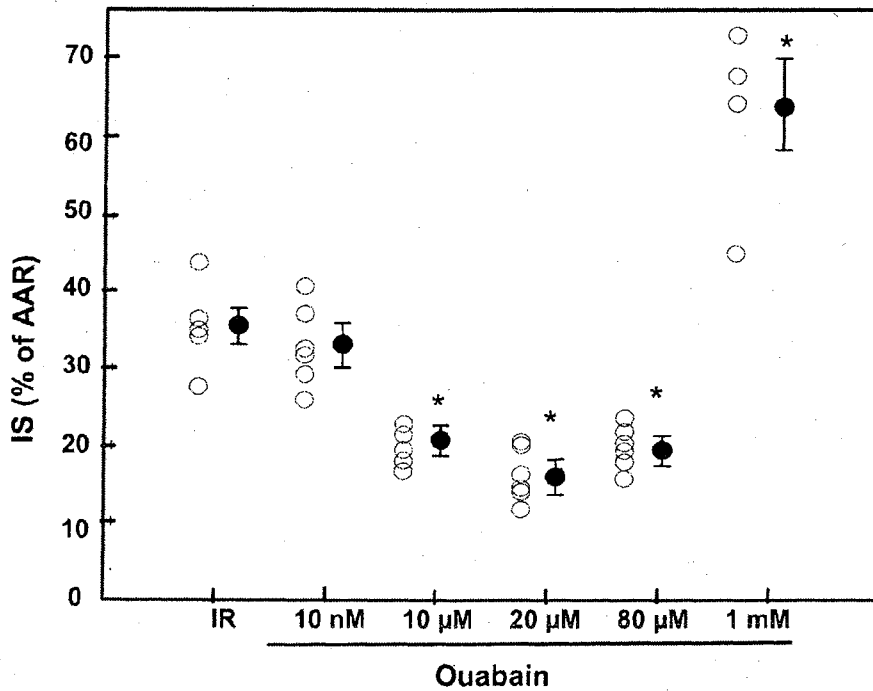
Figure 3.4. *Effect of ouabain on mitochondrial respiration in skinned fibers.*

Shown are respiration values measured in KCl medium in the absence of ADP (black bars), in the presence of 2 mM ADP (gray bars), and in the presence of 2 mM ADP + 10 µM cytC (dashed bars). See "Materials and Methods" and "protocol A" of Fig. 3.1 for details on perfusion protocols. ‡ indicates $p < 0.05$ *vs.* Control; * indicates $p < 0.05$ *vs.* State 3 IR.
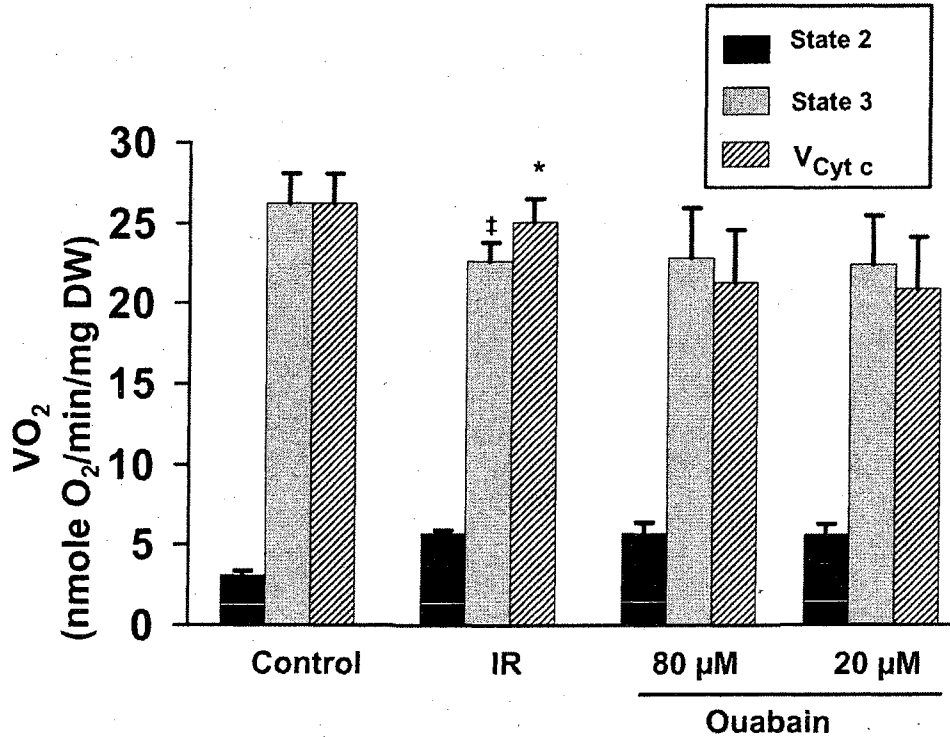
Figure 3.5. *Effect of ouabain on control of outer membrane permeability to ADP.*

$K_{1/2}^{ADP}$ for respiration was assessed as a measure of outer membrane permeability to ADP in the presence (hatched bars) or absence (black bars) of 20 mM creatine. Respiration was evaluated in permeabilized fibers prepared from the left ventricle of isolated rat hearts, as describe in "Materials and Methods" and "protocol A" of fig 3.1. * indicates $p < 0.05$ vs IR, and †indicates $p<0.05$ vs in presence of creatine.
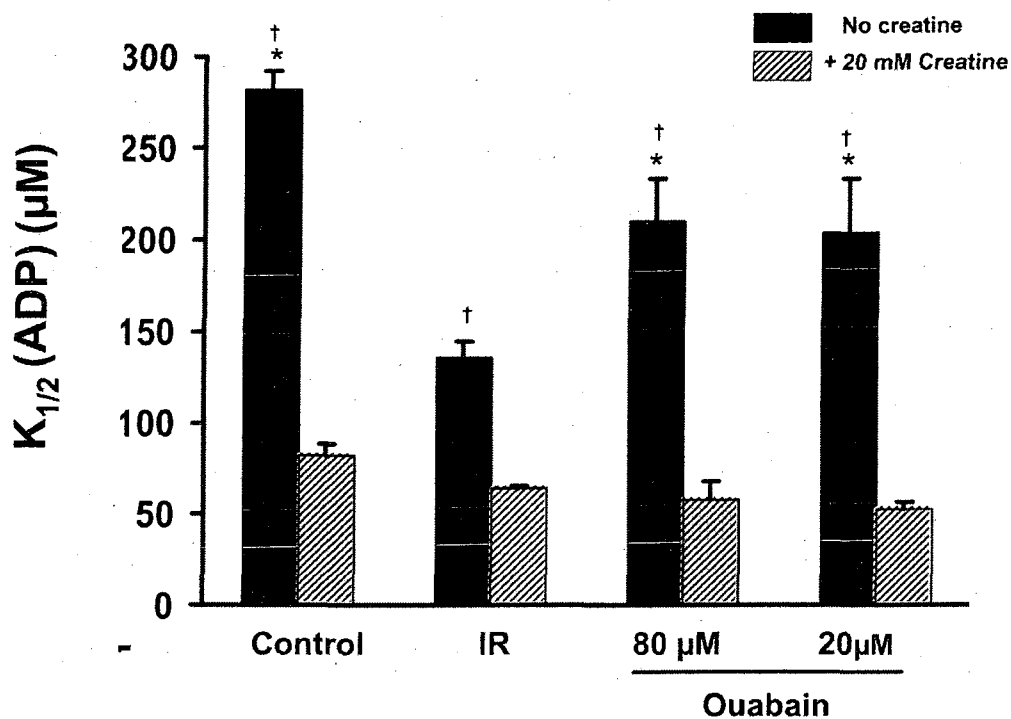
contracture during index ischemia (Fig. 3.2B) and significantly improved

functional recovery upon reperfusion (Fig. 3.2A).

Effects of ouabain on infarct size

The area at risk (AAR) was identical in each group (Figure 3.1 protocol

B) and averaged 28 ± 2 % of left ventricular mass. As shown in Fig. 3.3, 40

min ischemia followed by 120 min reperfusion resulted in an infarction of 29.8

± 2.5 % of the AAR. Fifteen min perfusion of 10, 20 or 80 μM ouabain

immediately before ischemia significantly decreased the infarct size to $12 \pm$

1.7%, 7.4 ± 2.1% and 11 ± 1.8% respectively (p < 0.05 vs IR). Perfusion of 10

nM ouabain did not afford any protection, whereas perfusion of 1 mM ouabain

exerted a toxic effect as evidenced by the significant increase in infarct size to

62 ± 6.4 % % of the AAR.

Effects of ouabain on mitochondrial function

Figure 3.4 contains results from assays of cytochrome c release (see

Materials and Methods). In the control group, maximal respiration was 26 ± 2

nmol O_2/min/ mg dw, and addition of cytochrome c did not induce any

stimulation. After 30 min ischemia followed by 20 min reperfusion, maximal

respiration was decreased by 16 % compared to control ($p < 0.05$). In these

fibers, the addition of exogenous cytochrome c accelerated respiration up to

the value measured in the control group. These data reflect alterations at the

level of the outer mitochondrial membrane leading to a loss of endogenous

77

cytochrome c. It is to be noted that ischemia followed by reperfusion had no

effect on state 2

respiration rates. In the ouabain groups, maximal respiration was not

significantly decreased, and addition of cytochrome c did not produce any

stimulation. These data indicate that ouabain protected against cytochrome c

loss from mitochondria.

The data in Fig. 3.5 contain $K_{1/2}^{ADP}$ values, determined in the presence

or absence of creatine (Cr), as described in "Materials and Methods". In fibers

from control hearts, the $K_{1/2}^{ADP}$ value was 282 ± 10 µM. This high value reflects

restriction of permeability to ADP at the level of the outer mitochondrial

membrane. In the presence of Cr, this value decreased to 82 ± 7 µM. As

previously discussed, the Cr-induced decrease in $K_{1/2}^{ADP}$ reflects functional

coupling between adenine nucleotide translocase (ANT) and mitochondrial

creatine kinase (195). In fibers from the IR group, $K_{1/2}^{ADP}$ was dramatically

decreased to 135 ± 8 µM ($p < 0.05$ $vs.$ control), and decreased to 64 ± 2 µM in

the presence of Cr. In contrast, $K_{1/2}^{ADP}$ in fibers from the ouabain-treated

hearts remained high, with values of 210 ± 23 µM (80 µM ouabain) and $204 \pm$

29 µM (20 µM ouabain). These values are significantly higher than the value

measured in fibers from the IR group, which reflects the preservation of the low

permeability of the outer mitochondrial membrane for ADP (47). Fibers

obtained from Ouab 10 group showed similar effects (data not shown).

Addition of Cr resulted in a decrease in $K_{1/2}^{ADP}$ to 57 ± 10 µM and 53 ± 4 µM, respectively, in fibers from the ouabain-treated hearts, reflecting the preservation of functional coupling of ANT and miCK, as observed in control group.

Ouabain versus bradykinin in cardioprotection

Cardioprotection by ouabain is a newly described phenomenon. We decided to begin an investigation of the signaling pathways involved in ouabain protection by comparing it with the well-characterized effects of bradykinin. Bradykinin and ouabain treatment caused improved post-ischemic functional recovery (Figs. 3.6a and 3.6b) as well as reduced infarct size (Fig. 3.7). As shown by Krieg, et al. (118, 120), cardioprotection by bradykinin involves src kinase, eNOS, guanylyl cyclase, PKG, mitoK$_{ATP}$ and ROS. Participation of these elements is confirmed by the data in Figs. 3.6 and 3.7, in which bradykinin protection against cardiac dysfunction (Fig. 3.6) and infarction (Fig. 3.7) is shown to be abolished by PP2, a src kinase inhibitor (86), ODQ, a guanylyl cyclase inhibitor (74), KT5823, a PKG inhibitor (103), 5-HD, a mitoK$_{ATP}$ blocker (94), and MPG, a free radical scavenger.

Ouabain protection against post-ischemic cardiac dysfunction (Fig. 3.6) and infarct size (Fig. 3.7) was also abolished by PP2, 5-HD and MPG, confirming participation of src, mitoK$_{ATP}$ and ROS in ouabain cardioprotection. Interestingly, however, ouabain protection was not abolished by ODQ or

KT5823, suggesting that signaling following administration of ouabain and bradykinin follows different pathways from the plasma membrane to mitochondria.

Ouabain protection versus ouabain-induced inotropy

Although this study was designed primarily to address cardioprotection by ouabain, we were also struck by the effects of drugs on the positive inotropic response to ouabain, which were observed in the pre-ischemic phase (see Fig. 3.6a). As shown in Fig. 3.8, 5-HD blocked the inotropic response, as previously shown (73). Additionally, the inotropic response to ouabain was blunted by MPG, PP2, KT5823, and ODQ. This data suggested that the positive inotropic effect of ouabain was mediated by PKG. To test this, we perfused with the cell-permeant cGMP CPT-cGMP in additon to ODQ and ouabain. This reinstated the positive inotropic effect of ouabain that had been inhibited by ODQ, confirming the requirement for PKG in ouabain-induced inotropy.

Figure 3.6. *Effects of ouabain versus bradykinin on left ventricular function.* (A) Functional cardiac recovery expressed as rate-pressure product (RPP). (B) Post-ischemic LVDP plotted as the average pressure (mm Hg) 30 minutes post-global ischemia, with error bars. See "Materials and Methods" and "protocol B" of Fig. 3.1 for details on perfusion protocols. 100nM bradykinin (Bk) protection was blocked by 300 μM 5-HD, 1 μM KT 5823 (KT), 1 mM MPG and 2 μM ODQ. Neither ODQ nor KT blocked 50 μM ouabain (Ouab) afforded cardioprotection, but 5-HD, MPG and PP2 blocked functional recovery. N is at least 4 in all trials. * indicates $p < 0.05$ vs. control.
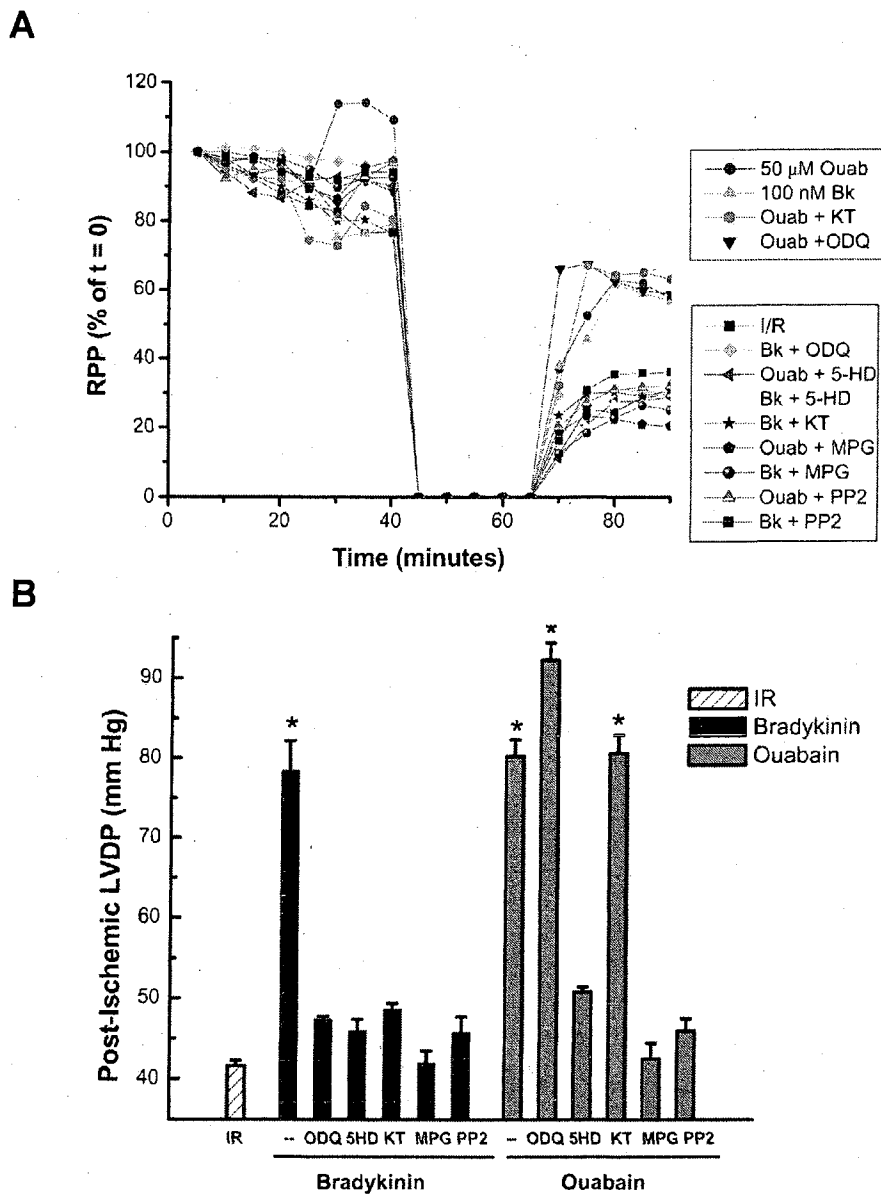
Figure 3.7. *Differential effects of agents on ouabain versus bradykinin cardioprotection.*

Infarct size is presented as percent of risk zone in isolated adult rat hearts subjected to 25 minutes global ischemia and 120 minutes reperfusion. See "Materials and Methods" and "protocol B" of Fig. 3.1 for details on perfusion protocols. Individual hearts (○) and group means (●) with standard error bars are shown. Hearts treated with 100 nM bradykinin or 50 μM ouabain had significantly smaller infarct size than untreated ischemia reperfusion (IR) hearts. In bradykinin treated hearts, this effect was blocked by all inhibitors tested: 300 μM 5-HD, 1 μM KT 5823 (KT), 2 μM ODQ, 1 mM MPG, and 1 μM PP2. In ouabain treated hearts protection was not blocked by ODQ or KT but was blocked by 5-HD, MPG and PP2. N is equal to at least 4 in all trials. * indicates $p < 0.05$ *vs.*
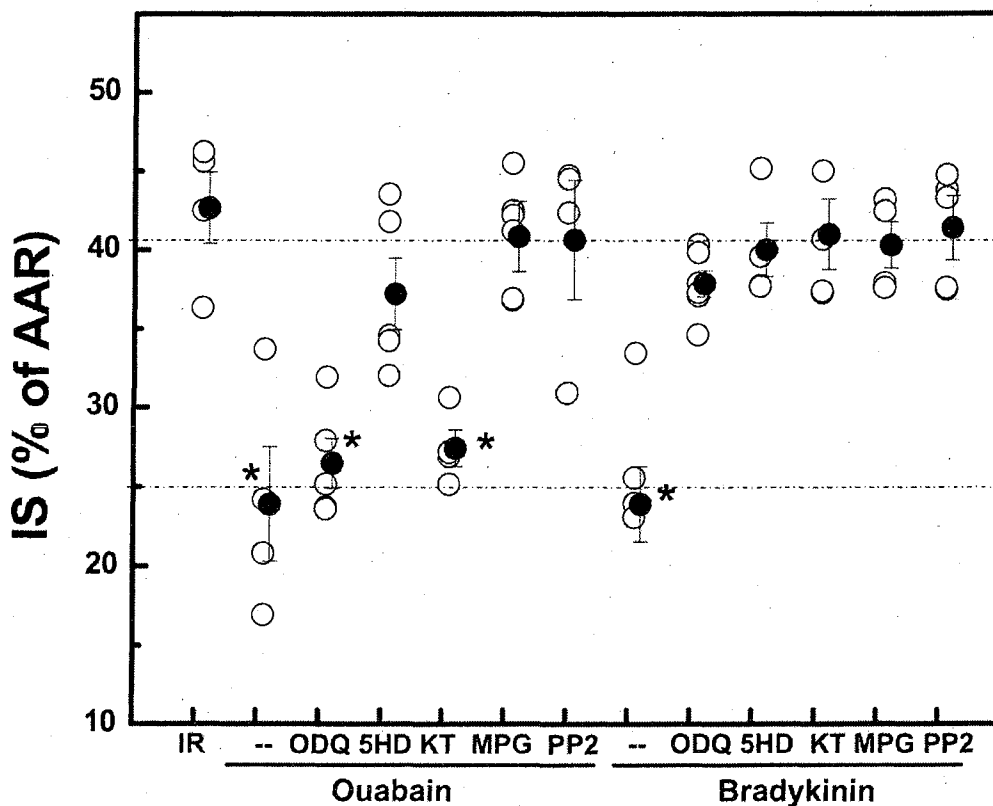
Figure 3.8. Differential effects of ODQ and KT5823 on ouabain-induced inotropy.

The inotropic response of the hearts is expressed as average of rate-pressure product (RPP) during the 15-minute drug treatment. The data have been normalized to the initial RPP at t = 0. Bradykinin does not have a positive inotropic effect; the positive inotropic response induced by 50 μM ouabain treatment was abolished by 300 μM 5-HD, 2 μM ODQ, 1 mM MPG, 1 μM KT5823 and 1 μM PP2. The ODQ-inhibited positive inotropy was restored by addition of the PKG activator CPT-cGMP (10 μM). * indicates $p < 0.05$ as compared to ouabain. † indicates $p < 0.05$ as compared to ODQ inhibited ouabain.
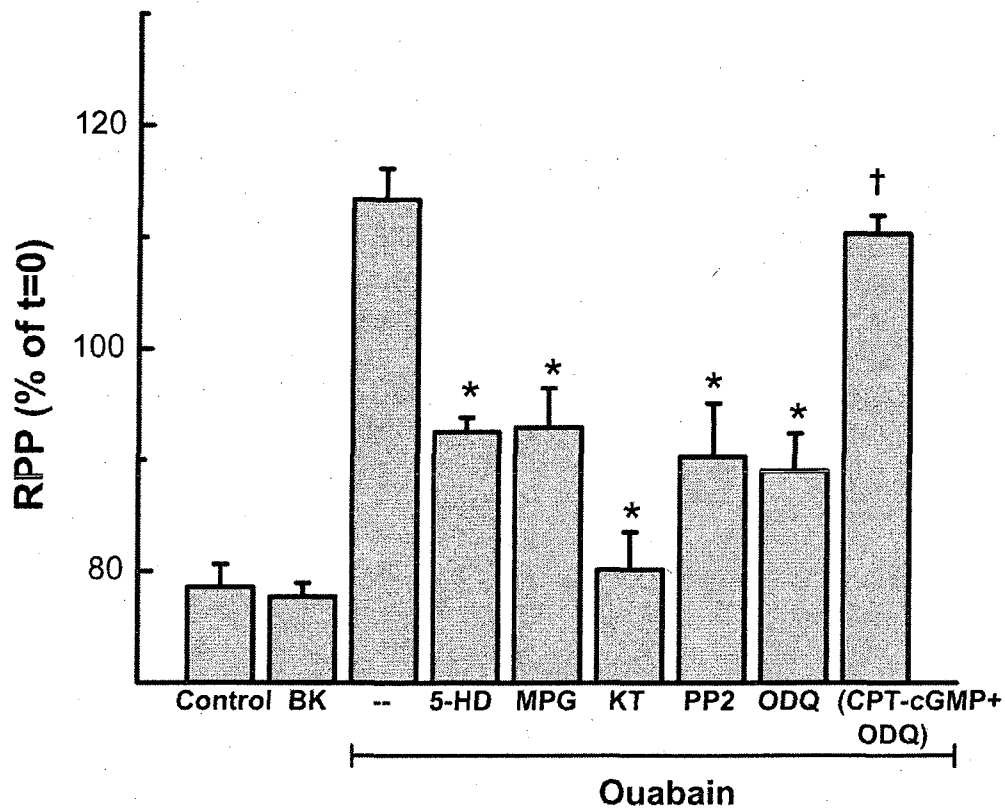
3.5 Discussion

Digitalis-like compounds have long been used in the treatment of heart failure for their inotropic effects. We recently demonstrated that mitoK$_{ATP}$ opening is necessary for the positive inotropic response, including that caused by ouabain (73). The implication of this result is that ouabain, like ischemic preconditioning (IPC), causes mitoK$_{ATP}$ opening by triggering an intracellular signaling pathway. Because mitoK$_{ATP}$ opening is cardioprotective, we decided to investigate whether ouabain itself is cardioprotective and to begin an investigation of its signaling pathway. The data in Figs. 3.2-5 show that perfusion of ouabain, in the micromolar range, before ischemia-reperfusion protects against infarction, protects heart function, and preserves adenine nucleotide compartmentation in mitochondria. In this regard, treatment with ouabain reproduces the effects of diazoxide and of ischemic preconditioning previously described (47, 121). Ouabain in the nanomolar range did not induce reduction in infarct size. This is in line with experiments performed on myocytes showing that ouabain in the nanomolar range does not block, but activates cardiac Na/K pumps (60). On the other hand, ouabain in the millimolar range induced a toxic effect as evidenced by the significant increase in infarct size shown in Figure 3.3. This might be explained by the damaging effect of increased mitochondrial Ca^{2+} overload in this condition (92).

All or most cardioprotective signaling pathways rely on Src kinase (21,

84

119, 226), mitoK$_{ATP}$ (71, 156, 231), and ROS (9, 165, 221, 230), and it is clear from the results in Figs. 3.6 and 3.7 that ouabain cardioprotection exhibits the same requirements. Thus, the Src inhibitor PP2, the mitoK$_{ATP}$ blocker 5-HD, and the ROS scavenger MPG each blocks protection against contractile failure and infarction after ischemia-reperfusion injury. In these respects, the effects of ouabain were the same as the effects of bradykinin, compared in Figs. 3.6 and 3.7.

It is most interesting, however, that the signaling pathways for the two ligands differ in important respects. Thus, bradykinin protection depends on PKG and guanylyl cyclase (160), whereas ouabain protection does not. This is manifested in the differential response to KT5823 and ODQ, inhibitors of PKG and guanylyl cyclase, respectively, and the effect is seen in both functional recovery and protection against infarction (Figs. 3.6 and 3.7). Addition of PKG + cGMP to isolated mitochondria is sufficient to open mitoK$_{ATP}$ (31); however these ligands appear not to be involved in the ouabain cardioprotective pathway, so there must be more than one mechanism to signal mitoK$_{ATP}$ opening at the level of the mitochondrion. We infer from these studies that mitoK$_{ATP}$ opening is necessary and sufficient for cardioprotection by ouabain and bradykinin.

Another original finding of this study is that KT5823 and ODQ inhibit the inotropic effect of ouabain (Fig. 3.8), in contrast to their lack of effect on

protection. This indicates that guanylyl cyclase and PKG are required for the inotropic response to ouabain. We showed that ouabain causes mitoK$_{ATP}$ opening and mitochondrial ROS production (217) and, moreover, that mitoK$_{ATP}$ opening is necessary for the inotropic response (73). From these results, we may conclude that mitoK$_{ATP}$ opening is necessary, but not sufficient, for the inotropic resonse.

Based on these findings and those from other studies, we infer that ouabain activates two different signaling platforms, as described in Fig. 3.9. One platform is the "mitoK$_{ATP}$-ROS platform" (4), which is activated by low concentrations of ouabain, as detected by mitoK$_{ATP}$-dependent cardioprotection. The other is a "Ca^{2+} regulating platform", such as has been observed in renal cells (141, 242), which is activated by higher concentrations of ouabain, as detected by the concentration-dependence of cardiac contractility. The data presented here show that cardioprotection requires only the mitoK$_{ATP}$-ROS signaling platform, whereas the inotropic response requires both platforms. It has been known for several years that the signaling pathway induced by ouabain through cardiac Na,K-ATPase relies on two intracellular mediators: Ca^{2+} and ROS. Removal of Ca^{2+} from the medium inhibits the ouabain-induced increase in intracellular Ca^{2+} in myocytes but does not affect ouabain-induced ROS production (130), which is mediated by mitoK$_{ATP}$ (217). Thus, the two pathways exhibit a certain degree of independence. However,

disruption of an upstream component of the cascade, such as the Na/K-ATPase /c-Src binary receptor (through inhibition of c-Src for example), prevents ouabain-induced increases in both Ca^{2+} and ROS, and, as shown here, prevents ouabain-induced inotropy and cardioprotection.

It appears that the common element connecting the two pathways is ROS, since $mitoK_{ATP}$-dependent ROS production is required for both cardioprotection and inotropy (73). Although earlier work by Xie and coworkers found no effect of N-acetyl-cysteine on contractility (216), a recent study from the same group found that ouabain-induced prolongation of the Ca^{2+} transient and increased contractility were blocked by N-acetyl-cysteine, and these effects were mimicked by incubation with 10 μM H_2O_2 (105). ROS are known to inhibit or activate most of the Ca^{2+} channels and transporters of the heart (reviewed by Zima and Blatter (245)); however levels of H_2O_2 achieved by $mitoK_{ATP}$ are unlikely to reach 10 μM. Moreover, a direct role of ROS in inotropy cannot account for the participation of guanylyl cyclase and PKG in the inotropic pathway, which implies a role for phosphorylation, either of a Ca^{2+} transporter or of the contractile mechanism (154). PKCs are activated by H_2O_2 (32) and are an essential component of the Ca^{2+}-regulating platform (144), and it is possible that $mitoK_{ATP}$-dependent H_2O_2 serves the role of activating a PKC in the system. Noland, et al. (154) showed that a PKC phosphorylates troponin I to sensitize the contractile system to Ca^{2+}, and Ogbi,

et al. (157) showed that PMA -activated PKCε increased contractile amplitude and increased the quiescent period between contractions in neonatal cardiomyocytes. In summary, our results show that the mitoK$_{ATP}$-ROS platform is activated at low concentrations of ouabain that do not increase contractility. Although the precise role of increased ROS in this system remains to be established, it may be required to activate a step within the Ca^{2+}-regulating platform, which then moves to increase cytosolic Ca^{2+} or Ca^{2+}-sensitivity and thereby initiate the inotropic response.

It is unclear at present how these mechanisms fit into the more established view of ouabain's mechanism of action, in which inhibition of Na,K-ATPase leads to elevation of [Na+]i, which causes reduced Ca2+ extrusion and, possibly, increased Ca^{2+} influx via the Na$^+$/Ca^{2+} exchanger (NCX) (20). Thus, Philipson and coworkers (188) found that NCX activity is essential for the action of cardiac glycosides, and Bers and coworkers (2) found that a Na+ gradient and a functional NCX is essential for glycoside-induced inotropy in cardiac myocytes.

Our finding here that ouabain-induced inotropy is blocked by ROS scavengers and inhibitors of Src, guanylyl cyclase, and PKG points to an essential role of cell signaling in the inotropic response to ouabain. These two sets of requirements are not, of course, mutually exclusive; however it remains for future work to determine how they are interconnected.

Figure 3.9. Proposed model of bradykinin and ouabain signaling in the heart.

The figure shows the signaling platforms associated with the bradykinin receptor (BK2) and the ouabain receptor (Na,K-ATPase). We propose that bradykinin and ouabain induce formation of two different mitoK$_{ATP}$ signaling platforms that cause mitoK$_{ATP}$ opening, an increase in mitochondrial ROS production, and cardioprotection. The bradykinin mitoK$_{ATP}$ platform includes Src, PI3-k Akt, eNOS, PKC, GC and PKG. The ouabain mitoK$_{ATP}$ platform also relies on Src activation for its formation, but little is known about the downstream components. In addition, and at higher doses, ouabain induces a Ca^{2+} platform that mediates the positive inotropic response. Interestingly, the ouabain-dependent Ca^{2+} platform requires ROS for activation and appears to contain the same components as the bradykinin-dependent mitoK$_{ATP}$ platform.
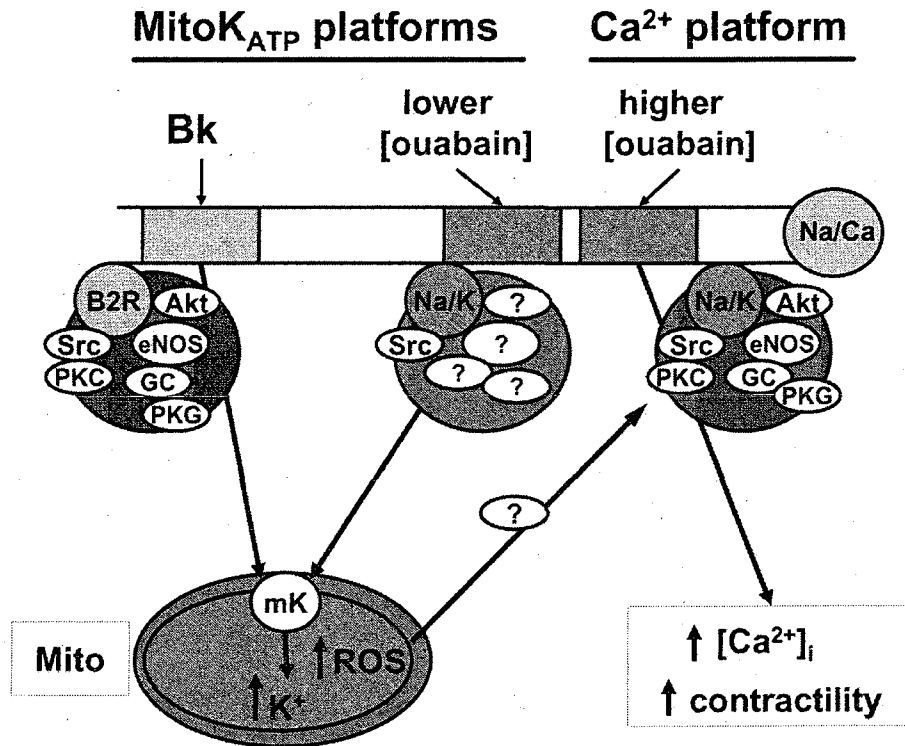
In summary, we have shown that ouabain is cardioprotective in the perfused rat heart model. The cardioprotective signaling pathway triggered by ouabain leads to mitoK$_{ATP}$ opening and mitochondrial ROS production, and this pathway differs from that triggered by bradykinin in that guanylyl cyclase and PKG are not involved in ouabain cardioprotection. The mitoK$_{ATP}$-ROS pathway is also necessary, but not sufficient, for the inotropic response, and we hypothesize that a second signaling pathway involving the Ca^{2+} regulating platform is also necessary for inotropy. These new features of ouabain signaling via the Na,K-ATPase clearly require additional investigation. Further investigation is also necessary to reveal whether the preconditioning effect of ouabain could explain, at least in part, why it remains more beneficial for the treatment of heart failure patients than the other drugs of the inotropic class (125, 240).

4. Conditioning the Heart Induces Formation of Signalosomes that Interact with Mitochondria to Open MitoK$_{ATP}$[3]

4.1 Summary

Perfusion of the heart with bradykinin triggers cellular signaling events that ultimately cause opening of mitochondrial ATP-sensitive K$^+$-channels (mitoK$_{ATP}$), increased H$_2$O$_2$ production, inhibition of the mitochondrial permeability transition (MPT), and cardioprotection. We hypothesize that bradykinin interaction with its receptor induces the assembly of a caveolar signaling platform (signalosome) that contains the enzymes of the signaling pathway and that migrates to mitochondria to induce mitoK$_{ATP}$ opening. We developed a novel method for isolating and purifying signalosomes from Langendorff-perfused rat hearts treated with bradykinin. Fractions containing the signalosomes were found to open mitoK$_{ATP}$ in mitochondria isolated from

untreated hearts via activation of a mitochondrial protein kinase C epsilon. MitoK$_{ATP}$ opening required signalosome-dependent phosphorylation of an outer membrane protein. Immunodetection analysis revealed the presence of the bradykinin B2 receptor only in the fraction isolated from bradykinin-treated hearts. Immunodetection and immunogold labeling of caveolin-3, as well as sensitivity to cholesterol depletion and resistance to Triton X-100, attested to the caveolar nature of the signalosomes. Ischemic preconditioning, ischemic postconditioning, and perfusion with ouabain, also led to active signalosome fractions that opened mitoK$_{ATP}$ in mitochondria from untreated hearts. These results provide initial support for a novel mechanism for signal transmission from plasma membrane receptor to mitoK$_{ATP}$.

4.2 Introduction

Bradykinin protects the heart against ischemia-reperfusion injury by a signaling process whose sequence has been well described by Downey and coworkers (160). Interaction of bradykinin with its receptor causes activation of phosphatidylinositol 3-kinase (PI3K), which phosphorylates membrane phospholipids to yield phosphatidylinositol trisphosphate, which then activates phospholipid dependent kinases (PDK), which in turn causes phosphorylation and activation of Akt. Akt phosphorylates endothelial nitric oxide synthase (eNOS), causing it to generate NO. NO activates soluble guanylyl cyclase (GC), causing it to synthesize cGMP which then activates protein kinase G (PKG). PKG acts on the mitochondrial outer membrane (MOM), causing opening of inner membrane mitoK$_{ATP}$ channels (31).

These temporal events take place within complex spatial domains. In particular, the signal must be transmitted from the plasma membrane to mitochondria through the cytosol. How does this occur? Cytosolic proteins are extensively hydrated, and the organization of this water causes a phase separation from bulk cell water. Minimization of the phase boundary, in turn, causes proteins to coalesce within their common hydration phase (65). If the proteins of the cardioprotective signaling pathway were randomly distributed in the cytosol, they too would coalesce within the hydration phase. The concerted sequential reactions of cardioprotection would be unlikely to take place by

random diffusional collisions in this milieu. Accordingly, we suggest that the signaling cascade is compartmentalized in a manner to promote metabolic channeling and that the entire reaction sequence moves through the cytosol as a unit. Thus, our working hypothesis is that cytosolic transmission of the signal to mitochondria takes place via vesicular, multimolecular signaling complexes called signalosomes (15, 55, 202). This hypothesis agrees with and extends the proposal by Ping and coworkers (182, 225) that intracellular signaling involves assembly and regulation of multiprotein complexes.

We show first that bradykinin treatment of perfused rat hearts caused a persistent open state of mitoK$_{ATP}$ that was reversed by exposing the inner membrane to the phosphatase PP2A. If this open state was caused by *in situ* interaction of signalosomes with mitochondria, as hypothesized, the signalosomes should be recoverable for study. Indeed, we were able to recover them from the mitochondrial suspension obtained from the treated hearts. Fractions containing the putative signalosomes from bradykinin-perfused hearts were added to mitochondria from untreated hearts and found to be functionally active. That is, they opened mitoK$_{ATP}$ to the same extent as diazoxide and also caused inhibition of the mitochondrial permeability transition (MPT). These effects were blocked by the specific PKG inhibitor KT5823, confirming that PKG is the terminal kinase of the bradykinin signalosome. The purified signalosomes were dissolved by the cholesterol-

binding agent methyl-β-cyclodextrin, and they were resistant to Triton X-100, indicating their caveolar nature. This was confirmed by immunodetection analysis showing the presence of caveolin-3, a marker for muscle caveolae (214). The bradykinin B2 receptor was also found in the signalosomes isolated from bradykinin-perfused hearts. The vesicular nature of the signalosomes was verified by electron microscopy, which revealed entities between 110 and 160 nm in diameter. Immunogold labeling showed a clear enrichment of the vesicles with caveolin-3. Signalosome formation appears to be a general phenomenon. We also recovered active signalosomes from hearts treated with ischemic preconditioning, ischemic postconditioning, and ouabain.

4.3 Materials and Methods

Isolated heart perfusions. Hearts from male Sprague-Dawley rats (200-220g) were perfused for 50-55 min as previously described (173). Control hearts were perfused for 50 min with Krebs Henseleit buffer containing (in mM) 118 NaCl, 5.9 KCl, 1.75 $CaCl_2$, 1.2 mM $MgSO_4$, 0.5 EDTA, 25 $NaHCO_3$, 16.7 glucose at pH 7.4. The perfusate was gassed with 95% O_2 - 5% CO_2. Treated hearts were perfused for 25 min with Krebs Henseleit buffer, then with buffer containing 100 nM bradykinin or 50 μM ouabain (173) for 15 min, followed by 10 min washout. The ischemic preconditioning (IPC) protocol was established by two cycles of 5 min global ischemia followed by 5 min reperfusion. Mitochondria were isolated promptly following the second reperfusion. Ischemic postconditioning was performed as described by Tsang, et al. (220), with 6 cycles of 10 s ischemia plus 10 s reperfusion. Infarct size was also measured after each of these treatments and found to be reduced to an extent similar to that reported elsewhere (121, 172). The experimental protocols complied with the Guiding Principles in the Use and Care of Animals published by the National Institutes of Health (NIH Publication No. 85-23, revised 1996).

Mitochondrial Isolation. Mitochondria from treated and untreated

donor rat hearts were isolated immediately following 50 min of Langendorff perfusion and used to isolate signalosomes. Mitochondria from untreated *assay* rat hearts were isolated without previous perfusion, purified in a Percoll gradient and used to assay for signalosome activity. A standard differential centrifugation isolation protocol was used (31). Mitoplasts were prepared from isolated mitochondria by digitonin treatment as described by Schnaitman et al (201). Briefly, an ice-cold 2% digitonin solution was added stepwise to mitochondria stirring on ice for 8 min. The digitonin was then washed out by dilution with mitochondrial isolation buffer (250 mM Sucrose, 10 mM HEPES (pH 7.2), 1 mM EGTA) and pelleted at 10,000 x g. Verification that the mitochondrial outer membrane (MOM) was disrupted was performed by respiratory assay in the presence and absence of cytochrome C. Interfibrillar mitochondria were prepared using a protocol slightly modified from Palmer, et al, (166). Briefly, the first low speed pellet from the standard isolation was resuspended in 150 mM KCl and 50 mM HEPES medium and re-homogenized with a tight-fitting teflon pestle. Following this step, the standard isolation protocol described in chapter 2 was followed (35). Mitochondrial protein concentration was estimated using the Biuret reaction (75).

Signalosome Purification. To determine if caveolar bodies associated with mitochondria following bradykinin treatment, donor mitochondria were further purified in a self-generated 24% Percoll gradient,

resulting in a purified mitochondrial fraction and a low-density fraction called

light-layer (LL). The LL was postulated to contain the signalosomes (see Fig.

4.1) but also contained plasma membrane fragments and broken

mitochondria. To purify the signalosomes, we used the non-detergent

caveolae isolation protocol of Smart et al (207). Briefly, the LL fraction was

adjusted to 2 ml, mixed with 50% Optiprep in buffer A (250 mM sucrose, 20

mM TRIS-Cl (pH 7.8), 1 mM EDTA), and placed in the bottom of a 12 ml

centrifuge tube (the sonication step

Figure 4.1. Schematic representation of the experimental protocol.
Each experiment required a donor preparation and an assay preparation.
The donor hearts were perfused with or without bradykinin on a
Langendorff apparatus, as described in "Methods". The assay hearts did
not undergo Langendorff perfusion. Mitochondrial fractions from both
hearts were purified on a 24% Percoll density gradient. The light layers
(LL) from donor hearts were assayed for their ability to open mitoK$_{ATP}$ in
assay mitochondria. In separate experiments, the LL were further purified
on an Optiprep gradient. These purified LL were used for light scattering
assays, immunoblot analysis, and electron microscopy.
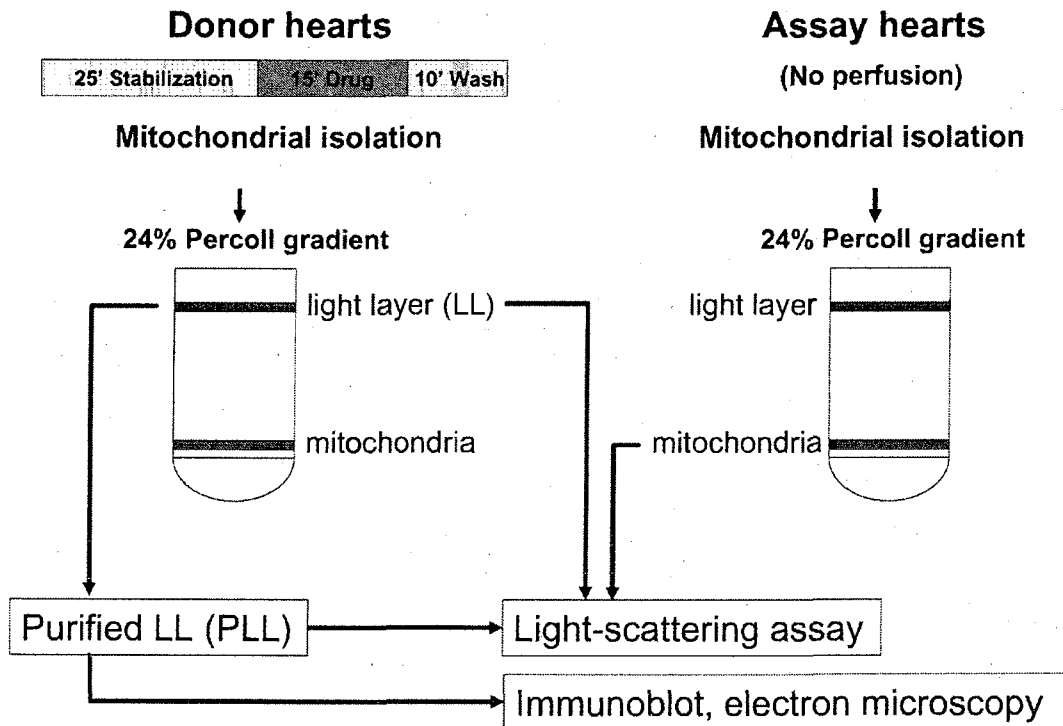
of the published protocol was eliminated). A 20-10% Optiprep gradient was layered on top, and the tubes were centrifuged at 52,000x*g* for 90 min. Following centrifugation, the top 5 ml were collected and mixed with 4 ml of the 50% Optiprep solution. This mixture was then overlayed with a 5% Optiprep solution and centrifuged again at 52,000x*g* for 90 min. The signalosome fraction was identified as an opaque band at the 5% interface. Validation of the purity of this fraction was demonstrated by Western blots that showed very little mitochondrial VDAC contamination and an enrichment of caveolins (fig 4.8).

MitoK$_{ATP}$ assays. MitoK$_{ATP}$ activity causes mitochondrial swelling, due to respiration-driven uptake of K$^+$ salts and water, and these volume changes were followed by light scattering, as previously described (16, 31, 35). Mitochondria from untreated assay hearts were added at 0.1 mg/ml to medium containing K$^+$ salts of Cl$^-$ (120 mM), HEPES pH 7.2 (10 mM), succinate (10 mM), and phosphate (5 mM) supplemented with MgCl$_2$ (0.5 mM), 5 μM rotenone , 0.67 μM oligomycin. LL or purified LL were added as indicated in figures. Data are summarized in bar graphs as "MitoK$_{ATP}$ activity (%)", given by

$$100 \times [V(x) - V(ATP)]/[V(0) - V(ATP)]$$

where V(x) is the observed steady-state volume at 120 s under the given experimental condition and V(ATP) and V(0) are observed values in the

presence and absence of ATP, respectively. Statistical significance of the difference of the means was assessed using unpaired Student's t-test. A value of $p < 0.05$ was considered significant. It should be noted that $mitoK_{ATP}$-dependent K^+ flux has been validated by 5 independent measurements - light scattering, direct measurements of K^+ flux, H^+ flux, respiration, and H_2O_2 production. Each of these was found to yield quantitatively identical measures of K^+ flux, using valinomycin-induced K^+ flux as a calibrating control (4, 35).

The LL are expected to contain microsomes and peroxisomes (139), which may be a source of H_2O_2. Because H_2O_2 opens $mitoK_{ATP}$ in a $PKC\varepsilon$-dependent manner (93). We examined whether the enzyme catalase (10 units/ml) and the reactive oxygen scavenger, mercapto-propionyl-glycine (MPG, 0.3 mM) inhibited LL-dependent $mitoK_{ATP}$ opening. This treatment had no effect on the ability of the LL to open $mitoK_{ATP}$ (n = 5).

LL-dependent $mitoK_{ATP}$ opening depends on the amount of LL added. The concentration-dependence was determined and the amount used in the assay was sufficient to give a near-V_{max} response. Importantly, the yield of LL from one donor preparation was just sufficient to treat the mitochondria from one assay preparation. Diazoxide was added at 30 μM, sufficient to yield a Vmax response (72).

MPT assays. Opening of the mitochondrial permeability transition (MPT) was synchronized by sequential additions to the assay medium

described above of $CaCl_2$ (100 μM free Ca^{2+}), ruthenium red (0.5 μM, to block further Ca^{2+} uptake), and CCCP (250 nM, to syncronize MPT opening) (32). Rates of volume change were obtained by taking the linear term of a second order polynomial fit of the light scattering trace, calculated over the initial 2 minutes after MPT induction by CCCP. MPT inhibition was calculated by taking the Ca^{2+}-induced swelling rates in the presence and absence of 1 μM cyclosporin A as 100 and 0 %, respectively.

Immunoblot analysis. Immunoblots were performed as described previously (93). 5 μg of protein was separated by SDS-PAGE using 10% acrylamide precast gels (BioRad) and transferred to polyvinylidine difluoride membranes (Millipore) by semi-dry transfer at 12 volts for 50 min. Membranes were blocked with 5% nonfat dry milk in 20 mM Tris-buffered saline and 0.5% Tween-20 (TBS-T) and incubated with primary antibody over night in TBS-T containing 5% BSA. The membrane was then incubated for one hour with the appropriate secondary antibody conjugated to horseradish peroxidase in TBS-T. The membranes were exposed to autoradiograph films, which were scanned. The primary antibody dilutions were as follows: BK2 1:5000 (Santa Cruz Biotechnology), Caveolin-3 1:10,000 (Affinity Bioreagents), VDAC 1:5000 (Affinity Bioreagents), Protein kinase G 1:20,000 (Stressgen), and eNOS 1:500 (BD Transductions Labs).

ImageQuant version 5.0 (Molecular Dynamics) was used to quantify Western blots. Quantification of gel band intensities was initiated by drawing rectangles around appropriate gel bands from the Western blots. By using the method of local averages for background correction, the software reports band intensities for each rectangle. The standard error of the mean for gel band intensities was determined from 4 to 6 replicate Western blots and represents the cumulative error for the total Western analysis assay.

Electron microscopy. For immunogold labeling, aliquots were washed in 20 mM KCl, mounted onto carbon-coated copper grids and fixed for 10 min in 3% paraformaldehyde. The grids were then incubated with Tris-buffered saline containing 0.2% bovine serum albumin (TBS-BSA) for 30 min and subsequently incubated with the primary antibody (20 µg/mL mouse monoclonal caveolin-3; BD Transduction Labs) in TBS-BSA for 30 min. The grids were washed three times for 5 min each in TBS-BSA and then incubated with the secondary antibody (1:100 dilution of 10 nm gold-conjugated goat anti-mouse IgG; Sigma) in TBS-BSA for 30 min. The grids were washed once in TBS-BSA and five more times in distilled H_2O. Control experiments were performed by omission of the primary antibody (42, 187, 207, 229). Grids were stained with 2% uranyl acetate, and examined with a JEOL TEM 100CX microscope.

Chemicals. KT5823 and protein phosphatase 2A (PP2A) were

103

purchased from Calbiochem. The PKC isoform-specific peptides εV_{1-2} and

$\Psi\varepsilon RACK$ were synthesized by EZ Biolabs (Westfield, IN), according to the

published amino acid sequences (27). Optiprep was purchased from Axis-

Schield PoC AS (Oslo, Norway). Bafilomycin A1, methyl-β-cyclodextrin and all

other chemicals were from Sigma.

4.4 Results

Bradykinin perfusion opens mitoK$_{ATP}$ by phosphorylation.

Bradykinin's cardioprotection is blocked by 5-hydroxydecanoate (5-HD) and

therefore presumed to require mitoK$_{ATP}$ opening (160, 173); however this has

not previously been demonstrated. Bradykinin-treatment acts via PKG, which

interacts with mitochondria to open mitoK$_{ATP}$ via a PKCϵ-mediated

phosphorylation (31). Thus, bradykinin perfusion should cause a persistent

open state of mitoK$_{ATP}$ that is reversed by dephosphorylation. We isolated

mitochondria from bradykinin-perfused and sham-perfusion hearts and

prepared mitoplasts to permit access of the phosphatase PP2A to the inner

membrane, which cannot cross the mitochondrial outer membrane (MOM).

The results are presented in Fig. 4.2. In mitoplasts from untreated hearts

("sham perfusion"), mitoK$_{ATP}$ was inhibited by ATP. As expected, ATP

inhibition was reversed by diazoxide, and PP2A had no effect (not shown). In

mitoplasts from bradykinin-treated hearts ("bradykinin perfusion"), mitoK$_{ATP}$

was resistant to inhibition by ATP unless PP2A was present (Fig. 4.2).

Bradykinin-dependent mitoK$_{ATP}$ opening was maximal, as shown by the fact

that diazoxide had no further effect and by the finding that the bradykinin-

dependent open state was equal to that observed in the presence of ATP +

PP2A + diazoxide. The data in Fig. 4.2 show for the first time that mitoK$_{ATP}$ is

Figure 4.2. Bradykinin-perfusion causes a persistent open state of mitoK$_{ATP}$. Shown are changes in "% MitoK$_{ATP}$ activity", calculated as described in "Methods". Mitoplasts were prepared from mitochondria isolated from perfused rat hearts, as described in "Methods". Mitoplasts from "sham-perfused" (no treatment) and "bradykinin-perfused" hearts were compared for the response of mitoK$_{ATP}$ to ATP (0.2 mM), ATP + protein phosphatase PP2A (11 ng/mL), ATP + diazoxide ("Dzx", 30 μM), and ATP + PP2A + Dzx. MitoK$_{ATP}$ from bradykinin-perfused hearts was open and unresponsive to ATP unless PP2A was added. This indicates that the persistence of the open state was due to phosphorylation. Data are averages ± SD of 3 experiments from 3 separate perfusions.
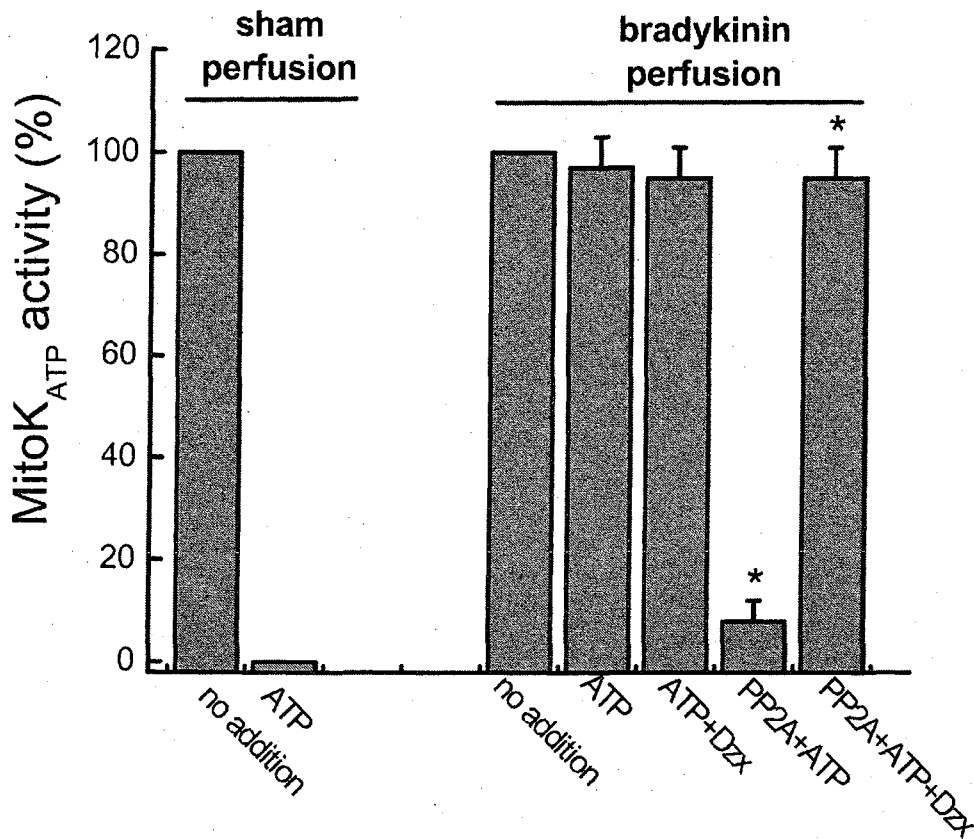
opened *ex vivo* when the heart is perfused with a cardioprotective agent.

Purified LL from bradykinin-treated hearts open mitoK$_{ATP}$ via PKG and mitochondrial PKCε. To test whether the mitochondria-associated LL contained signaling enzymes capable of opening mitoK$_{ATP}$, we added LL aliquots to purified mitochondria from untreated assay hearts. The representative traces in Fig. 4.3 show that both the LL and the purified LL from bradykinin-treated hearts reversed the ATP inhibition and opened mitoK$_{ATP}$. LL from untreated hearts ("sham LL") and residual LL ("RLL") from bradykinin-treated hearts had no effect. (RLL contain the proteins that remained after purified LL were isolated from LL).

Light scattering data from an extensive series of experiments are summarized in Fig. 4.4. LL from control hearts ("sham LL)" and isolated plasma membrane caveolae ("caveolae") had no effect on mitoK$_{ATP}$ or on the effect of diazoxide (n = 10). The LL from bradykinin-treated hearts ("bradykinin LL") opened mitoK$_{ATP}$ to the same extent as diazoxide (n = 10). Addition of diazoxide plus the bradykinin-LL had no further effect, so the bradykinin LL opened mitoK$_{ATP}$ maximally. MitoK$_{ATP}$ opening by the bradykinin-LL was blocked by 5-HD, acting directly on the channel.

Figure 4.3. LL and Purified LL from bradykinin-treated hearts open mitoK$_{ATP}$ in isolated mitochondria. Mitochondrial matrix volume is plotted versus time. Aliquots of LL ("LL", 10-15 µg/ml), purified LL ("PLL", 0.5 µg/ml), and residual LL ("RLL", 10-15 µg/ml) were added to medium one second after the mitochondria. ATP (0.2 mM) was present in each run. KT5823, a PKG inhibitor, was added at 0.5 µM. Traces are representative of at least 5 independent experiments. 6 separate traces are plotted in the figure, and some of them are superimposed.
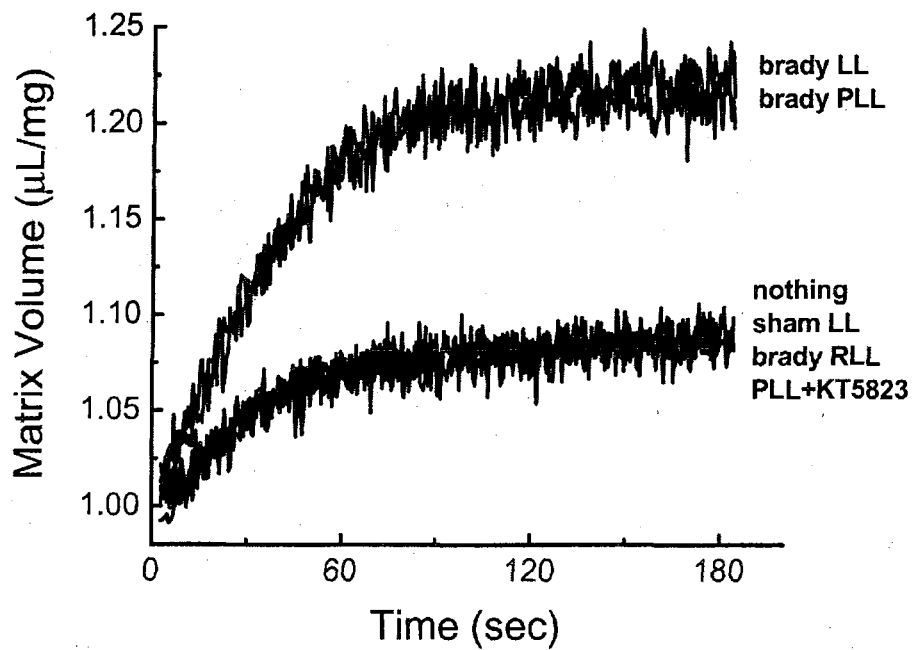
Figure 4.4. Properties of LL-induced mitoK$_{ATP}$ opening. Shown are changes in "MitoK$_{ATP}$ activity (%)". LL from sham-perfused hearts ("sham LL") had no effect on mitoK$_{ATP}$ activity (n = 3). Caveolae isolated from untreated hearts (206) did not open mitoK$_{ATP}$ at amounts up to 700 µg per mg of mitochondrial protein. (Shown are data using 300 µg/mg of caveolae, n = 3). The bradykinin LL induced mitoK$_{ATP}$-opening that was inhibited by 5-HD (1.0 mM) and εV_{1-2} (0.5 µM). Note that a higher concentration of 5-HD is required to block mitoK$_{ATP}$ after it has been opened by phosphorylation (31). The bradykinin LL opened mitoK$_{ATP}$ to the same extent as diazoxide ("dzx"), and diazoxide had no additional effect in the presence of the bradykinin LL. Bradykinin data are averages ± SD of at least 4 independent experiments.

109
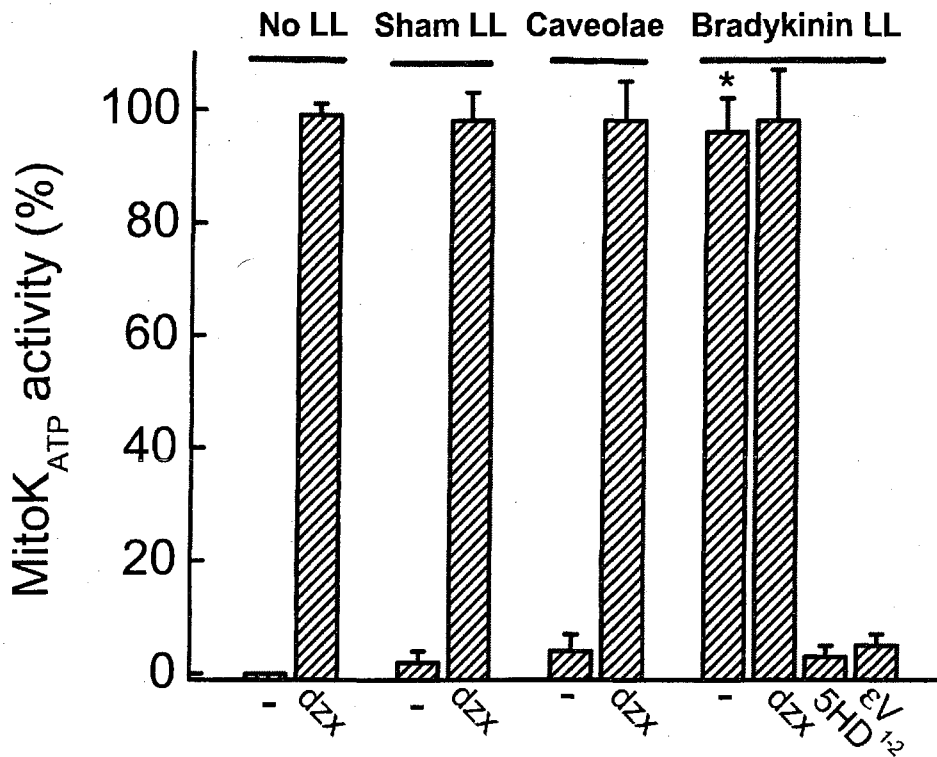
It was also blocked by εV_{1-2}, showing that LL-dependent mitoK$_{ATP}$ opening was mediated via PKCε. A complete set of experiments (N = 8) was also carried out with the bradykinin purified LL (not shown), which exhibited results identical to those of the bradykinin LL. For the practical reason that purified LL are more time-consuming to prepare, we carried out the majority of functional experiments using LL.

Expressed per mg of mitochondrial protein, LL from bradykinin-perfused and sham-perfused hearts were 130 μg/mg and 100 μg/mg, respectively. Purified LL from treated and sham were 8 μg/mg and 3.7 μg/mg, respectively. Thus, the LL purification removed 94% of the LL protein, and the 16-fold increase in specific activity of the purified LL shows a strong purification of functionality. The 1:125 protein ratio (purified LL to mitochondrial protein) permits a rough estimate to be made of the size of the putative signalosomes. Assuming that the protein ratio is roughly equal to the volume ratio, we calculate the diameter of the signalosomes to be about 140 nm, in excellent agreement with the size observed by electron microscopy, described below.

LL recovered from hearts after ouabain perfusion, ischemic preconditioning, and ischemic postconditioning open mitoK$_{ATP}$. We carried out experiments with other models of cardioprotection in order to

estimate the generality of this mechanism. We performed ischemic preconditioning, ischemic postconditioning, or perfused the hearts with the known protective ligand, ouabain (173), then isolated the LL and determined their effects on mitochondria from untreated hearts. As can be seen in Fig. 4.5 (first bar of each group), each of these treatments led to signalosomes capable of opening $mitoK_{ATP}$. LL-dependent $mitoK_{ATP}$ opening by each treatment was blocked by 5-HD and εV_{1-2}, acting at the level of inner membrane $mitoK_{ATP}$ and $PKC\varepsilon$, respectively (93) (not shown).

As shown in Fig. 4.5, the effects of bradykinin perfusion, ischemic preconditioning, and ischemic postconditioning were blocked by KT5823, indicating that these GPCR-coupled protective mechanisms act on mitochondria via PKG contained in the signalosome. The $mitoK_{ATP}$ opening effects of ouabain LL were not blocked by KT5823, indicating that PKG is not the terminal kinase of these signalosomes. This is in agreement with the finding in perfused hearts that KT5823 blocked cardioprotection by bradykinin but did not block cardioprotection by ouabain (173). In further experiments not shown, we found that other models of cardioprotection, including acetylcholine and elevated perfusate Ca^{2+} also led to LL that open $mitoK_{ATP}$ (n = 1 to 3 for

Figure 4.5. LL-induced mitoK_ATP opening following IPC and ouabain treatment. Shown are changes in "MitoK_ATP activity (%)" when bradykinin LL, IPC LL, ouabain LL, or ischemic postconditioning LL were added to assay mitochondria. Also shown are the effects of PP2A (11 ng/mL) and KT5823 ("KT", 0.5 µM) added to the assay. Note that PP2A cannot cross the MOM of intact mitochondria, so the effect is on the MOM. Data are averages ± SD of 3 to 4 independent experiments.
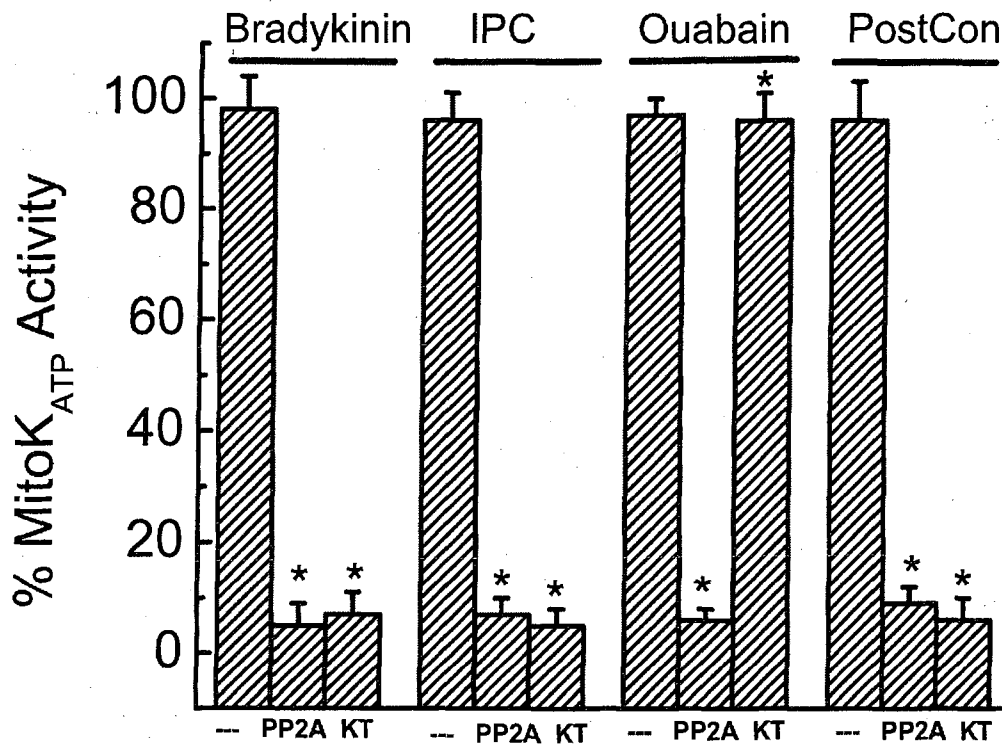
each treatment).

Role of the mitochondrial outer membrane (MOM) in LL signaling.
As shown in Fig. 4.5, LL-induced mitoK$_{ATP}$ opening was blocked in each case
by PP2A added to the assay medium. In these experiments, in contrast to
those of Fig. 4.2, the MOM was intact. Because PP2A cannot cross the MOM,
the results indicate that signalosome activity required phosphorylation of a
MOM protein. We used mitoplasts to study the effects of MOM removal on
mitoK$_{ATP}$ opening by various treatments. The findings (not shown) may be
summarized as follows: MOM removal had no effect on diazoxide-induced
mitoK$_{ATP}$ opening, but it abolished the abilities of PKG + cGMP and the
bradykinin, ouabain, and IPC LL to open mitoK$_{ATP}$. Thus the MOM is essential
for the action of the LL, and the effect of PP2A (Fig. 4.5) indicates that the LL
is phosphorylating a MOM protein, whose identity is not yet known.

LL from interfibrillar mitchondria of bradykinin-treated hearts
opens mitoK$_{ATP}$. Cardiomyocytes contain two populations of mitochondria,
subsarcolemmal (SSM) and interfibrillar (IFM), that exhibit subtle bioenergetic
differences (166). Standard isolation yields a primarily subsarcolemmal
population. We investigated whether active LL could also be isolated from
IFM, which largely supply ATP to contractile ATPases. We found that LL from
IFM opened mitoK$_{ATP}$ to the same extent as diazoxide and otherwise behaved
identically with LL from SSM (data not shown, n = 5). Separation of SSM and

IFM is imperfect; however, the fact that aliquots of LL from each fraction opened mitoK$_{ATP}$ maximally indicates that we were not studying a mixture of active and inactive fractions.

Bradykinin LL inhibits the mitochondrial permeability transition (MPT). The elevated calcium and ROS that occurs during ischemia-reperfusion causes MPT opening, and this is inhibited by cardioprotective agents (87). PKG-dependent MPT inhibition is a result of mitoK$_{ATP}$ opening, an increase in mitochondrial ROS production, and activation of an inner membrane PKCε that inhibits MPT ((32) and see Fig. 4.10). Thus, ROS are necessary for both initiation and prevention of MPT opening (32). As shown in Fig. 4.6, the bradykinin LL inhibited MPT opening and did so to the same extent as diazoxide. MPT inhibition by the bradykinin LL follows the same pattern as was observed in Fig. 4.6 for mitoK$_{ATP}$ opening - it is abolished by 5-HD, KT5823, and PP2A.

Activity of the bradykinin LL Is sensitive to methyl-β-cyclodextrin and bafilomycin a1, but not to triton x-100. Hearts were treated with bafilomycin A1, an inhibitor of receptor recycling (98), for 5 min prior to and during treatment with bradykinin. LL and purified LL obtained from these hearts failed to open mitoK$_{ATP}$ (Fig. 4.7). Treatment of the LL with the cholesterol binding agent, methyl-β-cyclodextrin, abolished LL-induced mitoK$_{ATP}$-opening (Fig. 4.7) and dissolved the purified LL, as revealed by the

Figure 4.6. LL-induced inhibition of the mitochondrial permeability transition (MPT). LL inhibition of MPT in isolated heart mitochondria and the effects of various antagonists are shown. Data are plotted as "MPT inhibition (%)". Additions were: LL (10-15 μg/ml), diazoxide ("dzx", 30 μM), 5-HD (0.3 mM), KT5823 ("KT", 0.5 μM), and PP2A (11 ng/ml). Data are shown as average ± SD of at least 4 independent experiments.
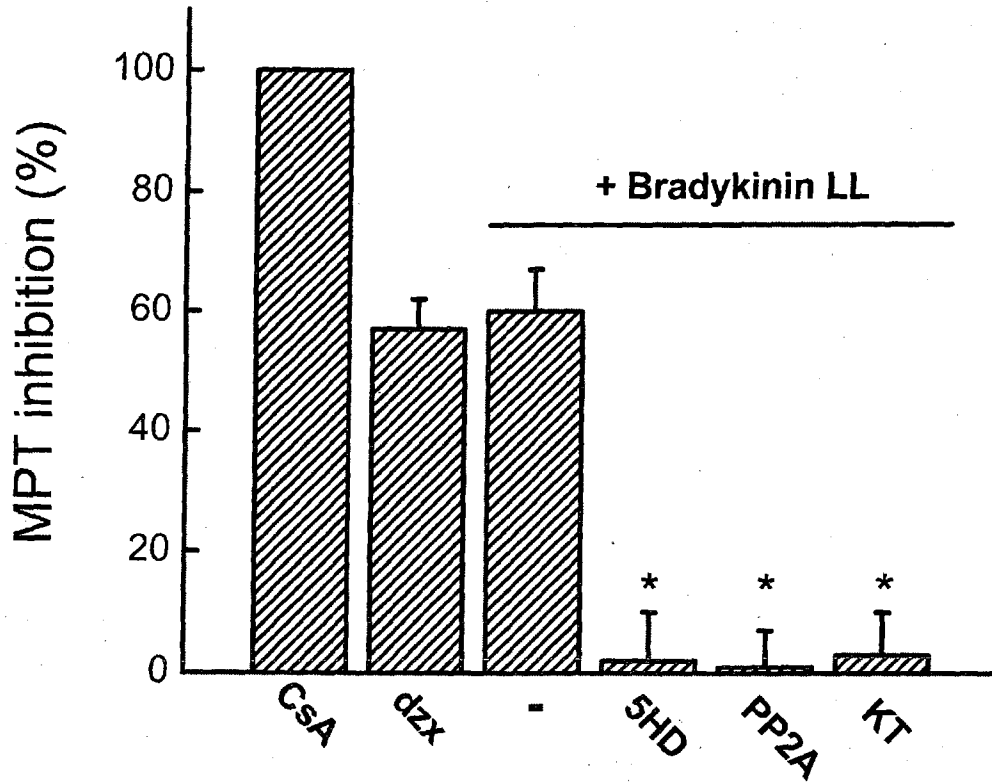
absence of a pellet after centrifugation. Neither of these treatments affected diazoxide-dependent mitoK_{ATP} opening, showing that the observed effects were due to inactivity of the LL and not to mitochondrial damage caused by adding the treated LL. To further characterize the nature of the purified LL, we investigated its response to the nonionic detergent Triton X-100. Activity of purified LL from bradykinin treated hearts was not affected by treatment with 1 % Triton X-100 (Fig. 4.7).

Presence of the bradykinin receptor and caveolin-3 in purified LL from treated hearts. Mitochondria ("Mito") and purified LL ("PLL") from donor hearts perfused with medium containing no bradykinin ("sham perfusion") or bradykinin ("bradykinin") were obtained as described in Fig. 4.1 and "Methods". As shown in Fig. 4.8A, the bradykinin receptor B2K was detected uniquely in the bradykinin Purified LL, and caveolin-3 was strongly enriched. The endothelial nitric oxide synthase (eNOS), a known component of bradykinin signal transduction (160), was also found to be enriched in the bradykinin fraction. PKG was found in all samples. Because the bradykinin purified LL contains twice as much protein as the sham purified LL and the same amount of protein was used for each sample, we estimate that the purified LL from bradykinin-treated hearts contained about twice as much total PKG as the purified LL from sham-treated hearts (Fig. 4.8B). VDAC was used as a mitochondrial marker, and its immunoblots demonstrate minimal

Figure 4.7. Bafilomycin A or methyl-β-cyclodextrin abolish LL-induced mitoK$_{ATP}$ opening, triton X-100 does not. Shown are changes in "MitoK$_{ATP}$ activity (%)". These experiments examine the effects of bafilomycin A (50 nM), methyl-β-cyclodextrin (MCD) (5%) and Triton X-100 (1%) on mitoK$_{ATP}$ opening induced by bradykinin LL. Bafilomycin was added to the heart perfusate prior to isolation of the LL. MCD, a cholesterol-binding agent, was incubated with LL at 30°C for 5 min prior to assay. Triton X-100 was incubated with purified LL for 10 min at 4° C. Prior to assay, the vesicles were pelleted in a microcentrifuge (16,000 x g for 15 min), washed twice in dilute salt solution, and resuspended in buffer without Triton X-100. Diazoxide ("dzx", 30 μM) was added at the same time as the LL aliquot (10-15 μg/ml). Data are average ± SD of at least 3 independent experiments.* indicates $p < 0.05$ vs. corresponding LL.
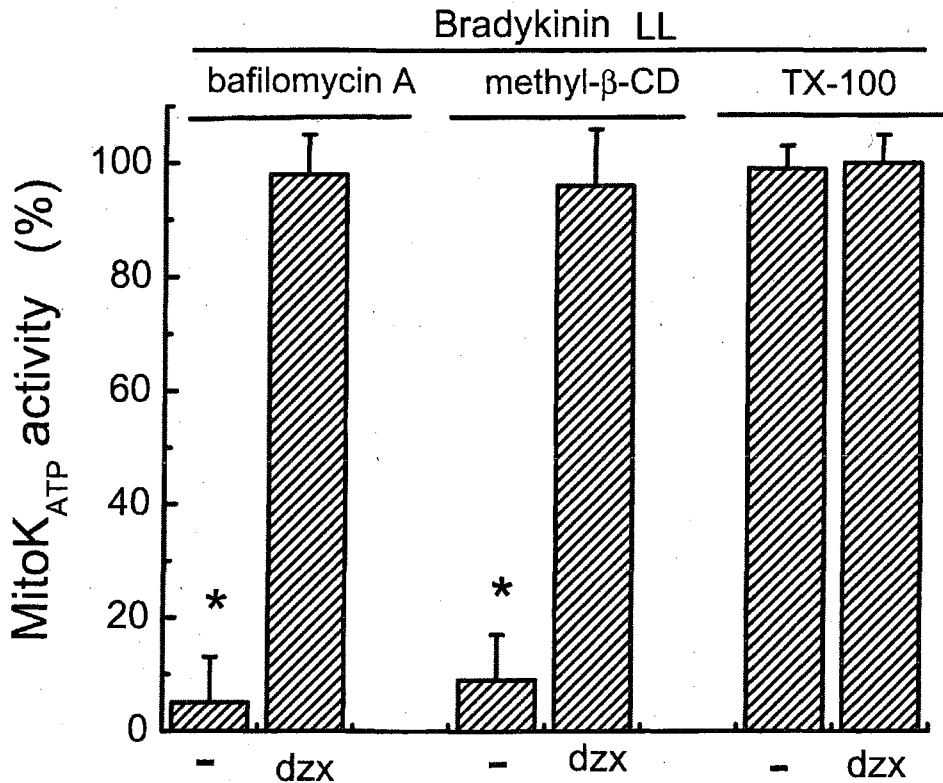
mitochondrial contamination in both purified LL. Fig. 4.8B shows the result of a densitometric analysis of the bands from six independent Western blots.

Immunogold labeling of caveolin-3 in the purified LL. We performed immunogold labeling studies using an antibody to caveolin-3. As shown by the representative example in Fig. 4.9A, each vesicle was decorated with several gold particles, indicating multiple copies of caveolin-3 in the vesicles. Fig. 4.9B, obtained in the absence of primary antibody shows no nonspecific binding of colloidal gold. Transmission electron micrography of Triton X-100-purified LL was also performed to measure vesicle dimensions. The mean diameter of the roughly spherical vesicles was 137 ± 25 nm (n = 48). The residual LL contained no vesicles. Purified LL from sham-perfused hearts contained 15-20% as many vesicles as purified LL from bradykinin-treated hearts, but these were ineffective in opening mitoK$_{ATP}$ (Fig. 4.3).

Figure 4.8. Immunodetection analysis of bradykinin signalosomes. (A)
Shown are representative immunoblots of 6 independent experiments. 5 µg of
mitochondria protein ("MITO") from perfused untreated-hearts, or 5 µg purified
LL ("PLL") from untreated ("sham-perfusion") or bradykinin-treated
("bradykinin") hearts, obtained as described in "Methods", were loaded. For
each antigen, the signal shown was obtained on samples loaded on the same
gel and processed under the same conditions.
(B) Pixel density analysis performed on each band of N = 6 Western blots.
"BG" is the pixel density of a protein-free region of the blot.

119
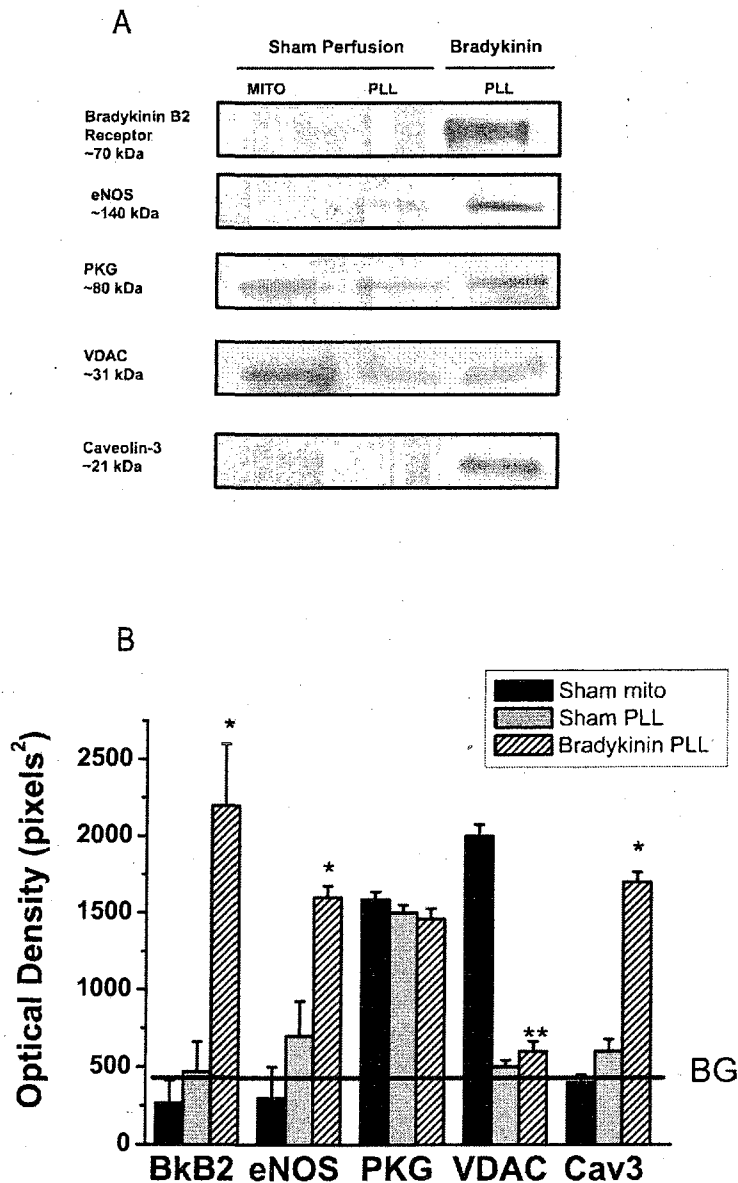
Figure 4.9. Immunogold staining of bradykinin signalosomes.
Transmission electron microscopic analysis of purified LL from bradykinin-perfused hearts. Samples were applied to carbon-coated grids, fixed, and processed for the presence of immunogold-labeling when treated either **(A)** with the primary antibody caveolin-3 or (Mag = 100,000x) **(B)** without the primary antibody, as a negative control (Mag = 67,000x).

A
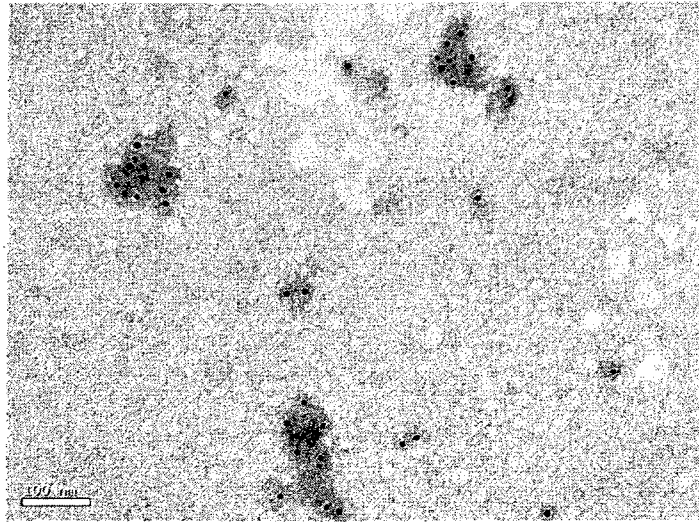
B
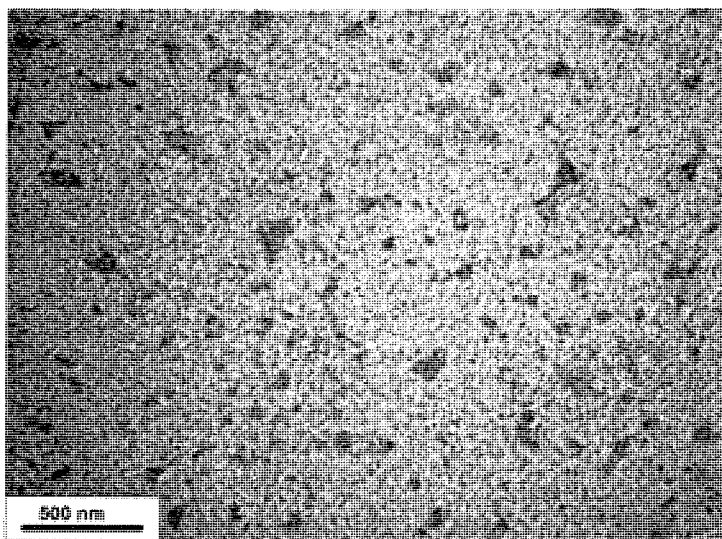
4.5 Discussion

The cardioprotective signal arising from bradykinin treatment is transmitted from the bradykinin receptor to the mitochondrial outer membrane (MOM), where it initiates the intramitochondrial signaling pathway described in recent publications (4, 31-33, 93) and in Fig. 4.10. The objective of the present study was to understand how the signal passes through the cytosol to mitochondria. We propose that the pathway is mediated by signalosomes, which are vesicular, multimolecular signaling complexes that are assembled in caveolae and deliver signals to cytosolic targets, including mitochondria. We first established that bradykinin treatment caused phosphorylation-dependent mitoK$_{ATP}$ opening in the donor mitochondria (Fig. 4.2). Using the protocols described in Fig. 4.1, we then isolated functionally active signalosomes from the same donor mitochondria. These were found to open mitoK$_{ATP}$ in mitochondria from untreated hearts (Fig. 4.3). This finding is consistent with, but does not prove, the suggestion that these vesicles were responsible for the mitoK$_{ATP}$ opening that was observed in the experiments of Fig.4.2.

The remaining experiments of this study focus on the functional effects of the isolated signalosomes, on their physical properties, and on the generality of the signalosome mechanism. The signalosome-containing LL and purified LL were able to open mitoK$_{ATP}$ in mitochondria from untreated

hearts to maximum capacity (Figs. 4.3 and 4.4). As expected from previous results (31, 32), mitoK$_{ATP}$ opening was blocked by 5-HD and ϵV_{1-2} acting at the level of the inner membrane (Figs. 4.4 and 4.10). Importantly, three different control preparations had no effect on mitoK$_{ATP}$ — a caveolar preparation isolated from cardiac sarcolemma (Fig 4.4), purified LL from untreated hearts (Figs. 4.3 and 4.4), and the residual LL (RLL) obtained after removal of the purified LL from the LL preparation (Fig. 4.3).

MitoK$_{ATP}$ opening by the bradykinin-LL was blocked by the PKG inhibitor KT5823 (Fig. 4.5), confirming previous studies showing that PKG is the terminal cytosolic kinase of the bradykinin signaling pathway (31, 32). LL-dependent mitoK$_{ATP}$ opening was also blocked by the Ser-Thr phosphatase PP2A (Fig. 4.5), indicating that phosphorylation of a MOM protein is an essential step in transmitting the signal to mitochondria. This was confirmed by the further finding that removal of the MOM abolished all effects of LL on mitoK$_{ATP}$ activity (not shown). Thus, the effects of bradykinin-LL on mitoK$_{ATP}$ were identical to the previously reported effects of adding exogenous PKG plus cGMP (31).

We have not yet identified the outer membrane target of PKG ("R1" in Fig. 4.10), and we can only speculate on the nature of the link between cytosolic PKG and mitochondrial PKCϵ. Several kinases have been observed associated with mitochondria in the cardioprotected

Figure 4.10. Signalosome hypothesis. It is proposed that interaction of bradykinin with its receptor induces formation of a vesicular caveolar signaling platform (signalosome) that phosphorylates a receptor (R1) on the mitochondrial outer membrane (MOM). The identity of R1 is unknown. The terminal kinase of the bradykinin signalosome is PKG, which phosphorylates R1 at a Ser/Thr residue. Following phosphorylation of the MOM receptor, the signal is transmitted across the intermembrane space to activate PKCε1 on the mitochondrial inner membrane. PKCε1, which is constitutively expressed in mitochondria (32) and localized in close association with mitoK$_{ATP}$ (123), causes mitoK$_{ATP}$ opening (31) and consequent increase in H_2O_2 production (4). The H_2O_2 then activates a second PKCε, PKCε2, which leads to reduction in necrosis through inhibition of the mitochondrial permeability transition (MPT) (32).
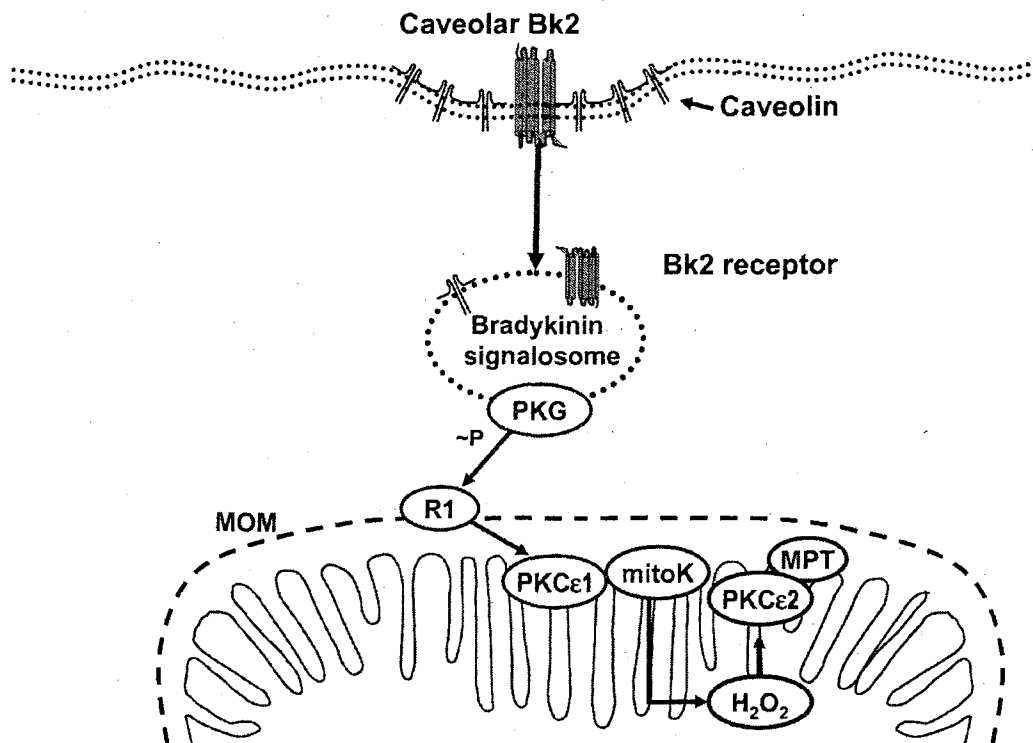
phenotype. Increased phosphorylation of mitochondrial mitogen-activated protein kinase (MAPK) has been observed, and PKCε has been shown to phosphorylate VDAC, but the functional consequences of these observations are not well understood (11, 12). Akt has been shown to phosphorylate hexokinase-II and modulate the MPT (142). Current experiments in our laboratory indicate a role for a MOM MAPK in cardioprotective conditioning mediated by the ouabain signalosome, but this MAPK is not involved in PKG signaling. We have found that PKG-dependent signaling from R1 to PKCε ("PKCε1" in Fig. 4.10) is not prevented by MPG, and therefore this step does not involve ROS. The mechanism of PKCε1 activation is unknown; however, PKCε1 is activated by ψεRACK (31), and we speculate that the connection between R1 and PKCε1 operates by a pseudo-RACK mechanism (receptor for activated C kinase) (190).

Signal transmission by signalosome appears to be a general phenomenon. Ischemic preconditioning, ischemic postconditioning, and ouabain perfusion each lead to LL that open mitoK$_{ATP}$ (Fig. 4.5). A limited survery showed that perfusion with acetylcholine or elevated Ca^{2+} also lead to LL that open mitoK$_{ATP}$.

The results of Fig. 4.6 show that the bradykinin LL causes inhibition of MPT, which is widely thought to be responsible for cell death from ischemia-reperfusion injury (38). We infer from this result that mitoK$_{ATP}$ opening by the

bradykinin signalosome mediates the MPT inhibition afforded by bradykinin (168).

Both clathrin-mediated and caveolar-mediated endocytosis and recycling depend on endosomal acidification by the vacuolar H(+)-ATPase (98, 140, 211), which occurs when the vesicles pinch off from the plasma membrane (140). Consistent with this, bafilomycin A1, a specific inhibitor of the vacuolar H(+)-ATPase, prevented signalosome function (Fig. 4.7). Interestingly, Western blots of the bradykinin purified LL were identical to those obtained in the absence of bafilomycin (data not shown), in agreement with the finding that bafilomycin blocks receptor return to the plasma membrane without affecting receptor internalization (14, 98). This suggests that signalosome-mediated delivery of the cardioprotective signal to mitochondria is a dynamic process that requires both internalization and return to the plasma membrane. Further investigation is warranted to test this hypothesis.

Resistance to Triton X-100 and sensitivity to methyl-β-cyclodextrin (Fig. 4.7), together with the Western blot data showing enrichment with caveolin-3 (Fig. 4.8), are consistent with a caveolar origin of the signaling platform (169, 205). The immunoblot analyses of Fig. 4.8 show that purified LL from bradykinin-perfused hearts contain the bradykinin receptor BK2, caveolin-3, PKG, and eNOS. Finally, electron microscopy of immunogold labeled purified LL revealed that the vesicles contain multiple copies of caveolin-3 (Fig. 4.9).

In general support of the signalosome hypothesis, there is considerable evidence from a variety of cell types that activated G-protein-coupled receptors first migrate to caveolae, where caveolins compartmentalize receptors and signaling molecules (36, 53, 129, 134, 175, 184), assemble them into a signaling platform (78, 225), and deliver the platform to the cytosol by internalization (85, 134, 138, 183, 184, 219). The hypothesis is also consistent with the findings of Tong, et al. (218), who showed that receptor internalization and recycling are essential for cardioprotection by IPC. Signalosome-mediated signaling has previously been postulated to occur in heart in conditions other than cardioprotection (15, 55, 180, 202). The data presented here appear to be the first demonstration of a specific functional property of purified cardiac signalosomes.

These findings represent an initial step in our effort to apprehend the organization of the complex signaling pathways of cardioprotection. The signalosome hypothesis offers a new perspective for understanding and studying cardioprotective signaling in the heart; however the concept remains a working hypothesis that will require additional critical experiments to test its predictions and validity.

5. Ouabain cardioprotection is mediated by a signalosome mechanism acting on mitochondrial p38-MAPK

5.1 Summary

This chapter serves to extend and strengthen the signalosome hypothesis for cardioprotection. The digitalis-like cardiac glycoside ouabain activates an intracellular signaling cascade that is cardioprotective. Ouabain cardioprotection is mediated by the mitochondrial ATP-sensitive K+ channel (mitoK$_{ATP}$), as well as kinases such as protein kinase C (PKC) and Src kinase. This study explores the enzymatic components of the ouabain cardioprotective pathway and proposes a hypothesis for their regulation. It is proposed that, similar to bradykinin, a cardioprotective signalosome is formed upon treatment with ouabain. The ouabain signalosome is a subfraction isolated from the mitochondrial fraction of ouabain-treated hearts. It is characterized as a low-density membrane compartment that is enriched in caveolin-3, Src kinase, and PKCε. Addition of the isolated signalosome to untreated mitochondria in an *in vitro* assay of mitoK$_{ATP}$ activity opens mitoK$_{ATP}$. This effect can be blocked by inhibitors Src kinase, PKCε, and p38 mitogen-activated protein kinase (p38 MAPK). These data suggest that ouabain cardioprotection is mediated by a p38 MAPK that is located in mitochondria and acting upstream of mitoK$_{ATP}$.

5.2 Introduction

The Na,K-ATPase has two functions in cardiac physiology. It is an energy transducer, using the energy from ATP hydrolysis to transport Na+ and K+ across the cell membrane against their electrochemical gradients. When activated by digitalis, the Na,K-ATPase is also a signal transducer, leading to activation of PI3K/Akt pathways implicated in the control of both physiological and pathological cardiac hypertrophy (132). The signaling function of the digitalis-Na,K-ATPase complex also plays a role in digitalis-induced positive inotropy. The accepted hypothesis for the mechanism of this effect is that partial inhibition of the Na,K-ATPase leads to an increase in $[Na^+]_i$ that exchanges with Ca^{2+} on the Na^+-Ca^{2+} exchanger. The elevated $[Ca^{2+}]_i$, in turn, acts on contractile proteins to increase contractile force (208). It was recently shown that the inotropic response of the perfused rat heart to elevated Ca^{2+}, dobutamine, or ouabain was substantially inhibited by two different blockers of the mitochondrial ATP-sensitive K^+ channel (mitoK$_{ATP}$) (73). Similar effects of mitoK$_{ATP}$ inhibition on contractility were observed in rat cardiomyocytes (217) and in human atrial fibers (73), implying that digitalis causes a signal to move rapidly to mitochondria.

The signaling function of the digitalis-Na,K-ATPase complex also leads to cardioprotection from ischemia-reperfusion injury (173, 181). Thus, ouabain administered to the perfused rat heart before ischemia provided improved

hemodynamic recovery and reduced infarct size after reperfusion. Similar

results have been obtained in the perfused rabbit heart (S. Pierre,

unpublished observations). Ouabain cardioprotection involves receptor-

activated recruitment of protein kinases such as Src kinase and Protein kinase

C (PKC) into signaling complexes that mediate cardioprotection (173, 181,

215). Here again, the signal moves to mitochondria, because It has been

shown that ouabain cardioprotection requires mitoK$_{ATP}$ activation and reactive

oxygen species (ROS) production.

In Chapter 4 of this study, I proposed that the signaling cascade in

response to bradykinin perfusion is assembled into a vesicular signalosome in

caveolae, after which it moves to mitochondria to open mitoK$_{ATP}$. We found

that hearts treated with bradykinin contained a mitochondria-associated

signalosome fraction that was recoverable for study (186). The signalosome

possessed a number of unique properties both biochemically and

physiologically, including its low-density caveolar nature as well as its ability to

open mitoK$_{ATP}$ *in vitro*. In the exploration of this hypothesis we also found that

there was some generality to the proposed mechanism in that hearts that had

undergone ischemic preconditioning, postconditioning or ouabain treatment

also contained a signalosome fraction that was capable of opening mitoK$_{ATP}$

and inhibiting the mitochondrial permeability transition (MPT).

In the present study, rat hearts perfused with ouabain yielded a mitochondria-associated low-density signalosome fraction enriched in caveolin-3, Src, PKCε and the α-subunit of the N^+,K^+-ATPase. We show that this subfraction is capable of opening mitoK_{ATP} and inhibiting MPT *in vitro*. We find that the signalosome-associated Src and PKCε behave as parallel terminal kinases to phosphorylate a p38 mitogen-activated protein kinase (MAPK) in the mitochondrial outer membrane (MOM) that resides upstream of mitoK_{ATP}. In further exploration of the role of p38 MAPK, we find that ouabain cardioprotection is blocked by the p38 MAPK inhibitor SB203580, and that cardioprotection afforded by the MAPK activator anisomycin is blocked by the mitoK_{ATP} blocker 5HD. These data support the hypothesis that ouabain-mediated cardioprotection is acting through a signalosome mechanism to activate a mitochondrial p38 MAPK.

5.3 Methods

Isolated heart perfusions:

Male Wistar rats (200-220g) were anesthetized with carbon dioxide and immediately decapitated. Hearts were rapidly excised, submerged in iced Krebs buffer, and perfused by an aortic cannula delivering normothermic (37°C) modified Krebs Henseleit solution containing (in mM) 118 NaCl, 5.9 KCl, 1.75 $CaCl_2$, 1.2 mM $MgSO_4$, 0.5 EDTA, 25 $NaHCO_3$, 16.7 glucose at pH 7.4. The perfusate was gassed with 95% O_2 - 5% CO_2, which results in a pO_2 above 600 mmHg at the level of the aortic canula. All perfusions prior to mitochondria and signalosome isolation were 50 min long. Drug perfusions were comprised of 25 min stabilization, 15 min bradykinin (100 nM) or ouabain (50 μM), and 10 min wash. Control perfusions were 50 min without interruption.

To assess infarct size and functional recovery following drug treatments and ischemia, seven groups of hearts were studied (n = 4-6 in each group). Following stabilization and pretreatment, all groups were exposed to 25-min zero-flow global ischemia followed by 120 min of reperfusion with standard Krebs solution. The ischemia-reperfusion group (IR) was allowed to stabilize under aerobic conditions for 40 min. Prior to ischemia, the ouabain- (Ouab) and bradykinin- (BK) treated groups were allowed to stabilize under aerobic conditions for 25 min, followed by 15 min perfusion with a buffer containing 50

131

mM of ouabain, 100 nM bradykinin, or 5 μM anisomycin, respectively. Where used, 5HD (300 μM) or SB203580 (1 μM), were added to the perfusate 5 min before ouabain, bradykinin or anisomycin, and included in the perfusate during the subsequent 15 min perfusion with ouabain, bradykinin or anisomycin.

Following ischemia, the hearts in each group were reperfused for 120 min and infarct size was estimated by the method of Ytrehus, et al. (241). The infarct staining protocol was as follows, 15 ml of 1% wt/vol 2,3,5-Triphenyltetrazolium chloride (TTC) in phosphate–buffered saline pH 7.4 at 37 °C was infused into the coronary circulation at a rate of 0.5 ml/gm/min. The eluted stain from the cardiac veins was collected and recirculated. After approximately 15 min of perfusion the epicardial surface was deep red. Hearts were then removed from the cannula and fixed overnight in 10 % Formalin. Hearts were removed from formalin, sectioned along the atrioventricular plane into ~1mm sections. Sections were placed between two microscope slides and computerized area analysis was performed using Scion image and the infarct size of each heart was expressed as a fraction of the total area at risk. Infarct size for each heart was determined by averaging the infarct area of the 5-6 cross-sections. The rate-pressure product (RPP) data shown if Fig. 5.7A were calculated using the average RPP measured during the 15-min drug treatment for each experimental condition. The experimental protocols complied with the Guiding Principles in the Use and Care of Animals published

by the National Institutes of Health (NIH Publication No. 85-23, revised 1996).

Mitochondria Isolation

Mitochondria from rat hearts were isolated immediately following 50 min

Langendorff perfusions. Mitochondria from untreated *assay* rat hearts and

livers were isolated by differential centrifugation without previous perfusion, as

thoroughly described in chapter 2 (31). The resulting crude mitochondrial

fractions were further purified in a self-generated 24% Percoll gradient,

resulting in a purified mitochondrial fraction and a low-density fraction enriched

in caveolin and signaling molecules, which we have termed the light layer or

LL. Mitochondrial protein concentration was estimated using the Biuret

reaction (75).

Signalosome isolation – Purified LL (PLL)

The purification was exactly as that described in chapter 4 and in the non-

detergent caveolae isolation protocol of Smart et al (207). Briefly, the LL

fraction was adjusted to 2 ml, mixed with 50% Optiprep in buffer A (250 mM

sucrose, 20 mM TRIS-Cl (pH 7.8), 1 mM EDTA), and placed in the bottom of a

12 ml centrifuge tube. A 20-10% Optiprep gradient was layered on top, and

the tubes were centrifuged at 52,000x*g* for 90 min. Following centrifugation,

the top 5 ml were collected and mixed with 4 ml of the 50% Optiprep solution.

This mixture was then overlayed with a 5% Optiprep solution and centrifuged

again at 52,000x*g* for 90 min. The signalosome fraction was identified as an opaque band at the 5% interface.

Matrix volume measurements

MitoK$_{ATP}$ assays. MitoK$_{ATP}$ activity is determined by monitoring changes in mitochondrial light scattering, as previously described (16, 31, 35). Mitochondria from untreated assay hearts were added at 0.1 mg/ml to medium containing K$^+$ salts of Cl$^-$ (120 mM), HEPES pH 7.2 (10 mM), succinate (10 mM), and phosphate (5 mM) supplemented with MgCl$_2$ (0.5 mM), 5 μM rotenone , 0.67 μM oligomycin. LL or purified LL were added as indicated in figures. Light scattering changes of 0.1 mg/ml mitochondrial suspensions were followed at 520 nm and 25 °C and are reported as "Matrix Volume", which is calculated based on inverse absorbance normalized for protein concentration, P$_s$:

$$\text{Matrix volume} = P_s \left(1/A - 1/A_\infty \right)$$

Data are summarized in bar graphs as "MitoK$_{ATP}$ activity (%)", given by

$$100 \times [V(x) - V(ATP)]/[V(0) - V(ATP)]$$

where V(x) is the observed steady-state volume at 120 s under the given experimental condition and V(ATP) and V(0) are observed values in the presence and absence of ATP, respectively. Statistical significance of the difference of the means was assessed using unpaired Student's t-test. A value of $p < 0.05$ was considered significant. It should be noted that mitoK$_{ATP}$-

134

dependent K^+ flux has been validated by 5 independent measurements - light scattering, direct measurements of K^+ flux, H^+ flux, respiration, and H_2O_2 production. Each of these was found to yield quantitatively identical measures of K^+ flux, using valinomycin-induced K^+ flux as a calibrating control (32).

Mitochondrial Permeability Transition Pore (MPT) Assay

In vitro studies of MPT opening were carried out by light scattering (32). Briefly, mitochondria (0.1 mg mitochondrial protein/ml) were incubated in the assay medium described above at 30 °C (t=0), $CaCl_2$ (100 μM as free Ca^{2+}) was added at 20 s, ruthenium red (0.5 μM) was added at 40 s to block further Ca^{2+} uptake, and CCCP was added at 60 s (250 nM), to synchronize MPT opening (178). These experiments were performed in the absence of MPG or catalase. The LL was added simultaneously with mitochondria. MPT data are summarized in bar graphs as "MPT inhibition (%)", which was calculated by taking Ca^{2+}-induced swelling rates in the absence and presence of 1 μM cyclosporin A as 0% and 100%, respectively. Statistical significance of the difference of the means was assessed using unpaired Student's t-test. A value of $p < 0.05$ was considered significant.

Assay of mitoK$_{ATP}$-opening by Recombinant PKCε and Src

Recombinant PKCε (expressed in sf 21 insect cells) was purchased from US Biologicals, and Recombinant c-Src p60 (expressed in sf9 insect cells) was

purchased from Upstate Biochemical. The enzymes were incubated for 1 min at 30°C in 40 µL of buffer containing 20 mM Tris (pH 7.5), 10 mM MgCl$_2$, 25 mM MnCl$_2$. Following the incubation, the enzymes were added to the mitochondrial light scattering assay.

Immunoblot Analysis

Proteins were separated by SDS-PAGE using 10% acrylamide precast gels (BioRad) and transferred to polyvinylidine difluoride membranes by semi-dry transfer. Membranes were blocked with 5% nonfat dry milk in 20 mM Tris-buffered saline and 0.5% Tween-20 (TBS-T) and incubated with primary antibody over night in 5% BSA-TBS-T. The membrane was then incubated for one hour with the appropriate secondary antibody conjugated to horseradish peroxidase in TBS-T. The membranes were exposed to autoradiograph films, which were scanned.

Chemicals

Anisomycin, SB203580, KT5823 , PP2, protein phosphotase 2A (PP2A) and protein tyrosine phosphotase B1 (PTPB1) were purchased from Calbiochem. PKC isoform-specific peptides were synthesized by EZ Biolabs (Westfield, IN), according to the published amino acid sequences (27). Antibodies against Src were from Santa Cruz, for Caveolin-3 from ABR Affinity Bioreagents, for the α1-subunit of Na/K-ATPase from ABCam Inc, for PKCε from BD Biosciences. Phospho-p38 MAPK (Thr 180/Tyr 182) and p38 MAPK were

purchased from Cell Signaling. Precast gels (10%) were from BioRad and PVDF membranes were from Millipore. Optiprep was purchased from Axis-Schield PoC AS (Oslo, Norway). Recombinant p38 MAPK (expressed in E. coli) and all other chemicals were from Sigma.

5.4 Results

The ouabain signalosome possesses caveolar properties

We hypothesize that ouabain interaction with the Na,K-ATPase initiates assembly of a signaling platform in sarcolemmal caveolae. This signalosome then buds off and moves to mitochondria, where it interacts with the mitochondrial outer membrane (MOM). The protocol described in "Methods" to isolate the ouabain signalosome exploits the low density of these cholesterol-rich vesicles. As shown in Fig. 1, the physical properties of the ouabain light layer (LL) are consistent with a previous study of signalosomes from bradykinin-treated hearts (186). Similarly to our previous work and the findings of Smart et al, we find that visualization and immunogold labeling of the vesicular structures indicates multiple copies of caveolin-3, the marker for cardiac caveolar structures (Fig. 5.1A) (206). Figure 5.1B contains a Western blot analysis of the isolated signalosome probed with antibodies for the Na+/K+-ATPase, PKCε, Src, and caveolin-3. The ouabain signalosome was enriched in each of these proteins as compared to fractions obtained from sham-perfused hearts. In further experiments not shown, we found that methyl-β-cyclodextrin, a cholesterol binding agent, abolished the ability of the ouabain signalosome to induce mitoK$_{ATP}$ opening when added to mitochondria from untreated hearts, whereas the nonionic detergent Triton X-100 had no effect.

Figure 5.1 The PLL is caveolar in nature and contains signaling molecules **(A)** Immunogold labeling with anti-caveolin-3 indicates that the isolated structures are caveolar in nature. Magnification = 67,000x **(B)** Immunoblot analysis shows a clear enrichment of the α-1 subunit of the N^+,K^+-ATPase, PKCε, Src, and caveolin-3 in PLL from ouabain-treated hearts vs a similar fraction isolated from sham-perfused hearts.

A

F

5 µg protein/lane
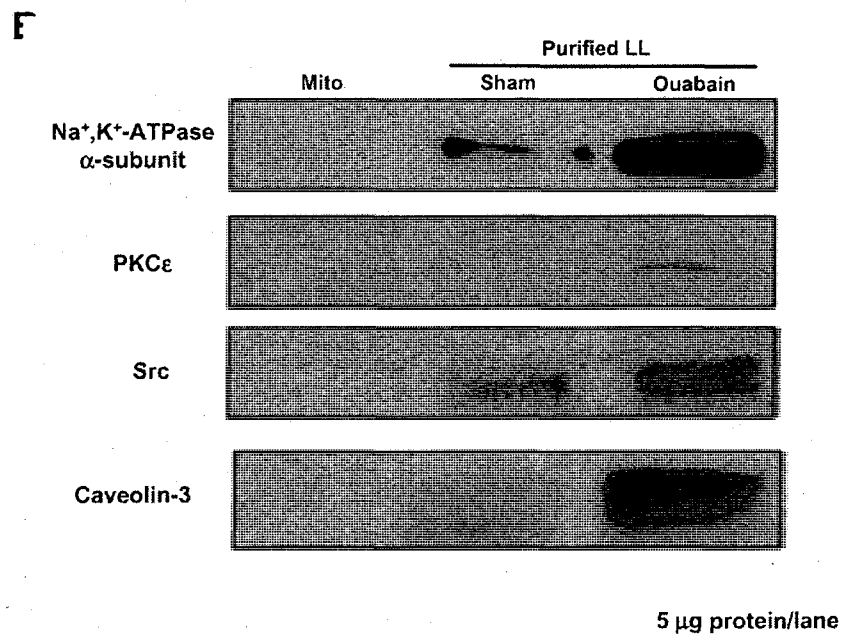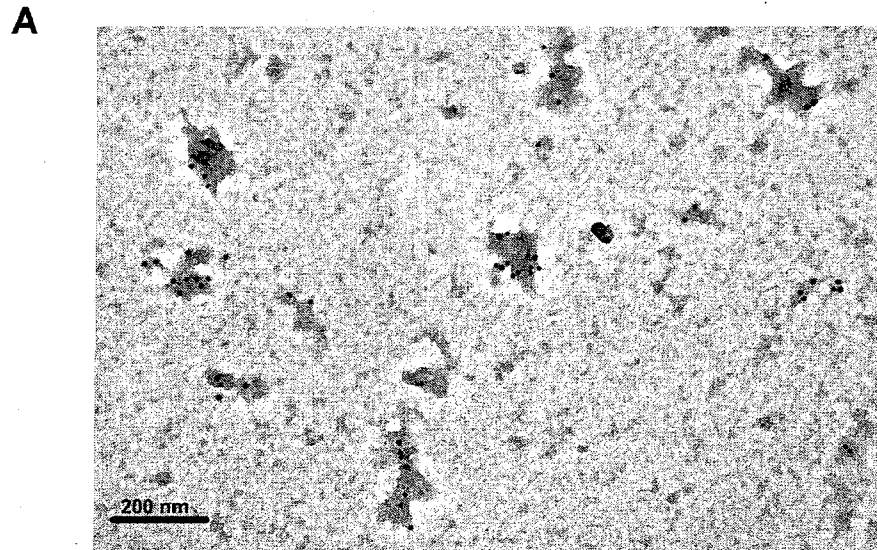
Sensitivity to methyl-β-cyclodextrin and resistance to Triton X-100 are

characteristic properties of caveolar membrane microdomains (3). These

results are similar to those previously obtained with the bradykinin

signalosome (186) and they support the notion that the isolated ouabain

signalosome is caveolar in nature.

The ouabain LL opens mitoK$_{ATP}$ and inhibits the mitochondrial

permeability transition (MPT)

The low-density signalosome fraction isolated from ouabain-treated

hearts, here called light-layer or LL, opens mitoK$_{ATP}$ to the same extent as

diazoxide in isolated mitochondria (Fig. 5.2 A). The traces contained in Fig.

5.2A show that both the LL and the purified LL (PLL, described in Methods)

from ouabain-treated hearts are capable of reversing the ATP-inhibited state

of mitoK$_{ATP}$. LL from sham-perfused hearts ("sham LL") and the residual LL

("RLL"), which are the proteins remaining after PLL are isolated, are unable to

open mitoK$_{ATP}$. A summary of these results is contained in fig. 5.2 B.

MitoK$_{ATP}$ opening induced by the ouabain LL was reversed by the

mitoK$_{ATP}$-blocker 5-hydroxydecanoate (5-HD), the PKCε inhibitor εV$_{1-2}$, the

Src inhibitor PP2, and the MAPK inhibitor SB203580 ("SB"). The effects of

Src and PKCε inhibitors implies that a phosphorylation event was required for

the observed effect. In light of this, we tested the ability of the serine/threonine

protein phosphatase 2A (PP2A), and the protein tyrosine phosphatase B1

(PTPB1), to inhibit the LL effect. Both phosphatases inhibited the activity of

the LL, suggesting that both a serine/threonine and a tyrosine phosphorylation

were important in this process (Fig. 5.2B). Finally, we show that the PKG

inhibitor KT5823 (KT), which blocks activity of the bradykinin signalosome

(186), did not inhibit the mitoK$_{ATP}$ opening by the ouabain LL. This is in full

agreement with a prior study that showed that protein kinase G (PKG) was not

involved in ouabain cardioprotection (173).

We showed previously that physiological or pharmacological opening

of mitoK$_{ATP}$ inhibits the mitochondrial permeability transition (MPT) (32). This

is caused by a mitoK$_{ATP}$-dependent increase in mitochondrial ROS

production and subsequent activation of a PKCε which is constitutively

expressed in mitochondria (32, 93). As shown in Fig. 5.2C, addition of the

ouabain LL to isolated mitochondria inhibited Ca^{2+}-initiated MPT by about

60%, which is approximately the same as the inhibition observed with

diazoxide (32). MPT inhibition by the LL was prevented by the mitoK$_{ATP}$

blocker 5-HD and the Src kinase inhibitor PP2. MPT inhibition was also

prevented by the phosphatases PP2A and PTPB1. These results are in

accordance with those contained in Fig. 5.2 B.

Figure 5.2 (A) LL and Purified LL from ouabain-treated hearts open mitoK$_{ATP}$ and inhibit MPT in isolated mitochondria. Mitochondrial matrix volume is plotted versus time. Aliquots of LL ("LL", 10-15 µg/ml), purified LL ("PLL", 0.5 µg/ml), and residual LL ("RLL", 10-15 µg/ml) were added to medium one second after the mitochondria. ATP (0.2 mM) was present in each run. Diazoxide, the mitoK$_{ATP}$ opener, was used at 30 µM, PP2, a Src inhibitor, was added at 0.5 µM. Also shown is the inability of the residual LL (RLL) or the sham-perfused LL (Sham LL) to open mitoK$_{ATP}$. Traces are representative of at least 5 independent experiments. 7 separate traces are plotted in the figure, and some of them are superimposed. **(B)** Shown is a summary of data with a series of inhibitors tested, plotted as "% mitoK$_{ATP}$ activity" as described in methods . Each inhibitor was added to the assay medium with the LL. Concentrations tested were 300 µM 5-hydroxydecanoate (5HD), 0.5 µM εV1-2, 0.5 µM KT5823 (KT), 0.5 µM PP2, 10 U/mL PP2A, 1 µM SB203580 (SB), 11 U/mL PTPB1. * indicates that data were significantly different from ATP alone, and ξ indicates that ATP were not significantly different than ATP alone ($p < 0.05$). **(C)** Inhibition of the mitochondrial Permeability Transition (MPT) by the addition of the LL was reversed by a similar panel of compounds as described above. * indicates that data were significantly different than the ouabain LL alone ($p < 0.05$).

142
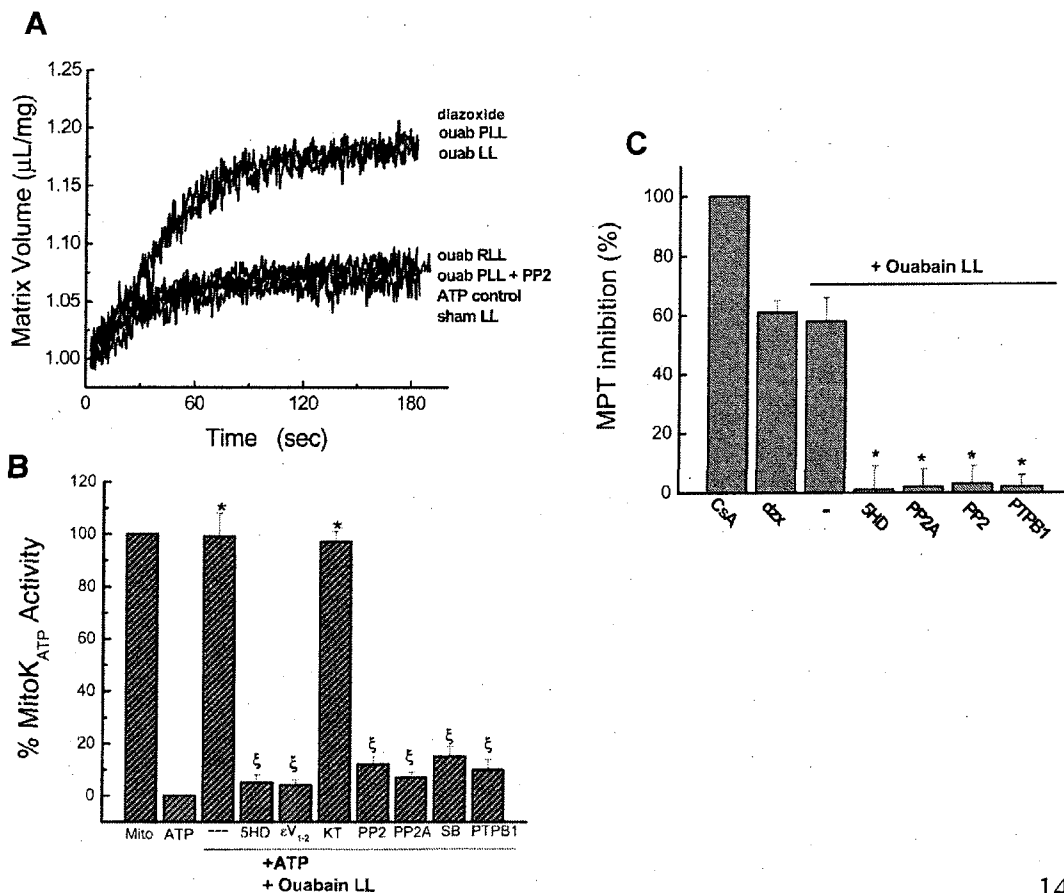
Signalosomes from rat heart open mitoK$_{ATP}$ in rat liver mitochondria

Signal transmission from plasma membrane to mitochondria is a feature of most cell types. We investigated whether signalosomes from heart would interact with liver mitochondria to open mitoK$_{ATP}$. The data in Fig. 3 show that they do. Both the ouabain LL (white bars) and the bradykinin LL (gray bars) open mitoK$_{ATP}$ in liver mitochondria, and they exhibit the same differences in inhibition by PP2, KT5823 and the phosphatases PP2A and PTPB1 that were observed in heart mitochondria. Thus, the signalosome mechanism is a general phenomenon.

PKCε plays dual roles in mitoK$_{ATP}$ opening induced by the ouabain signalosome

We have previously shown that there is an endogenous mitochondrial PKCε that mediates mitoK$_{ATP}$ opening (32, 34, 93). It was necessary to distinguish between the mitochondrial and signalosome PKCε, each of which is presumably inhibited by the specific peptide inhibitor εV$_{1-2}$. We achieved this distinction by simple dilution, as demonstrated by the data in Fig. 4A. To study the signalosome PKCε, we preincubated signalosomes with the same concentration of εV$_{1-2}$ (0.5 μM) that we found by dose-response to inactivate PKCε in mitochondria. Incubation of the ouabain LL was carried out for 1 min

at 30° C, and the LL aliquot was then diluted 150-fold to 3 nM in the assay medium. In separate experiments, we verified that this concentration, which is well below concentrations required to inhibit PKCε (32, 199), had no effect on mitoK$_{ATP}$ opening. In experiments not shown here, we that the ability of the bradykinin signalosome to open mitoK$_{ATP}$ is not affected by preincubation with εV$_{1-2}$, but is blocked if 0.5 μM εV$_{1-2}$ is present in the assay medium, reflecting inhibition of the mitochondrial, but not the signalosome PKCε. These results are contained in Fig. 5.4A and show that the two PKCεs are necessary here, one in the ouabain signalosome and one within mitochondria associated with mitoK$_{ATP}$.

Western blot analysis of the PLL and mitochondria confirmed the presence of PKCε in both the ouabain PLL and mitochondria (Fig. 5.4B). The PLL fraction is a highly purified membrane fraction that contains a total of 7-15 μg of protein per heart, and 5 μg protein was typically loaded on to the gels. As shown, the PLL of ouabain hearts contained an enrichment of PKCε as compared to sham perfusion. As we have shown before, heart mitochondrial PKCε is a very low-abundance protein (93). and we therefore loaded the gel with 50 μg protein in order to observe it. This produces a sharp band, as shown in Fig. 5.4 B.

Figure 5.3 Ouabain- and bradykinin-treated LL open mitoK$_{ATP}$ in isolated liver mitochondria. Both the bradykinin and ouabain open mitoK$_{ATP}$ in liver, but respond differently to inhibitors. The ouabain LL is not sensitive to the PKG inhibitor, KT5823 (KT) or the tyrosine phosphatase PTPB1, but unlike the bradykinin LL is sensitive to the Src inhibitor PP2. All concentrations were the same as those describe in figure 5.2.
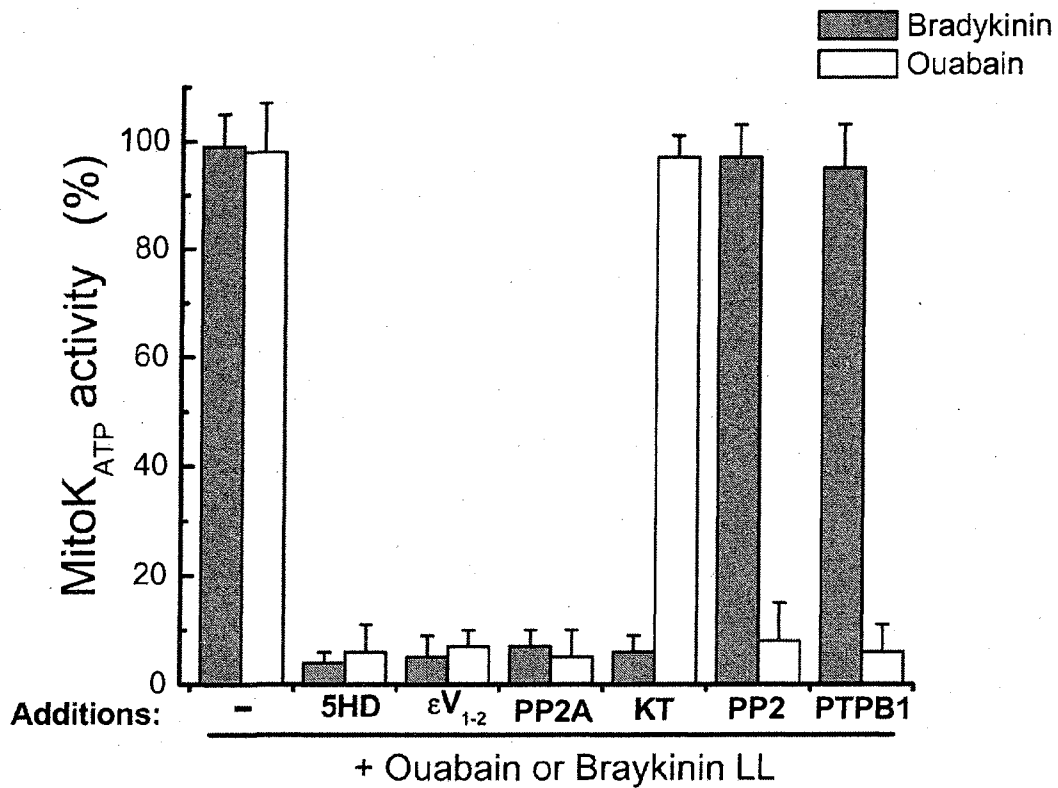
Figure 5.4 Dual PKCεs are mediating mitoK$_{ATP}$-opening in this system.
(A) Shown is the assay to differentiate between the PKCε present in the ouabain LL and the PKCε present in mitochondria. 0.5 μM εV$_{1-2}$, when used in the assay medium with mitochondria and the LL will inhibit PKCε present in both locations (4th bar, "assay"). To inhibit only the LL PKCε we incubated an aloquot of the LL with 0.5 μM εV$_{1-2}$ for 1 min at 30°C and diluted the aloquot into 3 mL assay medium (5th bar, "incub."). This makes the effective concentration of εV$_{1-2}$ in the medium 3 nM. As the final bar shows, 3 nM εV$_{1-2}$ is not a sufficient dose to inhibit the mitochondrial PKCε. **(B)** The immunoblots show that PKCε is present in both the mitochondrial and PLL fractions, but that it is very low abundance in mitochondria, therefore substantially more protein must be loaded in order to observe it.
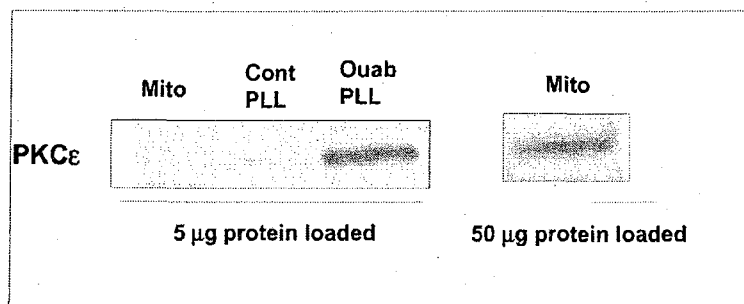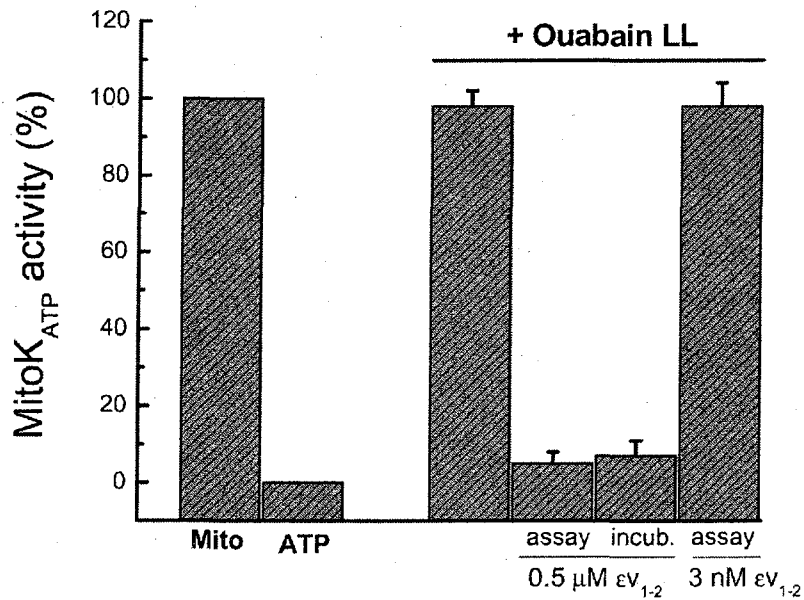
Figure 5.5 Recombinant Src and PKCε open mitoK$_{ATP}$

50 ng recombinant PKCε (specific activity = 1865 Units/mg) and/or 6 units Src were incubated at 30°C for 1 min. Neither kinase alone induced mitoK$_{ATP}$-opening, but the combination did. This opening was sensitive to 300 μM 5HD and 1 μM SB203580. * indicates that $p < 0.05$ vs. either kinase alone.
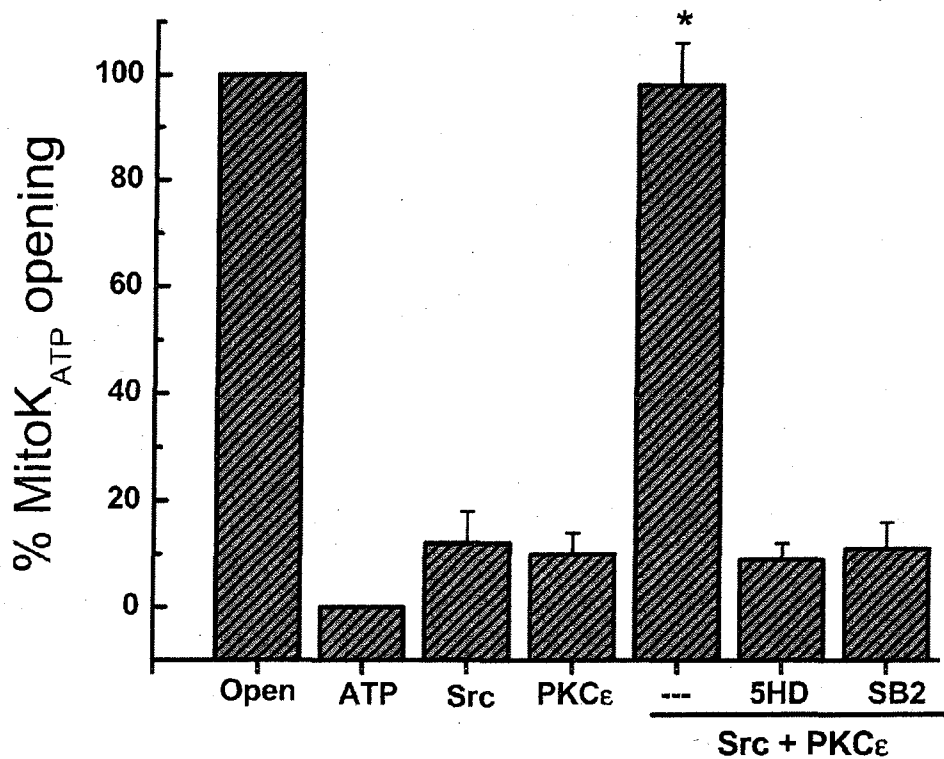
The terminal kinases of the ouabain signalosome are Src and PKCε

Signalosomes contain a number of enzymes, including the terminal kinases that interact with the MOM. Thus, the terminal kinase of the bradykinin signalosome is PKG (186). The physiological data in Fig. 5.2 indicate that both PKCε and Src are required for mitoK$_{ATP}$ opening by the ouabain signalosome. To further test this hypothesis, we assayed the ability of recombinant PKCε and Src to open mitoK$_{ATP}$ *in vitro*. As can be seen in Fig. 5.5, the addition of either kinase alone (third and fourth bars) did not open mitoK$_{ATP}$, but the combination (fifth bar) did. This opening was sensitive to 5HD as well as the MAPK inhibitor SB203580.

The role of p38 MAPK in ouabain-induced mitoK$_{ATP}$ opening

The data in Fig. 5.5 imply that p38 MAPK is the target of Src and PKCε. Since Src and PKCε are the terminal kinases, and since signalosome function is blocked by the phosphatases PP2A and PTPB1 (Fig. 2B), p38 MAPK must be in the MOM. Indeed the immunoblot of Fig. 5.6 demonstrates the presence p38 MAPK in Percoll-purified mitochondria. We also observe an increase in phosphorylation of p38 MAPK (Thr 180/Tyr 182) after the heart has been treated with ouabain. Thus, mitochondria contain p38 MAPK, and it is acting as receptor for the ouabain signalosome that confers the signal to open

148

mitoK$_{ATP}$.

It has not previously been shown that p38 MAPK is involved in ouabain cardioprotection. We now show, in the Langendorff perfused heart model, that cardioprotection afforded by ouabain is blocked by SB203580, the inhibitor of p38 MAPK (Figs. 5.7A and B). We also show that cardioprotection can be induced by direct activation of p38 MAPK with anisomycin and that this protection can be blocked by 5-HD. Finally, to emphasize the distinct differences between the cardioprotective pathways triggered by ouabain and bradykinin (173), we show that SB203580 did not block bradykinin cardioprotection (Figs. 5.7A and B).

Figure 5.6 Mitochondria from ouabain-treated hearts shows increased phosphorylation of p38 MAPK

50 µg of Percoll purified mitochondria was loaded per lane and samples were probed with anti-phosphorylated p38 MAPK (Thr 180/Tyr 182) and anti-p38 MAPK. The positive control was 5 µg recombinant MAPK. Mitochondria isolated from ouabain-treated hearts (ouab) showed enhanced phosphorylation of p38 MAPK as compared to sham perfused hearts (sham).
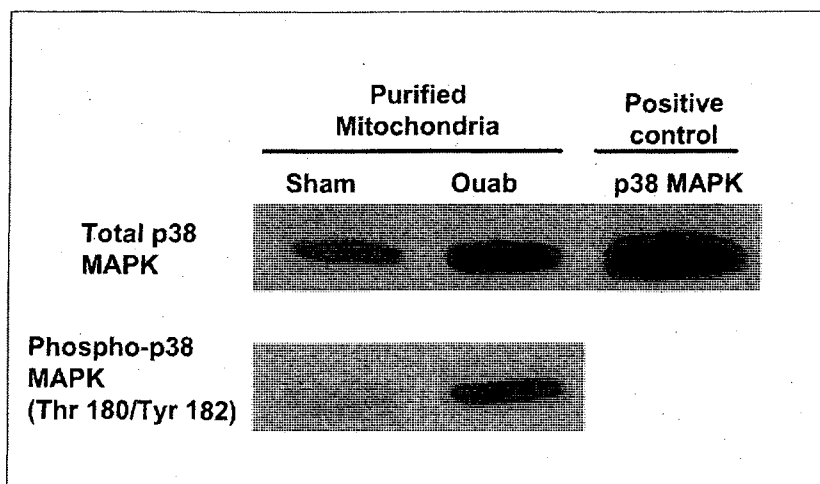
Figure 5.7. *Effects of p38 MAPK inhibition on ouabain and bradykinin cardioprotection.* **(A)** Functional cardiac recovery expressed as rate-pressure product (RPP). See "Materials and Methods" for details on perfusion protocols. Ischemia-reperfusion (IR) is used as the standard for cardiac damage. 50 µM ouabain (Ouab) or 5 µM anisomycin afforded cardioprotection, both were inhibited by 1 µM of the p38 MAPK inhibitor SB203580 (SB) and 300 µM 5HD. The cardioprotective dose of bradykinin, 100 nM, was not blocked by 1 µM SB203580. **(B)** Infarct size measurements, expressed as percent of area at risk, indicate that this measure of cellular necrosis mirrors the functional cardiac recovery. Individual hearts (○) and group means (●) with standard error bars are shown. * indicates $p < 0.05$ *vs.* control IR.

151
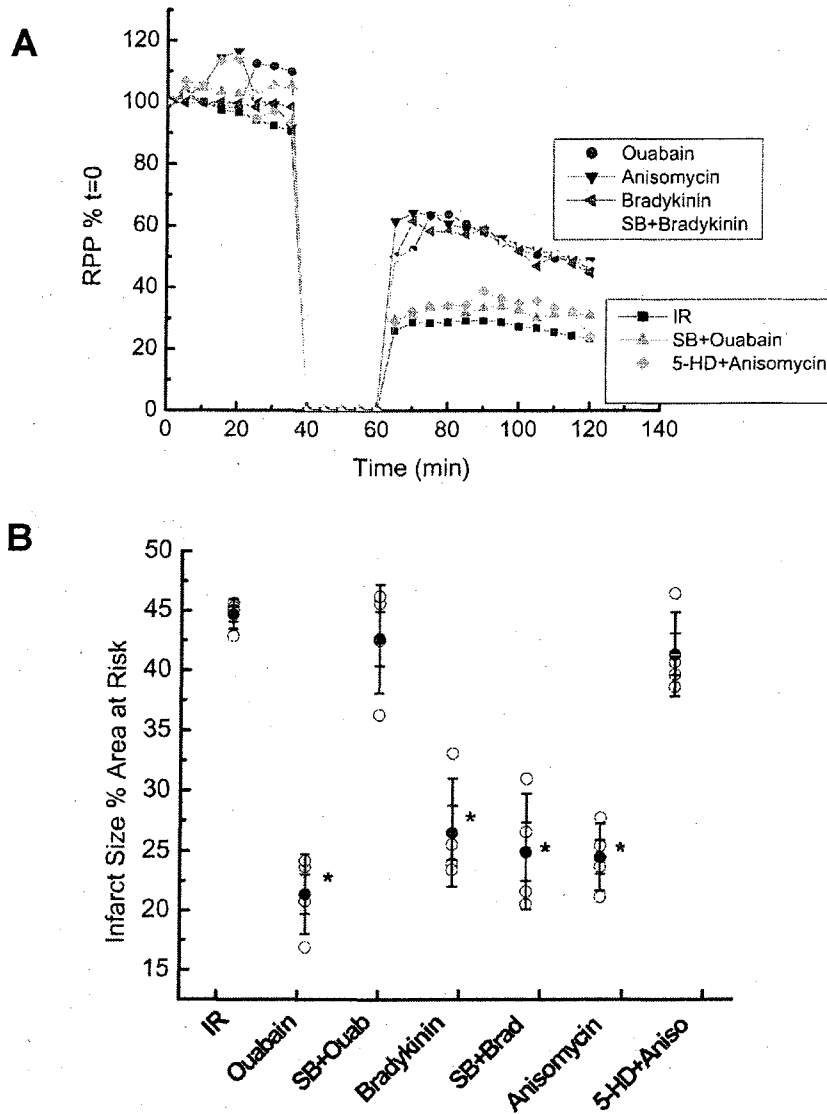
5.5 Discussion

The primary function of the N^+,K^+-ATPase is to transport ions across the cell membrane; the signaling functions of N^+,K^+-ATPase have been more recently described. For example, the N^+,K^+-ATPase is capable of modulating its own gene expression and the expression of genes involved in cell growth (150, 158). Ouabain binding to the N^+,K^+-ATPase has been linked to nonproliferative cell growth (hypertrophy) in the heart through the instigation of signal transduction pathways that originate at the N^+,K^+-ATPase and promote induction or repression of the transcription of several cardiac marker genes known to be involved in the hypertrophic response (144, 234, 235). Ouabain treatment has been shown to cause a rapid activation of Src family kinases with associated recruitment and activation of phosphlipase $C\gamma$ (144, 228). The downstream activation of enzymes such as PKC and ERK has also been observed (144, 180, 235, 242). The presence of multiple binding motifs that foster protein-protein intereaction suggest the N^+,K^+-ATPase as a prime candidate for receptor-mediated signal transduction (228). In fact, the N^+,K^+-ATPase signalosome hypothesis was put forth by Xie and colleagues in 2003 (236).

The presence of the N^+,K^+-ATPase in caveolae strengthens the signalosome hypothesis, 20-30% of the $\alpha 1$-subunit of Na,K-ATPase is

normally located in caveolae (131). Caveolae are membrane microdomains that sequester and regulate signaling molecules (127, 129). Caveolins interact with cholesterol and signaling proteins including receptors, Src family kinases, and adapter proteins. Recent studies have indicated that many of these interactions are mediated through the binding of caveolin scaffolding domains to caveolin-binding motifs of the target proteins. Based on sequence analysis, two caveolin-binding motifs seem likely on the $\alpha 1$ subunit of N^+,K^+-ATPase (236). Significantly, ouabain appears to regulate the interaction of caveolin-1 with the N^+,K^+-ATPase and induce the formation of the N^+,K^+-ATPase –Src–caveolin-1 complex. Ouabain also stimulates tyrosine phosphorylation of caveolin-1 in LLC-PK1 cells, and caveolar p42/44 MAPKs in cardiac myocytes (131, 228).

This study proposes that ouabain cardioprotection is mediated by a signalosome mechanism. The cardioprotective signalsome hypothesis states that binding of ouabain to its receptor, the N^+,K^+-ATPase, instigates the formation of a caveolar signaling complex that mediates the opening of mitoK_{ATP} and inhibition of celluar necrosis. This hypothesis is supported by experiments that assay the composition and behavior of the isolated signalosome from ouabain-treated hearts. The signalosome is a low-density fraction enriched in caveolin-3, the α-subunit of N^+,K^+-ATPase, Src, and PKCε. It is subfractionated from the mitochondrial fraction of treated hearts,

and because it contains activated kinases, can be used to open mitoK$_{ATP}$ in isolated untreated mitochondria.

As shown in Figs. 5.2 and 5.3, the ouabain signalosome fraction (LL) opened mitoK$_{ATP}$ in untreated heart and liver and this effect was sensitive to inhibitors of mitoK$_{ATP}$, Src, PKCε, and MAPK, but not PKG. This is in agreement with a recent study that compared the cardioprotective profile of the peptide bradykinin with that of ouabain. We found that although both pathways required Src, mitoK$_{ATP}$, and ROS, only bradykinin utilized protein kinase G (PKG) and guanylyl cyclase (173). Ouabain cardioprotection was not affected by inhibitors of PKG or guanylyl cyclase. Studies in both the perfused heart and isolated mitochondria have determined that PKG acts immediately proximal to mitoK$_{ATP}$-opening in bradykinin-mediated pahtways (31, 161). Most recently, in a study describing the signalosome hypothesis for bradykinin cardioprotection, we found that the isolated signalosome fraction from bradykinin-treated hearts contained activated PKG that mediated mitoK$_{ATP}$-opening in vitro (186). The fact that PKG did not appear to be involved in ouabain cardioprotection suggested that the upstream pathways must be divergent and result in mitoK$_{ATP}$-opening via different terminal kinases.

It has been proposed that PKCε and Src coexist in signaling complexes that mediate cardioprotection (181, 226). Our data agree with this; the ouabain signalosome contains active Src and PKCε working in concert to

mediate mitoK$_{ATP}$-opening (figs 5.2, 5.3, and 5.4). It is of note that we propose

that three PKCεs are acting in this system, one within the signalosome, and

two within mitochondria associated with mitoK$_{ATP}$ and MPT. Our previous

work indicates that these PKCε play distinct roles in mitochondria modulating

both mitoK$_{ATP}$ and MPT (34, 93, 186).

We also investigated the ability of the recombinant forms of PKCε and

Src to mimic the effects of the ouabain signalosome. As shown in Fig. 5.5,

neither recombinant kinase alone could instigate mitoK$_{ATP}$-opening, but

incubation with both opened mitoK$_{ATP}$, and this opening was sensitive to

SB203580, the p38 MAPK inhibitor. The ability of the recombinant enzymes

to mimic the mitoK$_{ATP}$-opening behavior of the ouabain signalosome suggests

that these are in fact the active elements of the ouabain signalosome. The

inhibition of the effect by SB203580 suggests that p38 MAPK must be present

in the outer membrane of mitochondria. Indeed, immuoblot analysis revealed

the presence of p38 MAPK in mitochondria and an increase in its

phosphorylated form following ouabain treatment (fig 5.6).

To establish the role of p38 MAPK in this system, we performed

cardioprotection experiments in the isolated perfused heart (fig. 7A and B).

We found that inhibition of p38 MAPK blocked ouabain cardioprotection, as

measured by both functional recovery and infarct size. Interestingly, bradykinin

cardioprotection was not blocked by SB203580, which further suggests a

divergence of these two cardioprotective pathways. Anisomycin, the p38 MAPK activator, protected the heart, and this protection was blocked by the mitoK$_{ATP}$ blocker, 5HD.

Both the presence of p38 MAPK in mitochondria, and its action as the receptor for the signalosome, suggest a new paradigm for the role of this enzyme in cardioprotection. There has been some controversy concerning the role of p38 MAPK in cardioprotection, some studies have found its activation to be cardioprotective, and alternately, other studies have found its inhibition to be cardioprotective (137, 143, 151). The relative role of p38 MAPK in preconditioning seems to be strongly contingent on the protocol, but it may also be which receptor-mediated pathway has been activated. As can be seen in figs. 7A and B, bradykinin cardioprotection was not blocked by inhibition of p38 MAPK with SB203580, whereas ouabain was. It may be that the role of p38 in cardioprotection is determined by its location and sequencial activation (136, 196, 243). The addition of p38 MAPK to the mitochondrial paradigm is novel. However, it has been demonstrated that PKCε and p38 MAPK co-localize with cardiac mitochondria and that this association increases with over expression of PKCε (12). It has also been shown that PKCε and Src modulate p38 MAPK following activation of muscarinic receptors (149). How the signal is being transduced from p38 to mitochondrial PKCε is of great interest and will certainly be the work of future studies.

Overall, these data offer support to the signalosome hypothesis for cardioprotection. As we have shown previously with bradykinin, we now show with ouabain, that treating the heart with cardioprotective agents initiates the formation of a signaling platform that can be isolated from mitochondria. The signalosome contains the enzymes necessary to open mitoK$_{ATP}$. The fact that the ligands induce activation of different enzymes (PKCε/Src or PKG) suggests that although the mechanism is general, the pathways are unique. In consideration of the highly specific nature of signaling cascades, it is not surprising that the signalosome contains the enzymes specific to its receptor-activated pathway. Future work will investigate the mechanisms of signalosome scaffolding and delivery, as well as further analyze the content and physiology of these platforms.

6. Conclusions and Future work

Recent years have brought robust advances in our understanding of cardiac signal transduction during cardioprotection against ischemia-reperfusion and particularly the pivotal role of mitochondria in these processes. This study seeks to describe a novel paradigm for integration of the signaling pathways that are instigated upon cardioprotective treatments, from activation of sarcolemmal receptors to mitochondrial permeability transition. We suggest that interaction of the cardioprotective ligand with its receptor induces the formation of a signaling platform (which we have termed the signalosome) that is scaffolded by caveolins and contains the activated enzymes of the pathway. Upon interaction of the signalosome with mitochondria, the intramitochondrial pathway is initiated, whereby $PKC\varepsilon$ activates $mitoK_{ATP}$, increased K^+ flux causes an increase in ROS production, and MPT is inhibited via a second, ROS-activated $PKC\varepsilon$.

This work, which explores the current understanding of the mechanistic link between plasma membrane receptors and mitochondrial targets of cardioprotection, also points to several areas that require further investigation. This study does not address the mechanism that is utilized in delivery of the signalsomes to mitochondria. It seems likely that the cytoskeleton would play a crucial role here, and future studies would benefit from analyzing the roles played by microtubles and microfilaments in scaffolding and transport. Also, if

158

this is in fact a general phenomenon, then one would expect to find signalosomes modulating many forms of receptor-mediated signaling. Examinations of the nucleus and sarcoplasmic reticulum could be very informative regarding signalosome-mediated changes in gene expression and Ca^{2+} handling, respectively.

The intramitochondrial signaling hypothesis has provided a suitable model within which to examine the pathways that are instigated by opening of $mitoK_{ATP}$ *in vivo*. There are still many aspects of this pathway that require further analysis. Though this study in particular does examine the details of these issues, it is interesting to speculate on the nature of these processes. For example, ROS production instigated by matrix alkalinization is thought to arise from complex I (5), and yet the mechanism of this production remains a mystery. In fact, much debate remains regarding the specific site within complex I that from which ROS arises (59). It is postulated that these ROS are activating PKCε, but it is possible that activation occurs by one of the other mechanisms known to activate PKCε such as binding to activating proteins or diacylglycerol. As discussed in the Introduction of this study, activation of PKCε is complex, and in light of the multiple PKCεs postulated to be acting in this system, it would be interesting to understand if these are being activated by different mechanisms (193).

In summary, the work presented here investigates the interactions

among cytosolic signaling components and mitochondria. It also examines the intramitochondrial signaling pathways that are triggered by cellular events. A mechanistic understanding of these pathways could lend powerful insight into the decision between cell survival and cell death during an acute myocardial infarction.

7. References

1.   **Akao M, Ohler A, O'Rourke B, and Marban E.** Mitochondrial ATP-sensitive potassium channels inhibit apoptosis induced by oxidative stress in cardiac cells. *Circ Res* 88: 1267-1275., 2001.

2.   **Altamirano J, Li Y, Desantiago J, Piacentino V, 3rd, Houser SR, and Bers DM.** The inotropic effect of cardioactive glycosides in ventricular myocytes requires Na+-Ca2+ exchanger function. *J Physiol* 575: 845-854 Epub 2006 Jul 2006, 2006.

3.   **Anderson RG.** The caveolae membrane system. *Annu Rev Biochem* 67: 199-225., 1998.

4.   **Andrukhiv A, Costa AD, West IC, and Garlid KD.** Opening mitoK$_{ATP}$ increases superoxide generation from Complex I of the electron transport chain. *Am J Physiol* 291: H2067-2074, 2006.

5.   **Andrukhiv A, Costa ADT, and Garlid KD.** MitoK$_{ATP}$ opening increases mitochondrial ROS production due to matrix alkalinization. *J Mol Cell Cardiol* 38: 813, 2005.

6.   **Anversa P, Cheng W, Liu Y, Leri A, Redaelli G, and Kajstura J.** Apoptosis and myocardial infarction. *Basic Res Cardiol* 93: 8-12., 1998.

7.   **Argaud L, Gateau-Roesch O, Raisky O, Loufouat J, Robert D, and**

Ovize M. Postconditioning inhibits mitochondrial permeability transition. *Circulation* 111: 194-197 Epub 2005 Jan 2010, 2005.

8.   **Auchampach JA, Grover GJ, and Gross GJ.** Blockade of ischaemic preconditioning in dogs by the novel ATP dependent potassium channel antagonist sodium 5-hydroxydecanoate. *Cardiovasc Res* 26: 1054-1062, 1992.

9.   **Baines CP, Goto M, and Downey JM.** Oxygen radicals released during ischemic preconditioning contribute to cardioprotection in the rabbit myocardium. *J Mol Cell Cardiol* 29: 207-216, 1997.

10.   **Baines CP, Kaiser RA, Purcell NH, Blair NS, Osinska H, Hambleton MA, Brunskill EW, Sayen MR, Gottlieb RA, Dorn GW, Robbins J, and Molkentin JD.** Loss of cyclophilin D reveals a critical role for mitochondrial permeability transition in cell death. *Nature* 434: 658-662, 2005.

11.   **Baines CP, Song CX, Zheng YT, Wang GW, Zhang J, Wang OL, Guo Y, Bolli R, Cardwell EM, and Ping P.** Protein kinase Cepsilon interacts with and inhibits the permeability transition pore in cardiac mitochondria. *Circ Res* 92: 873-880, 2003.

12.   **Baines CP, Zhang J, Wang G-W, Zheng Y-T, Xiu JX, Cardwell EM, Bolli R, and Ping P.** Mitochondrial PKCε and MAPK form signaling modules in the murine heart: enhanced mitochondrial PKCε-MAPK interactions and

differential MAPK activation in PKCε-induced cardioprotection. *Circ Res* 90:

390-397, 2002.

13.   **Bajgar R, Seetharaman S, Kowaltowski AJ, Garlid KD, and**

Paucek P. Identification and properties of a novel intracellular (mitochondrial)

ATP-sensitive potassium channel in brain. *J Biol Chem* 276: 33369-33374,

2001.

14.   **Balbis A, Baquiran G, Dumas V, and Posner BI.** Effect of inhibiting

vacuolar acidification on insulin signaling in hepatocytes. *J Biol Chem* 279:

12777-12785, 2004.

15.   **Bauman AL, Michel JJ, Henson E, Dodge-Kafka KL, and Kapiloff**

MS. The mAKAP signalosome and cardiac myocyte hypertrophy. *IUBMB Life*

59: 163-169, 2007.

16.   **Beavis AD, Brannan RD, and Garlid KD.** Swelling and contraction of

the mitochondrial matrix. I. A structural interpretation of the relationship

between light scattering and matrix volume. *J Biol Chem* 260: 13424-13433,

1985.

17.   **Beavis AD and Garlid KD.** Evidence for the allosteric regulation of the

mitochondrial K^+/H^+ antiporter by matrix protons. *J Biol Chem* 265: 2538-

2545, 1990.

18.   **Beavis AD, Lu Y, and Garlid KD.** On the regulation of K^+ uniport in

intact mitochondria by adenine nucleotides and nucleotide analogs. *J Biol Chem* 268: 997-1004., 1993.

19.   **Becher A and McIlhinney RA.** Consequences of lipid raft association on G-protein-coupled receptor function. *Biochem Soc Symp*: 151-164, 2005.

20.   **Bers DM.** *Excitation-Contraction Coupling and Cardiac Contractile Force, 2nd edition*: Kluwer Academic Publishers, the Netherlands., 2001.

21.   **Bolli R, Dawn B, Tang XL, Qiu Y, Ping P, Xuan YT, Jones WK, Takano H, Guo Y, and Zhang J.** The nitric oxide hypothesis of late preconditioning. *Basic Res Cardiol* 93: 325-338, 1998.

22.   **Brierley GP, Panzeter ES, and Jung DW.** Regulation of mitochondrial K^+/H^+ antiport activity by hydrogen ions. *Arch Biochem Biophys* 288: 358-367., 1991.

23.   **Bright GR, Fisher GW, Rogowska J, and Taylor DL.** Fluorescence ratio imaging microscopy. *Methods Cell Biol* 30: 157-192, 1989.

24.   **Brookes PS, Salinas EP, Darley-Usmar K, Eiserich JP, Freeman BA, Darley-Usmar VM, and Anderson PG.** Concentration-dependent effects of nitric oxide on mitochondrial permeability transition and cytochrome c release. *J Biol Chem* 275: 20474-20479, 2000.

25.   **Byron KL, Babnigg G, and Villereal ML.** Bradykinin-induced Ca2+

entry, release, and refilling of intracellular Ca2+ stores. Relationships revealed by image analysis of individual human fibroblasts. *J Biol Chem* 267: 108-118, 1992.

26. **Cao Z, Liu L, and Van Winkle DM.** Activation of delta- and kappa-opioid receptors by opioid peptides protects cardiomyocytes via KATP channels. *Am J Physiol Heart Circ Physiol* 285: H1032-1039, 2003.

27. **Chen L, Hahn H, Wu G, Chen CH, Liron T, Schechtman D, Cavallaro G, Banci L, Guo Y, Bolli R, Dorn GW, 2nd, and Mochly-Rosen D.** Opposing cardioprotective actions and parallel hypertrophic effects of delta PKC and epsilon PKC. *Proc Natl Acad Sci U S A* 98: 11114-11119., 2001.

28. **Cohen AW, Hnasko R, Schubert W, and Lisanti MP.** Role of caveolae and caveolins in health and disease. *Physiol Rev* 84: 1341-1379, 2004.

29. **Cohen MV, Baines CP, and Downey JM.** Ischemic preconditioning: from adenosine receptor of K_{ATP} channel. *Annu Rev Physiol* 62: 79-109., 2000.

30. **Cohen MV, Yang XM, Liu GS, Heusch G, and Downey JM.** Acetylcholine, bradykinin, opioids, and phenylephrine, but not adenosine, trigger preconditioning by generating free radicals and opening mitochondrial K_{ATP} channels. *Circ Res* 89: 273-278., 2001.

31. **Costa AD, Garlid KD, West IC, Lincoln TM, Downey JM, Cohen**

MV, and Critz SD. Protein Kinase G Transmits the Cardioprotective Signal From Cytosol to Mitochondria. *Circ Res* 97: 329-336, 2005.

32. **Costa AD, Jakob R, Costa CL, Andrukhiv K, West IC, and Garlid KD.** The mechanism by which mitoK$_{ATP}$ opening and H$_2$O$_2$ inhibit the mitochondrial permeability transition. *J Biol Chem* 281: 20801-20808, 2006.

33. **Costa AD, Pierre SV, Cohen MV, Downey JM, and Garlid KD.** cGMP Signaling in Pre- and Postconditioining: The Role of Mitochondria. *Cardiovasc Res* 77: 344-352, 2008.

34. **Costa ADT and Garlid KD.** Intramitochondrial signaling: interactions among mitoK$_{ATP}$, PKCε , ROS, and MPT. *Am J Physiol* 295: H874-882, 2008.

35. **Costa ADT, Quinlan C, Andrukhiv A, West IC, and Garlid KD.** The direct physiological effects of mitoK$_{ATP}$ opening on heart mitochondria. *Am J Physiol* 290: H406-415, 2006.

36. **Couet J, Li S, Okamoto T, Ikezu T, and Lisanti MP.** Identification of peptide and protein ligands for the caveolin-scaffolding domain. Implications for the interaction of caveolin with caveolae-associated proteins. *J Biol Chem* 272: 6525-6533., 1997.

37. **Crompton M.** Bax, bid and the permeabilization of the mitochondrial outer membrane in apoptosis. *Curr Opin Cell Biol* 12: 414-419, 2000.

38.   **Crompton M.** The mitochondrial permeability transition pore and its role in cell death. *Biochem J* 341: 233-249, 1999.

39.   **Crompton M, Ellinger H, and Costi A.** Inhibition by cyclosporin A of a Ca2+-dependent pore in heart mitochondria activated by inorganic phosphate and oxidative stress. *Biochem J* 255: 357-360, 1988.

40.   **Crompton M, Virji S, Doyle V, Johnson N, and Ward JM.** The mitochondrial permeability transition pore. *Biochem Soc Symp* 66: 167-179., 1999.

41.   **D'Alessio A, Al-Lamki RS, Bradley JR, and Pober JS.** Caveolae participate in tumor necrosis factor receptor 1 signaling and internalization in a human endothelial cell line. *Am J Pathol* 166: 1273-1282, 2005.

42.   **Dalskov SM, Immerdal L, Niels-Christiansen LL, Hansen GH, Schousboe A, and Danielsen EM.** Lipid raft localization of GABA A receptor and Na+, K+-ATPase in discrete microdomain clusters in rat cerebellar granule cells. *Neurochem Int* 46: 489-499, 2005.

43.   **Das DK, Maulik N, Sato M, and Ray PS.** Reactive oxygen species function as second messenger during ischemic preconditioning of heart. *Mol Cell Biochem* 196: 59-67, 1999.

44.   **Das M, Parker JE, and Halestrap AP.** Matrix volume measurements challenge the existence of diazoxide/glibencamide-sensitive K_{ATP} channels in

rat mitochondria. *J Physiol* 547: 893-902, 2003.

45.   **Di Lisa F, Menabo R, Canton M, Barile M, and Bernardi P.** Opening

of the mitochondrial permeability transition pore causes depletion of

mitochondrial and cytosolic NAD$^+$ and is a causative event in the death of

myocytes in postischemic reperfusion of the heart. *J Biol Chem* 276: 2571-

2575, 2001.

46.   **Dordick RS, Brierley GP, and Garlid KD.** On the mechanism of

A23187-induced potassium efflux in rat liver mitochondria. *J Biol Chem* 255:

10299-10305, 1980.

47.   **Dos Santos P, Kowaltowski AJ, Laclau MN, Seetharaman S,**

Paucek P, Boudina S, Thambo JB, Tariosse L, and Garlid KD.

Mechanisms by which opening the mitochondrial ATP- sensitive K$^+$ channel

protects the ischemic heart. *Am J Physiol* 283: H284-295., 2002.

48.   **Dos Santos P, Laclau MN, Boudina S, and Garlid KD.** Alterations of

the bioenergetics systems of the cell in acute and chronic myocardial

ischemia. *Mol Cell Biochem* 256/257: 157-166, 2004.

49.   **Downey JM and Cohen MV.** Signal transduction in ischemic

preconditioning. *Adv Exp Med Biol* 430: 39-55, 1997.

50.   **Downey JM, Davis AM, and Cohen MV.** Signaling pathways in

ischemic preconditioning. *Heart Fail Rev* 12: 181-188, 2007.

51.   **Drab M, Verkade P, Elger M, Kasper M, Lohn M, Lauterbach B, Menne J, Lindschau C, Mende F, Luft FC, Schedl A, Haller H, and Kurzchalia TV.** Loss of caveolae, vascular dysfunction, and pulmonary defects in caveolin-1 gene-disrupted mice. *Science* 293: 2449-2452, 2001.

52.   **Elsasser A, Suzuki K, and Schaper J.** Unresolved issues regarding the role of apoptosis in the pathogenesis of ischemic injury and heart failure. *J Mol Cell Cardiol* 32: 711-724., 2000.

53.   **Escriche M, Burgueno J, Ciruela F, Canela EI, Mallol J, Enrich C, Lluis C, and Franco R.** Ligand-induced caveolae-mediated internalization of A1 adenosine receptors: morphological evidence of endosomal sorting and receptor recycling. *Exp Cell Res* 285: 72-90, 2003.

54.   **Facundo HT, de Paula JG, and Kowaltowski AJ.** Mitochondrial ATP-sensitive K(+) channels are redox-sensitive pathways that control reactive oxygen species production. *Free Radic Biol Med* 42: 1039-1048 Epub 2007 Jan 1038, 2007.

55.   **Feron O and Balligand JL.** Caveolins and the regulation of endothelial nitric oxide synthase in the heart. *Cardiovasc Res* 69: 788-797, 2006.

56.   **Forbes RA, Steenbergen C, and Murphy E.** Diazoxide-Induced Cardioprotection Requires Signaling Through a Redox-Sensitive Mechanism. *Circ Res* 88: 802-809, 2001.

57.   **Frank PG, Woodman SE, Park DS, and Lisanti MP.** Caveolin,

caveolae, and endothelial cell function. *Arterioscler Thromb Vasc Biol* 23:

1161-1168, 2003.

58.   **Fryer RM, Schultz JE, Hsu AK, and Gross GJ.** Importance of PKC

and tyrosine kinase in single or multiple cycles of preconditioning in rat hearts.

Am J Physiol 276: H1229-1235, 1999.

59.   **Galkin A and Brandt U.** Superoxide radical formation by pure complex

I (NADH: Ubiquinone oxidoreductase) from Yarrowia lipolytica. *J Biol Chem*

28: 28, 2005.

60.   **Gao J, Wymore RS, Wang Y, Gaudette GR, Krukenkamp IB,

Cohen IS, and Mathias RT.** Isoform-specific stimulation of cardiac Na/K

pumps by nanomolar concentrations of glycosides. *J Gen Physiol* 119: 297-

312, 2002.

61.   **Garg V and Hu K.** Protein kinase C isoform-dependent modulation of

ATP-sensitive K+ channels in mitochondrial inner membrane. *Am J Physiol*

293: H322-332, 2007.

62.   **Garlid KD.** Cation transport in mitochondria--the potassium cycle.

Biochim Biophys Acta 1275: 123-126, 1996.

63.   **Garlid KD.** On the mechanism of regulation of the mitochondrial K^+/H^+

exchanger. *J Biol Chem* 255: 11273-11279, 1980.

64.   **Garlid KD.** Opening mitochondrial K_{ATP} in the heart--what happens, and what does not happen. *Basic Res Cardiol* 95: 275-279., 2000.

65.   **Garlid KD.** The state of water in biological systems. *Int Rev Cytol* 192: 281-302., 2000.

66.   **Garlid KD.** Unmasking the mitochondrial K/H exchanger: tetraethylammonium-induced K^+-loss. *Biochem Biophys Res Commun* 87: 842-847, 1979.

67.   **Garlid KD and Beavis AD.** Swelling and contraction of the mitochondrial matrix. II. Quantitative application of the light scattering technique to solute transport across the inner membrane. *J Biol Chem* 260: 13434-13441, 1985.

68.   **Garlid KD, DiResta DJ, Beavis AD, and Martin WH.** On the mechanism by which dicyclohexylcarbodiimide and quinine inhibit K^+ transport in rat liver mitochondria. *J Biol Chem* 261: 1529-1535, 1986.

69.   **Garlid KD, Dos Santos P, Xie Z-J, Costa ADT, and Paucek P.** Mitochondrial potassium transport: the role of the mitochondrial ATP-sensitive K^+ channel in cardiac function and cardioprotection. *Biochim Biophys Acta* 1606: 1-21, 2003.

70.   **Garlid KD and Paucek P.** Mitochondrial potassium transport: the K^+ cycle. *Biochim Biophys Acta* 1606: 23-41, 2003.

71.   **Garlid KD, Paucek P, Yarov-Yarovoy V, Murray HN, Darbenzio RB, D'Alonzo AJ, Lodge NJ, Smith MA, and Grover GJ.** Cardioprotective effect of diazoxide and its interaction with mitochondrial ATP-sensitive K^+ channels. Possible mechanism of cardioprotection. *Circ Res* 81: 1072-1082, 1997.

72.   **Garlid KD, Paucek P, Yarov-Yarovoy V, Sun X, and Schindler PA.** The mitochondrial K_{ATP} channel as a receptor for potassium channel openers. *J Biol Chem* 271: 8796-8799, 1996.

73.   **Garlid KD, Puddu PE, Pasdois P, Costa ADT, Beauvoit B, Criniti A, Tariosse L, Diolez P, and Dos Santos P.** Inhibition of cardiac contractility by 5-hydroxydecanoate and tetraphenylphosphonium ion: a possible role of mitoK_{ATP} in the response to inotropic stress. *Am J Physiol* 291: H152-160, 2006.

74.   **Garthwaite J, Southam E, Boulton CL, Nielsen EB, Schmidt K, and Mayer B.** Potent and selective inhibition of nitric oxide-sensitive guanylyl cyclase by 1H-[1,2,4]oxadiazolo[4,3-a]quinoxalin-1-one. *Mol Pharmacol* 48: 184-188, 1995.

75.   **Gornall AG, Bardawill CJ, and David MM.** Determination of serum proteins by means of the biuret reaction. *J Biol Chem* 177: 751-766, 1949.

76.   **Goto M, Liu Y, Yang XM, Ardell JL, Cohen MV, and Downey JM.** Role of bradykinin in protection of ischemic preconditioning in rabbit hearts.

Circ Res 77: 611-621, 1995.

77.   **Gottlieb RA and Engler RL.** Apoptosis in myocardial ischemia-

reperfusion. *Ann N Y Acad Sci* 874: 412-426, 1999.

78.   **Graziani A, Bricko V, Carmignani M, Graier WF, and Groschner K.**

Cholesterol- and caveolin-rich membrane domains are essential for

phospholipase A2-dependent EDHF formation. *Cardiovasc Res* 64: 234-242,

2004.

79.   **Gross ER and Gross GJ.** Ligand triggers of classical preconditioning

and postconditioning. *Cardiovasc Res* 70: 212-221, 2006.

80.   **Gross GJ and Auchampach JA.** Blockade of ATP-sensitive

potassium channels prevents myocardial preconditioning in dogs. *Circ Res*

70: 223-233, 1992.

81.   **Grover GJ, D'Alonzo AJ, Garlid KD, Bajgar R, Lodge NJ, Sleph**

PG, Darbenzio RB, Hess TA, Smith MA, Paucek P, and Atwal KS.

Pharmacologic characterization of BMS-191095, a mitochondrial K_{ATP} opener

with no peripheral vasodilator or cardiac action potential shortening activity. *J*

Pharmacol Exp Ther 297: 1184-1192, 2001.

82.   **Grover GJ and Garlid KD.** ATP-Sensitive potassium channels: a

review of their cardioprotective pharmacology. *J Mol Cell Cardiol* 32: 677-

695., 2000.

83.   **Grover GJ, Newburger J, Sleph PG, Dzwonczyk S, Taylor SC, Ahmed SZ, and Atwal KS.** Cardioprotective effects of the potassium channel opener cromakalim: stereoselectivity and effects on myocardial adenine nucleotides. *J Pharmacol Exp Ther* 257: 156-162, 1991.

84.   **Gui G, Hegazy MG, Mironova G, Mahdi F, Beavis A, and Garlid KD.** Purification and reconstitution of the mitochondrial K+ channel. *J Mol Cell Cardiol* 23: S78, 1991.

85.   **Haasemann M, Cartaud J, Muller-Esterl W, and Dunia I.** Agonist-induced redistribution of bradykinin B2 receptor in caveolae. *J Cell Sci* 111: 917-928, 1998.

86.   **Hanke JH, Gardner JP, Dow RL, Changelian PS, Brissette WH, Weringer EJ, Pollok BA, and Connelly PA.** Discovery of a novel, potent, and Src family-selective tyrosine kinase inhibitor. Study of Lck- and FynT-dependent T cell activation. *J Biol Chem* 271: 695-701, 1996.

87.   **Hausenloy DJ, Yellon DM, Mani-Babu S, and Duchen MR.** Preconditioning protects by inhibiting the mitochondrial permeability transition. *Am J Physiol* 287: H841-849, 2004.

88.   **Hide EJ and Thiemermann C.** Limitation of myocardial infarct size in the rabbit by ischaemic preconditioning is abolished by sodium 5-hydroxydecanoate. *cardiovascular research* 31: 941-946, 1996.

89.   **Holmuhamedov EL, Wang L, and Terzic A.** ATP-sensitive K^+ channel openers prevent Ca^{2+} overload in rat cardiac mitochondria. *J Physiol (Lond)* 519 Pt 2: 347-360, 1999.

90.   **Honda HM, Korge P, and Weiss JN.** Mitochondria and ischemia/reperfusion injury. *Ann N Y Acad Sci* 1047: 248-258, 2005.

91.   **Inoue I, Nagase H, Kishi K, and Higuti T.** ATP-sensitive K+ channel in the mitochondrial inner membrane. *Nature* 352: 244-247, 1991.

92.   **Ishida H, Hirota Y, Genka C, Nakazawa H, Nakaya H, and Sato T.** Opening of mitochondrial K(ATP) channels attenuates the ouabain-induced calcium overload in mitochondria. *Circ Res* 89: 856-858, 2001.

93.   **Jaburek M, Costa ADT, Burton JR, Costa CL, and Garlid KD.** Mitochondrial PKCepsilon and $mitoK_{ATP}$ co-purify and co-reconstitute to form a functioning signaling module in proteoliposomes. *Circ Res* 99: 878-883, 2006.

94.   **Jaburek M, Yarov-Yarovoy V, Paucek P, and Garlid KD.** State-dependent inhibition of the mitochondrial K_{ATP} channel by glyburide and 5-hydroxydecanoate. *J Biol Chem* 273: 13578-13582, 1998.

95.   **Jezek P, Mahdi F, and Garlid KD.** Reconstitution of the beef heart and rat liver mitochondrial K^+/H^+ (Na^+/H^+) antiporter. Quantitation of K^+ transport with the novel fluorescent probe, PBFI. *J Biol Chem* 265: 10522-

10526, 1990.

96. **Jiang MT, Ljubkovic M, Nakae Y, Shi Y, Kwok WM, Stowe DF, and Bosnjak ZJ.** Characterization of human cardiac mitochondrial ATP-sensitive potassium channel and its regulation by phorbol ester in vitro. *Am J Physiol* 290: H1770-1776, 2006.

97. **Johnson JA, Gray MO, Chen CH, and Mochly-Rosen D.** A protein kinase C translocation inhibitor as an isozyme-selective antagonist of cardiac function. *J Biol Chem* 271: 24962-24966, 1996.

98. **Johnson LS, Dunn KW, Pytowski B, and McGraw TE.** Endosome acidification and receptor trafficking: bafilomycin A1 slows receptor externalization by a mechanism involving the receptor's internalization motif. *Mol Biol Cell* 4: 1251-1266, 1993.

99. **Jones SP and Bolli R.** The ubiquitous role of nitric oxide in cardioprotection. *J Mol Cell Cardiol* 40: 16-23, 2006.

100. **Ju H, Venema VJ, Liang H, Harris MB, Zou R, and Venema RC.** Bradykinin activates the Janus-activated kinase/signal transducers and activators of transcription (JAK/STAT) pathway in vascular endothelial cells: localization of JAK/STAT signalling proteins in plasmalemmal caveolae. *Biochem J* 351: 257-264, 2000.

101. **Juhaszova M, Zorov DB, Kim SH, Pepe S, Fu Q, Fishbein KW, Ziman BD, Wang S, Ytrehus K, Antos CL, Olson EN, and Sollott SJ.**

Glycogen synthase kinase-3beta mediates convergence of protection signaling to inhibit the mitochondrial permeability transition pore. *J Clin Invest* 113: 1535-1549, 2004.

102. **Jung DW, Davis MH, and Brierley GP.** Estimation of matrix pH in isolated heart mitochondria using a fluorescent probe. *Anal Biochem* 178: 348-354, 1989.

103. **Kase H, Iwahashi K, Nakanishi S, Matsuda Y, Yamada K, Takahashi M, Murakata C, Sato A, and Kaneko M.** K-252 compounds, novel and potent inhibitors of protein kinase C and cyclic nucleotide-dependent protein kinases. *Biochem Biophys Res Commun* 142: 436-440, 1987.

104. **Kazanietz MG, Bustelo XR, Barbacid M, Kolch W, Mischak H, Wong G, Pettit GR, Bruns JD, and Blumberg PM.** Zinc finger domains and phorbol ester pharmacophore. Analysis of binding to mutated form of protein kinase C zeta and the vav and c-raf proto-oncogene products. *J Biol Chem* 269: 11590-11594, 1994.

105. **Kennedy DJ, Vetteth S, Xie M, Periyasamy S, Xie Z, Han C, Basrur V, Mutgi KA, Fedorov V, Malhotra D, and Shapiro JI.** Ouabain Decreases Sarcoplasmic Reticulum Calcium ATPase (SERCA2a) Activity in Rat Hearts by a Process Involving Protein Oxidation. *Am J Physiol Heart Circ Physiol* 21: 21, 2006.

106. **Kevin LG, Camara AKS, Riess ML, Novalija E, and Stowe DF.**

Ischemic preconditioning alters real-time measure of O2 radicals in intact hearts with ischemia and reperfusion. *Am J Physiol* 284: H566-574, 2003.

107.   **Kholodenko BN.** Four-dimensional organization of protein kinase signaling cascades: the roles of diffusion, endocytosis and molecular motors. *J Exp Biol* 206: 2073-2082, 2003.

108.   **Kim JS, He L, Qian T, and Lemasters JJ.** Role of the mitochondrial permeability transition in apoptotic and necrotic death after ischemia/reperfusion injury to hepatocytes. *Curr Mol Med* 3: 527-535, 2003.

109.   **Kim JS, Ohshima S, Pediaditakis P, and Lemasters JJ.** Nitric oxide protects rat hepatocytes against reperfusion injury mediated by the mitochondrial permeability transition. *Hepatology* 39: 1533-1543, 2004.

110.   **Kim JS, Ohshima S, Pediaditakis P, and Lemasters JJ.** Nitric oxide: a signaling molecule against mitochondrial permeability transition- and pH-dependent cell death after reperfusion. *Free Radic Biol Med* 37: 1943-1950, 2004.

111.   **Klumpp S and Krieglstein J.** Serine/threonine protein phosphatases in apoptosis. *Curr Opin Pharmacol* 2: 458-462, 2002.

112.   **Korge P, Honda HM, and Weiss JN.** Protection of cardiac mitochondria by diazoxide and protein kinase C: implications for ischemic preconditioning. *Proc Natl Acad Sci U S A* 99: 3312-3317., 2002.

113. **Korichneva I, Hoyos B, Chua R, Levi E, and Hammerling U.** Zinc release from protein kinase C as the common event during activation by lipid second messenger or reactive oxygen. *J Biol Chem* 277: 44327-44331, 2002.

114. **Kositprapa C, Ockaili RA, and Kukreja RC.** Bradykinin B2 receptor is involved in the late phase of preconditioning in rabbit heart. *J Mol Cell Cardiol* 33: 1355-1362, 2001.

115. **Kowaltowski AJ, Seetharaman S, Paucek P, and Garlid KD.** Bioenergetic consequences of opening the ATP-sensitive K^+ channel of heart mitochondria. *Am J Physiol* 280: H649-657, 2001.

116. **Krajewska WM and Maslowska I.** Caveolins: structure and function in signal transduction. *Cell Mol Biol Lett* 9: 195-220, 2004.

117. **Krenz M, Oldenburg O, Wimpee H, Cohen MV, Garlid KD, Critz SD, Downey JM, and Benoit JN.** Opening of ATP-sensitive potassium channels causes generation of free radicals in vascular smooth muscle cells. *Basic Res Cardiol* 97: 365-373., 2002.

118. **Krieg T, Philipp S, Cui L, Dostmann WR, Downey JM, and Cohen MV.** Peptide blockers of PKG inhibit ROS generation by acetylcholine and bradykinin in cardiomyocytes but fail to block protection in the whole heart. *Am J Physiol Heart Circ Physiol* 288: H1976-1981, 2005.

119. **Krieg T, Qin Q, McIntosh EC, Cohen MV, and Downey JM.** ACh and adenosine activate PI3-kinase in rabbit hearts through transactivation of receptor tyrosine kinases. *Am J Physiol* 283: H2322-2330, 2002.

120. **Krieg T, Qin Q, Philipp S, Alexeyev MF, Cohen MV, and Downey JM.** Acetylcholine and bradykinin trigger preconditioning in the heart through a pathway that includes Akt and NOS. *Am J Physiol* 287: 2606-2611, 2004.

121. **Laclau MN, Boudina S, Thambo JB, Tariosse L, Gouverneur G, Bonoron-Adele S, Saks VA, Garlid KD, and Dos Santos P.** Cardioprotection by ischemic preconditioning preserves mitochondrial function and functional coupling between adenine nucleotide translocase and creatine kinase. *J Mol Cell Cardiol* 33: 947-956, 2001.

122. **Lamb ME, Zhang C, Shea T, Kyle DJ, and Leeb-Lundberg LM.** Human B1 and B2 bradykinin receptors and their agonists target caveolae-related lipid rafts to different degrees in HEK293 cells. *Biochemistry* 41: 14340-14347, 2002.

123. **Lawrence CL, Billups B, Rodrigo GC, and Standen NB.** The K_{ATP} channel opener diazoxide protects cardiac myocytes during metabolic inhibition without causing mitochondrial depolarization or flavoprotein oxidation. *Br J Pharmacol* 134: 535-542., 2001.

124. **Lebuffe G, Schumacker PT, Shao ZH, Anderson T, Iwase H, and Vanden Hoek TL.** ROS and NO trigger early preconditioning: relationship to

mitochondrial K_{ATP} channel. *Am J Physiol* 284: H299-308, 2003.

125. **Leier CV.** General overview and update of positive inotropic therapy.

Am J Med 81: 40-45, 1986.

126. **Lemasters JJ, Qian T, Bradham CA, Brenner DA, Cascio WE,**

Trost LC, Nishimura Y, Nieminen AL, and Herman B. Mitochondrial

dysfunction in the pathogenesis of necrotic and apoptotic cell death. *J*

Bioenerg Biomembr 31: 305-319, 1999.

127. **Li S, Couet J, and Lisanti MP.** Src tyrosine kinases, Galpha subunits,

and H-Ras share a common membrane-anchored scaffolding protein,

caveolin. Caveolin binding negatively regulates the auto-activation of Src

tyrosine kinases. *J Biol Chem* 271: 29182-29190., 1996.

128. **Li S, Seitz R, and Lisanti MP.** Phosphorylation of caveolin by src

tyrosine kinases. The alpha-isoform of caveolin is selectively phosphorylated

by v-Src in vivo. *J Biol Chem* 271: 3863-3868, 1996.

129. **Lisanti MP, Scherer PE, Tang Z, and Sargiacomo M.** Caveolae,

caveolin and caveolin-rich membrane domains: a signalling hypothesis.

Trends Cell Biol 4: 231-235, 1994.

130. **Liu J, Tian J, Haas M, Shapiro JI, Askari A, and Xie Z.** Ouabain

interaction with cardiac Na+/K+-ATPase initiates signal cascades

independent of changes in intracellular Na+ and Ca2+ concentrations. *J Biol*

Chem 275: 27838-27844, 2000.

131.   **Liu L, Mohammadi K, Aynafshar B, Wang H, Li D, Liu J, Ivanov AV, Xie Z, and Askari A.** Role of caveolae in signal-transducing function of cardiac Na$^+$/K$^+$-ATPase. *Am J Physiol* 284: C1550-1560, 2003.

132.   **Liu L, Zhao X, Pierre SV, and Askari A.** Association of PI3K-Akt signaling pathway with digitalis-induced hypertrophy of cardiac myocytes. *Am J Physiol* 293: C1489-1497, 2007.

133.   **Liu Y, Sato T, O'Rourke B, and Marban E.** Mitochondrial ATP-dependent potassium channels: novel effectors of cardioprotection? *Circulation* 97: 2463-2469, 1998.

134.   **Maniatis NA, Brovkovych V, Allen SE, John TA, Shajahan AN, Tiruppathi C, Vogel SM, Skidgel RA, Malik AB, and Minshall RD.** Novel mechanism of endothelial nitric oxide synthase activation mediated by caveolae internalization in endothelial cells. *Circ Res* 99: 870-877, 2006.

135.   **Maniatis NA, Brovkovych V, Allen SE, John TA, Shajahan AN, Tiruppathi C, Vogel SM, Skidgel RA, Malik AB, and Minshall RD.** Novel Mechanism of Endothelial Nitric Oxide Synthase Activation Mediated by Caveolae Internalization in Endothelial Cells 10.1161/01.RES.0000245187.08026.47. *Circ Res* 99: 870-877, 2006.

136.   **Marais E, Genade S, Salie R, Huisamen B, Maritz S, Moolman JA,**

and Lochner A. The temporal relationship between p38 MAPK and HSP27 activation in ischaemic and pharmacological preconditioning. *Basic Res Cardiol* 100: 35-47 Epub 2004 Nov 2003, 2005.

137. **Marais E, Genade S, Strijdom H, Moolman JA, and Lochner A.** p38 MAPK activation triggers pharmacologically-induced beta-adrenergic preconditioning, but not ischaemic preconditioning. *J Mol Cell Cardiol* 33: 2157-2177, 2001.

138. **Miaczynska M, Pelkmans L, and Zerial M.** Not just a sink: endosomes in control of signal transduction. *Curr Opin Cell Biol* 16: 400-406, 2004.

139. **Mickelson JR, Greaser ML, and Marsh BB.** Purification of skeletal-muscle mitochondria by density-gradient centrifugation with Percoll. *Anal Biochem* 109: 255-260, 1980.

140. **Mineo C and Anderson RG.** A vacuolar-type proton ATPase mediates acidification of plasmalemmal vesicles during potocytosis. *Exp Cell Res* 224: 237-242, 1996.

141. **Miyakawa-Naito A, Uhlen P, Lal M, Aizman O, Mikoshiba K, Brismar H, Zelenin S, and Aperia A.** Cell signaling microdomain with Na,K-ATPase and inositol 1,4,5-trisphosphate receptor generates calcium oscillations. *J Biol Chem* 278: 50355-50361, 2003.

142.   **Miyamoto S, Murphy AN, and Brown JH.** Akt mediates mitochondrial protection in cardiomyocytes through phosphorylation of mitochondrial hexokinase-II. *Cell Death Differ* 15: 521-529 Epub 2007 Dec 2007, 2008.

143.   **Mocanu MM, Baxter GF, Yue Y, Critz SD, and Yellon DM.** The p38 MAPK inhibitor, SB203580, abrogates ischaemic preconditioning in rat heart but timing of administration is critical. *Basic Res Cardiol* 95: 472-478, 2000.

144.   **Mohammadi K, Kometiani P, Xie Z, and Askari A.** Role of protein kinase C in the signal pathways that link Na+/K+-ATPase to ERK1/2. *J Biol Chem* 276: 42050-42056., 2001.

145.   **Moreau C, Jacquet H, Prost AL, D'Hahan N, and Vivaudou M.** The molecular basis of the specificity of action of K_{ATP} channel openers. *Embo J* 19: 6644-6651., 2000.

146.   **Murphy E and Steenbergen C.** Preconditioning: the mitochondrial connection. *Annu Rev Physiol* 69: 51-67, 2007.

147.   **Murriel CL and Mochly-Rosen D.** Opposing roles of delta and epsilonPKC in cardiac ischemia and reperfusion: targeting the apoptotic machinery. *Arch Biochem Biophys* 420: 246-254, 2003.

148.   **Murry CE, Jennings RB, and Reimer KA.** Preconditioning with ischemia: a delay of lethal cell injury in ischemic myocardium. *Circulation* 74:

1124-1136, 1986.

149. **Nagao M, Yamauchi J, Kaziro Y, and Itoh H.** Involvement of protein kinase C and Src family tyrosine kinase in Galphaq/11-induced activation of c-Jun N-terminal kinase and p38 mitogen-activated protein kinase. *J Biol Chem* 273: 22892-22898, 1998.

150. **Nakagawa Y, Rivera V, and Larner AC.** A role for the Na/K-ATPase in the control of human c-fos and c-jun transcription. *J Biol Chem* 267: 8785-8788., 1992.

151. **Nakano A, Cohen MV, Critz S, and Downey JM.** SB 203580, an inhibitor of p38 MAPK, abolishes infarct-limiting effect of ischemic preconditioning in isolated rabbit hearts. *Basic Res Cardiol* 95: 466-471, 2000.

152. **Nakano A, Cohen MV, and Downey JM.** Ischemic preconditioning. From basic mechanisms to clinical applications. *Pharmacol Ther* 86: 263-275, 2000.

153. **Nakashima RA and Garlid KD.** Quinine inhibition of Na^+ and K^+ transport provides evidence for two cation/H^+ exchangers in rat liver mitochondria. *J Biol Chem* 257: 9252-9254, 1982.

154. **Noland TA, Jr., Raynor RL, Jideama NM, Guo X, Kazanietz MG, Blumberg PM, Solaro RJ, and Kuo JF.** Differential regulation of cardiac actomyosin S-1 MgATPase by protein kinase C isozyme-specific

phosphorylation of specific sites in cardiac troponin I and its phosphorylation site mutants. *Biochemistry* 35: 14923-14931, 1996.

155. **Obata T and Yamanaka Y.** Block of cardiac ATP-sensitive K$^+$ channels reduces hydroxyl radicals in the rat myocardium. *Arch Biochem Biophys* 378: 195-200., 2000.

156. **Ockaili R, Emani VR, Okubo S, Brown M, Krottapalli K, and Kukreja RC.** Opening of mitochondrial K$_{ATP}$ channel induces early and delayed cardioprotective effect: role of nitric oxide. *Am J Physiol* 277: H2425-2434, 1999.

157. **Ogbi M, Wingard CJ, Ogbi S, Johnson JA, Chew CS, Pohl J, and Stuchlik O.** Epsilon protein kinase C lengthens the quiescent period between spontaneous contractions in rat ventricular cardiac myocytes and trabecula. *Naunyn Schmiedebergs Arch Pharmacol* 370: 251-261, 2004.

158. **Ohmori Y, Reynolds E, and Hamilton TA.** Modulation of Na+/K+ exchange potentiates lipopolysaccharide-induced gene expression in murine peritoneal macrophages. *J Cell Physiol* 148: 96-105., 1991.

159. **Oldenburg O, Cohen MV, Yellon DM, and Downey JM.** Mitochondrial K$_{ATP}$ channels: role in cardioprotection. *Cardiovasc Res* 55: 429-437, 2002.

160. **Oldenburg O, Qin Q, Krieg T, Yang X-M, Philipp S, Critz SD,**

Cohen MV, and Downey JM. Bradykinin induces mitochondrial ROS generation via NO, cGMP, PKG, and mitoK$_{ATP}$ channel opening and leads to cardioprotection. *Am J Physiol* 286: H468-476, 2004.

161.   **Oldenburg O, Qin Q, Krieg T, Yang X-M, Philipp S, Critz SD, Cohen MV, and Downey JM.** Bradykinin induces mitochondrial ROS generation via NO, cGMP, PKG, and mitoKATP channel opening and leads to cardioprotection 10.1152/ajpheart.00360.2003. *Am J Physiol Heart Circ Physiol* 286: H468-476, 2004.

162.   **Oldenburg O, Yang XM, Krieg T, Garlid KD, Cohen MV, Grover GJ, and Downey JM.** P1075 opens mitochondrial K$_{ATP}$ channels and generates reactive oxygen species resulting in cardioprotection of rabbit hearts. *J Mol Cell Cardiol* 35: 1035-1042., 2003.

163.   **Ostrom RS.** New determinants of receptor-effector coupling: trafficking and compartmentation in membrane microdomains. *Mol Pharmacol* 61: 473-476, 2002.

164.   **Ovide-Bordeaux S, Ventura-Clapier R, and Veksler V.** Do modulators of the mitochondrial K$_{ATP}$ channel change the function of mitochondria in situ? *J Biol Chem* 275: 37291-37295, 2000.

165.   **Pain T, Yang XM, Critz SD, Yue Y, Nakano A, Liu GS, Heusch G,**

Cohen MV, and Downey JM. Opening of mitochondrial K$_{ATP}$ channels triggers the preconditioned state by generating free radicals. *Circ Res* 87: 460-466, 2000.

166.   Palmer JW, Tandler B, and Hoppel CL. Biochemical properties of subsarcolemmal and interfibrillar mitochondria isolated from rat cardiac muscle. *J Biol Chem* 252: 8731-8739, 1977.

167.   Park DS, Woodman SE, Schubert W, Cohen AW, Frank PG, Chandra M, Shirani J, Razani B, Tang B, Jelicks LA, Factor SM, Weiss LM, Tanowitz HB, and Lisanti MP. Caveolin-1/3 double-knockout mice are viable, but lack both muscle and non-muscle caveolae, and develop a severe cardiomyopathic phenotype. *Am J Pathol* 160: 2207-2217, 2002.

168.   Park SS, Zhao H, Mueller RA, and Xu Z. Bradykinin prevents reperfusion injury by targeting mitochondrial permeability transition pore through glycogen synthase kinase 3beta. *J Mol Cell Cardiol*, 2006.

169.   Parolini I, Sargiacomo M, Lisanti MP, and Peschle C. Signal transduction and glycophosphatidylinositol-linked proteins (lyn, lck, CD4, CD45, G proteins, and CD55) selectively localize in Triton-insoluble plasma membrane domains of human leukemic cell lines and normal granulocytes. *Blood* 87: 3783-3794, 1996.

170.   Parton RG. Caveolae--from ultrastructure to molecular mechanisms. *Nat Rev Mol Cell Biol* 4: 162-167, 2003.

171. **Parton RG and Richards AA.** Lipid rafts and caveolae as portals for endocytosis: new insights and common mechanisms. *Traffic* 4: 724-738, 2003.

172. **Pasdois P, Beauvoit B, Tariosse L, Vinassa B, Bonoron-Adele S, and Santos PD.** MitoK(ATP)-dependent changes in mitochondrial volume and in complex II activity during ischemic and pharmacological preconditioning of Langendorff-perfused rat heart. *J Bioenerg Biomembr* 38: 101-112, 2006.

173. **Pasdois PP, Quinlan CL, Rissa A, Tariosse L, Vinassa B, Pierre SV, Dos Santos P, and Garlid KD.** Ouabain protects rat hearts against ischemia-reperfusion injury via a pathway involving src kinase, $mitoK_{ATP}$, and ROS. *Am J Physiol* 292: H1470-1478, 2007.

174. **Pastore D, Stoppelli MC, Di Fonzo N, and Passarella S.** The existence of the K(+) channel in plant mitochondria. *J Biol Chem* 274: 26683-26690., 1999.

175. **Patel HH, Head BP, Petersen HN, Niesman IR, Huang D, Gross GJ, Insel PA, and Roth DM.** Protection of adult rat cardiac myocytes from ischemic cell death: role of caveolar microdomains and delta opioid receptors. *Am J Physiol* 291: H344-350, 2006.

176. **Pelc LR, Gross GJ, and Warltier DC.** Mechanism of coronary vasodilation produced by bradykinin. *Circulation* 83: 2048-2056, 1991.

177. **Penna C, Rastaldo R, Mancardi D, Raimondo S, Cappello S, Gattullo D, Losano G, and Pagliaro P.** Post-conditioning induced cardioprotection requires signaling through a redox-sensitive mechanism, mitochondrial ATP-sensitive K+ channel and protein kinase C activation. *Basic Res Cardiol* 101: 180-189, 2006.

178. **Petronilli V, Cola C, Massari S, Colonna R, and Bernardi P.** Physiological effectors modify voltage sensing by the cyclosporin A-sensitive permeability transition pore of mitochondria. *J Biol Chem* 268: 21939-21945, 1993.

179. **Pierce KL, Premont RT, and Lefkowitz RJ.** Seven-transmembrane receptors. *Nat Rev Mol Cell Biol* 3: 639-650, 2002.

180. **Pierre SV and Xie Z.** The Na,K-ATPase Receptor Complex: Its Organization and Membership. *Cell Biochem Biophys* 46: 303-316, 2006.

181. **Pierre SV, Yang C, Yuan Z, Seminerio J, Mouas C, Garlid KD, Dos Santos P, and Xie Z.** Ouabain triggers preconditioning through activation of the Na,k-ATPase signaling cascade in rat hearts. *Cardiovasc Res* 73: 488-496, 2007.

182. **Ping P, Zhang J, Pierce WM, Jr., and Bolli R.** Functional proteomic analysis of protein kinase C epsilon signaling complexes in the normal heart and during cardioprotection. *Circ Res* 88: 59-62., 2001.

183. **Pizard A, Blaukat A, Muller-Esterl W, Alhenc-Gelas F, and Rajerison RM.** Bradykinin-induced internalization of the human B2 receptor requires phosphorylation of three serine and two threonine residues at its carboxyl tail. *J Biol Chem* 274: 12738-12747, 1999.

184. **Prabhakar P, Thatte HS, Goetz RM, Cho MR, Golan DE, and Michel T.** Receptor-regulated translocation of endothelial nitric-oxide synthase. *J Biol Chem* 273: 27383-27388, 1998.

185. **Puddu PE, Garlid KD, Monti F, Iwashiro K, Picard S, Dawodu AA, Criniti A, Ruvolo G, and Campa PP.** Bimakalim: A promising KATP channel activating agent. *Cardiovasc Drug Rev* 18: 25-46, 2000.

186. **Quinlan CL, Costa ADT, Costa CL, Pierre SV, Dos Santos P, and Garlid KD.** Conditioning the Heart Induces Formation of Signalosomes that Interact with Mitochondria to Open MitoK$_{ATP}$. *Amer J Phys*: In press, 2008.

187. **Ralston E and Ploug T.** Caveolin-3 is associated with the T-tubules of mature skeletal muscle fibers. *Exp Cell Res* 246: 510-515, 1999.

188. **Reuter H, Henderson SA, Han T, Ross RS, Goldhaber JI, and Philipson KD.** The Na+-Ca2+ exchanger is essential for the action of cardiac glycosides. *Circ Res* 90: 305-308, 2002.

189. **Riess ML, Costa AD, Carlson R, Jr., Garlid KD, Heinen A, and Stowe DF.** Differential increase of mitochondrial matrix volume by sevoflurane

in isolated cardiac mitochondria. *Anesth Analg* 106: 1049-1055, 2008.

190. **Ron D and Mochly-Rosen D.** An autoregulatory region in protein

kinase C: the pseudoanchoring site. *Proc Natl Acad Sci U S A* 92: 492-496,

1995.

191. **Rosamond W, Flegal K, Friday G, Furie K, Go A, Greenlund K,**

Haase N, Ho M, Howard V, Kissela B, Kittner S, Lloyd-Jones D,

McDermott M, Meigs J, Moy C, Nichol G, O'Donnell CJ, Roger V,

Rumsfeld J, Sorlie P, Steinberger J, Thom T, Wasserthiel-Smoller S, and

Hong Y. Heart Disease and Stroke Statistics--2007 Update: A Report From

the American Heart Association Statistics Committee and Stroke Statistics

Subcommittee. *Circulation* 115: e69-171, 2007.

192. **Rousou AJ, Ericsson M, Federman M, Levitsky S, and McCully**

JD. Opening of mitochondrial KATP channels enhances cardioprotection

through the modulation of mitochondrial matrix volume, calcium accumulation,

and respiration. *Am J Physiol* 287: H1967-1976 Epub 2004 Jul 1968, 2004.

193. **Rybin VO, Sabri A, Short J, Braz JC, Molkentin JD, and Steinberg**

SF. Cross-regulation of novel protein kinase C (PKC) isoform function in

cardiomyocytes. Role of PKC epsilon in activation loop phosphorylations and

PKC delta in hydrophobic motif phosphorylations. *J Biol Chem* 278: 14555-

14564, 2003.

194.   **Sadir R, Lambert A, Lortat-Jacob H, and Morel G.** Caveolae and clathrin-coated vesicles: two possible internalization pathways for IFN-gamma and IFN-gamma receptor. *Cytokine* 14: 19-26, 2001.

195.   **Saks VA, Vasil'eva E, Belikova Yu O, Kuznetsov AV, Lyapina S, Petrova L, and Perov NA.** Retarded diffusion of ADP in cardiomyocytes: possible role of mitochondrial outer membrane and creatine kinase in cellular regulation of oxidative phosphorylation. *Biochim Biophys Acta* 1144: 134-148, 1993.

196.   **Sanada S, Kitakaze M, Papst PJ, Hatanaka K, Asanuma H, Aki T, Shinozaki Y, Ogita H, Node K, Takashima S, Asakura M, Yamada J, Fukushima T, Ogai A, Kuzuya T, Mori H, Terada N, Yoshida K, and Hori M.** Role of phasic dynamism of p38 mitogen-activated protein kinase activation in ischemic preconditioning of the canine heart. *Circ Res* 88: 175-180., 2001.

197.   **Sasaki N, Sato T, Ohler A, O'Rourke B, and Marban E.** Activation of mitochondrial ATP-dependent potassium channels by nitric oxide. *Circulation* 101: 439-445, 2000.

198.   **Sato T, O'Rourke B, and Marbán E.** Modulation of mitochondrial ATP-dependent K$^+$ channels by protein kinase C. *Circ Res* 83: 110-114, 1998.

199. **Schechtman D and Mochly-Rosen D.** Isozyme-specific inhibitors and activators of protein kinase C. *Methods Enzymol* 345: 470-489., 2002.

200. **Scherer PE, Lewis RY, Volonte D, Engelman JA, Galbiati F, Couet J, Kohtz DS, van Donselaar E, Peters P, and Lisanti MP.** Cell-type and tissue-specific expression of caveolin-2. Caveolins 1 and 2 co-localize and form a stable hetero-oligomeric complex in vivo. *J Biol Chem* 272: 29337-29346, 1997.

201. **Schnaitman C and Greenawalt JW.** Enzymatic properties of the inner and outer membranes of rat liver mitochondria. *J Cell Biol* 38: 158-175, 1968.

202. **Schoner W and Scheiner-Bobis G.** Endogenous and exogenous cardiac glycosides: their roles in hypertension, salt metabolism, and cell growth. *Am J Physiol* 293: C509-536, 2007.

203. **Shajahan AN, Tiruppathi C, Smrcka AV, Malik AB, and Minshall RD.** Gbetagamma activation of Src induces caveolae-mediated endocytosis in endothelial cells. *J Biol Chem* 279: 48055-48062 Epub 42004 Sep 48052, 2004.

204. **Shamraj OI, Grupp IL, Grupp G, Melvin D, Gradoux N, Kremers W, Lingrel JB, and De Pover A.** Characterisation of Na/K-ATPase, its isoforms, and the inotropic response to ouabain in isolated failing human hearts. *Cardiovasc Res* 27: 2229-2237., 1993.

205. **Shaul PW and Anderson RG.** Role of plasmalemmal caveolae in signal transduction. *Am J Physiol* 275: L843-851, 1998.

206. **Smart E, Ying Y, Mineo C, and Anderson R.** A Detergent-Free Method for Purifying Caveolae Membrane from Tissue Culture Cells 10.1073/pnas.92.22.10104. *PNAS* 92: 10104-10108, 1995.

207. **Smart EJ, Ying YS, Mineo C, and Anderson RG.** A detergent-free method for purifying caveolae membrane from tissue culture cells. *Proc Natl Acad Sci U S A* 92: 10104-10108, 1995.

208. **Smith TW.** Digitalis. Mechanisms of action and clinical use. *N Engl J Med* 318: 358-365, 1988.

209. **Song KS, Sargiacomo M, Galbiati F, Parenti M, and Lisanti MP.** Targeting of a G alpha subunit (Gi1 alpha) and c-Src tyrosine kinase to caveolae membranes: clarifying the role of N-myristoylation. *Cell Mol Biol (Noisy-le-grand)* 43: 293-303, 1997.

210. **Souroujon MC and Mochly-Rosen D.** Peptide modulators of protein-protein interactions in intracellular signaling. *Nat Biotechnol* 16: 919-924, 1998.

211. **Sprenger RR, Fontijn RD, van Marle J, Pannekoek H, and Horrevoets AJ.** Spatial segregation of transport and signalling functions between human endothelial caveolae and lipid raft proteomes. *Biochem J*

400: 401-410, 2006.

212. **Steinberg SF.** Distinctive activation mechanisms and functions for protein kinase Cdelta. *Biochem J* 384: 449-459, 2004.

213. **Sweadner KJ.** Enzymatic properties of separated isozymes of the Na,K-ATPase. Substrate affinities, kinetic cooperativity, and ion transport stoichiometry. *J Biol Chem* 260: 11508-11513, 1985.

214. **Tang Z, Scherer PE, Okamoto T, Song K, Chu C, Kohtz DS, Nishimoto I, Lodish HF, and Lisanti MP.** Molecular cloning of caveolin-3, a novel member of the caveolin gene family expressed predominantly in muscle. *J Biol Chem* 271: 2255-2261, 1996.

215. **Tian J, Cai T, Yuan Z, Wang H, Liu L, Haas M, Maksimova E, Huang XY, and Xie ZJ.** Binding of Src to Na^+/K^+-ATPase forms a functional signaling complex. *Mol Biol Cell* 17: 317-326, 2006.

216. **Tian J, Gong X, and Xie Z.** Signal-transducing function of Na^+-K^+-ATPase is essential for ouabain's effect on [Ca2+]i in rat cardiac myocytes. *Am J Physiol* 281: H1899-1907., 2001.

217. **Tian J, Liu J, Garlid KD, Shapiro JI, and Xie Z.** Involvement of Mitogen-activated Protein Kinases and Reactive Oxygen Species in the Inotropic Action of Ouabain on Cardiac Myocytes. A Potential Role for Mitochondrial K_{ATP} Channels. *Mol Cell Biochem* 242: 181-187, 2003.

218. **Tong H, Rockman HA, Koch WJ, Steenbergen C, and Murphy E.**
G protein-coupled receptor internalization signaling is required for
cardioprotection in ischemic preconditioning. *Circ Res* 94: 1133-1141, 2004.

219. **Trincavelli ML, Tuscano D, Cecchetti P, Falleni A, Benzi L, Klotz
KN, Gremigni V, Cattabeni F, Lucacchini A, and Martini C.** Agonist-
induced internalization and recycling of the human A(3) adenosine receptors:
role in receptor desensitization and resensitization. *J Neurochem* 75: 1493-
1501, 2000.

220. **Tsang A, Hausenloy DJ, Mocanu MM, and Yellon DM.**
Postconditioning: a form of "modified reperfusion" protects the myocardium by
activating the phosphatidylinositol 3-kinase-Akt pathway. *Circ Res* 95: 230-
232, 2004.

221. **Vanden Hoek TL, Becker LB, Shao Z, Li C, and Schumacker PT.**
Reactive oxygen species released from mitochondria during brief hypoxia
induce preconditioning in cardiomyocytes. *J Biol Chem* 273: 18092-18098,
1998.

222. **Veksler VI, Kuznetsov AV, Sharov VG, Kapelko VI, and Saks VA.**
Mitochondrial respiratory parameters in cardiac tissue: a novel method of
assessment by using saponin-skinned fibers. *Biochim Biophys Acta* 892:
191-196, 1987.

223. **Vohra HA and Galinanes M.** Myocardial preconditioning against

ischemia-induced apoptosis and necrosis in man. *J Surg Res* 134: 138-144 Epub 2006 Feb 2020, 2006.

224. **Vondriska TM, Klein JB, and Ping P.** Use of functional proteomics to investigate PKC epsilon-mediated cardioprotection: the signaling module hypothesis. *Am J Physiol* 280: H1434-1441., 2001.

225. **Vondriska TM, Pass JM, and Ping P.** Scaffold proteins and assembly of multiprotein signaling complexes. *J Mol Cell Cardiol* 37: 391-397, 2004.

226. **Vondriska TM, Zhang J, Song C, Tang XL, Cao X, Baines CP, Pass JM, Wang S, Bolli R, and Ping P.** Protein kinase C epsilon-Src modules direct signal transduction in nitric oxide-induced cardioprotection: complex formation as a means for cardioprotective signaling. *Circ Res* 88: 1306-1313., 2001.

227. **Wang G, Liem DA, Vondriska TM, Honda HM, Korge P, Pantaleon DM, Qiao X, Wang Y, Weiss JN, and Ping P.** Nitric oxide donors protect murine myocardium against infarction via modulation of mitochondrial permeability transition. *Am J Physiol* 288: H1290-1295, 2005.

228. **Wang H, Haas M, Liang M, Cai T, Tian J, Li S, and Xie Z.** Ouabain assembles signaling cascades through the caveolar Na^+/K^+-ATPase. *J Biol Chem* 279: 17250-17259, 2004.

229. **Wang J, Gunning W, Kelley KM, and Ratnam M.** Evidence for

segregation of heterologous GPI-anchored proteins into separate lipid rafts within the plasma membrane. *J Membr Biol* 189: 35-43, 2002.

230.　**Wang S, Cone J, and Liu Y.** Dual roles of mitochondrial K_{ATP} channels in diazoxide-mediated protection in isolated rabbit hearts. *Am J Physiol* 280: H246-255., 2001.

231.　**Wang Y, Hirai K, and Ashraf M.** Activation of mitochondrial ATP-sensitive K^+ channel for cardiac protection against ischemic injury is dependent on protein kinase C activity. *Circ Res* 85: 731-741, 1999.

232.　**Wang Y, Kudo M, Xu M, Ayub A, and Ashraf M.** Mitochondrial K(ATP) channel as an end effector of cardioprotection during late preconditioning: triggering role of nitric oxide. *J Mol Cell Cardiol* 33: 2037-2046, 2001.

233.　**Wojtovich AP and Brookes PS.** The endogenous mitochondrial complex II inhibitor malonate regulates mitochondrial ATP-sensitive potassium channels: Implications for ischemic preconditioning. *Biochim Biophys Acta*, 2008.

234.　**Xie Z.** Ouabain interaction with cardiac Na/K-ATPase reveals that the enzyme can act as a pump and as a signal transducer. *Cell Mol Biol* 47: 383-390., 2001.

235.　**Xie Z and Askari A.** Na(+)/K(+)-ATPase as a signal transducer. *Eur J Biochem* 269: 2434-2439, 2002.

236.   **Xie Z and Cai T.** Na+-K+-ATPase-mediated signal transduction: from protein interaction to cellular function. *Mol Interv* 3: 157-168, 2003.

237.   **Yaguchi Y, Satoh H, Wakahara N, Katoh H, Uehara A, Terada H, Fujise Y, and Hayashi H.** Protective effects of hydrogen peroxide against ischemia/reperfusion injury in perfused rat hearts. *Circ J* 67: 253-258, 2003.

238.   **Yang XM, Krieg T, Cui L, Downey JM, and Cohen MV.** NECA and bradykinin at reperfusion reduce infarction in rabbit hearts by signaling through PI3K, ERK, and NO. *J Mol Cell Cardiol* 36: 411-421, 2004.

239.   **Yoshida H, Kusama Y, Kodani E, Yasutake M, Takano H, Atarashi H, Kishida H, and Takano T.** Pharmacological preconditioning with bradykinin affords myocardial protection through NO-dependent mechanisms. *Int Heart J* 46: 877-887, 2005.

240.   **Young JB.** Whither Withering's Legacy? Digoxin's role in our contemporary pharmacopeia for heart failure. *J Am Coll Cardiol* 46: 505-507, 2005.

241.   **Ytrehus K, Liu Y, Tsuchida A, Miura T, Liu GS, Yang XM, Herbert D, Cohen MV, and Downey JM.** Rat and rabbit heart infarction: effects of anesthesia, perfusate, risk zone, and method of infarct sizing. *Am J Physiol* 267: H2383-2390, 1994.

242.   **Yuan Z, Cai T, Tian J, Ivanov AV, Giovannucci DR, and Xie Z.**

Na/K-ATPase tethers phospholipase C and IP3 receptor into a calcium-regulatory complex. *Mol Biol Cell* 16: 4034-4045, 2005.

243. **Yue Y, Qin Q, Cohen MV, Downey JM, and Critz SD.** The relative order of mK_{ATP} channels, free radicals and p38 MAPK in preconditioning's protective pathway in rat heart. *Cardiovasc Res* 55: 681-689, 2002.

244. **Zhang DX, Chen YF, Campbell WB, Zou AP, Gross GJ, and Li PL.** Characteristics and superoxide-induced activation of reconstituted myocardial mitochondrial ATP-sensitive potassium channels. *Circ Res* In press, 2001.

245. **Zima AV and Blatter LA.** Redox regulation of cardiac calcium channels and transporters. *Cardiovasc Res* 71: 310-321 Epub 2006 Mar 2006, 2006.